Identification and Treatment of Splice Defects in Ciliary Genes *RPGR* and *BBS1* Causing Retinitis Pigmentosa

---

Dissertation

zur

Erlangung der naturwissenschaftlichen Doktorwürde

(Dr. sc. nat.)

vorgelegt der

Mathematisch-naturwissenschaftlichen Fakultät

der

Universität Zürich

von

Fabian Schmid

von

Schübelbach (SZ)

Promotionskomitee

Prof. Dr. Wolfgang Berger (Vorsitz)

Dr. John Neidhardt (Leitung der Dissertation)

Prof. Dr. Stephan Neuhauss

Prof. Dr. Christian Grimm

Zürich, 2011

Declaration

I declare that the present thesis was composed by myself and the whole experimental work was performed by my own.
This dissertation has not been submitted anywhere else in order to get any other degree or professional qualification.

Fabian Schmid, 2011

Table of Contents

Zusammenfassung

Retinitis pigmentosa (RP) ist eine genetisch und klinisch heterogene Krankheit, die zur Degeneration von Photorezeptoren führt und vollständige Blindheit verursachen kann. Zirka eine von 3000 bis 4000 Personen erkrankt an RP und weltweit sind mind. 1.5 Millionen Menschen betroffen. RP kann auch Teil einer syndromalen Krankheit, wie zum Beispiel dem Bardet-Biedl Syndrom (BBS) sein.

Wir haben Mutationen in den Genen *RPGR* und *BBS1* gefunden, welche für das Funktionieren des Verbindenden Ziliums (connecting cilium) im Photorezeptor wichtig sind. Die Mutationen führen zu Defekten im Spleissen der pre-mRNA. Mutationen in *BBS1* sind normalerweise mit BBS assoziiert, wohingegen die meisten *RPGR* Mutationen nicht syndromale RP verursachen. Unsere Patienten zeigen aber Symptome, die dem zu erwartenden Krankheitsbild widersprechen. In der Familie des einen Patienten mit Spleissdefekten in *RPGR*, sind heterozygote Trägerinnen der Mutation ebenfalls betroffen. Im anderen Fall leidet der Patient zusätzlich zu RP an einer milden Höhrschwäche. Die zwei Patienten mit der Splice Donor Mutation in *BBS1* zeigen RP, aber keine weiteren Symptome von BBS. Unsere Beobachtungen deuten an, dass Spleissdefekte das Krankheitsbild und den Krankheitsverlauf modifizieren können.

Die zwei *RPGR* Mutationen verändern die exprimierte Menge von neu entdeckten, alternativen *RPGR* Transkriptisoformen. Wir haben gefunden, dass deren Menge in gesunden Menschen gewebespezifisch reguliert ist. Dies impliziert, dass eine Misregulation dieser Isoformen Schäden in den entsprechenden Geweben verursachen oder den Schweregrad der Krankheit erhöhen könnte. Im Gegensatz dazu, führt die *BBS1* Mutation zu RP, höchstwahrscheinlich durch eine Reduktion der Menge an funktionellem BBS1 Protein. Die reduzierte Menge an BBS1 scheint auf die anderen Gewebe aber keinen Einfluss zu haben.

In unserer Gruppe wurde ein gentherapeutischer Ansatz entwickelt, um die pathogenen Effekte von Spleissendefekten zu mildern. Der Ansatz basiert auf der Expression einer modifizierten Form des U1 small nuclear Ribonukleoproteins (U1). U1 ist ein Spleissfaktor der direkt am Pozess des Transkriptspleissens beteiligt ist. Höchstwahrscheinlich stört die Mutation in *BBS1* die Interaktion von U1 mit dem Transkript, was dadurch den Spleissdefekt verursacht. Um die Interaktion von U1 mit

dem Transkript und damit die Erkennung des von der Mutation betroffenen Exons zu verbessern, wurde U1 an die Mutation angepasst. Die Behandlung von Patientenzellen mit dem angepassten U1 verhindert das Überspringen von Exon 5 und erhöht die Menge an korrekt gespleisstem *BBS1* Transkript. Diese Resultate, werden möglicherweise dazu beitragen, eine Behandlungsmethode für solche Mutationen in betroffenen Patienten zu etablieren.

Summary

Retinitis pigmentosa (RP) is a genetically and clinically heterogeneous disease leading to the degeneration of photoreceptors and can cause complete blindness. The prevalence of the disease is about 1 in 3000 to 4000 people with more than 1.5 million affected worldwide. RP can be a part of several syndromic disorders, as for example the Bardet-Biedl syndrome (BBS).

We have identified mutations in the genes *RPGR* and *BBS1* which are important for the functioning of the photoreceptor's connecting cilium. The mutations lead to defects in pre-mRNA splicing. Mutations in *BBS1* are generally associated with BBS, whereas most of the mutations in *RPGR* cause non-syndromic RP. However, our patients show different phenotypes. In the family of one of the two male RP patients who show *RPGR* splice defects, heterozygous female carriers are affected. The other patient suffers from mild hearing impairments in addition to RP. Furthermore, the two patients with a splice site mutation in *BBS1* show RP without any further signs of BBS. Our findings implicate that defects in mRNA splicing might modify progression and expression of the disease. The two mutations found in *RPGR* change the amount of novel, alternative transcript isoforms. We have found that the novel *RPGR* isoforms were expressed in a tissue-dependent manner in healthy individuals which suggests that misregulation of these variants could affect other tissues or increase disease severity. In contrast, the splice site mutation in *BBS1* causes RP, most probably by reducing the amount of functional protein, whereas other tissues remain unaffected.

To correct spliced defects a gene therapeutic approach using a modified form of the U1 small nuclear ribonucleoprotein has been developed in our group. U1 is a splicing factor directly involved in the general splicing process. The mutation in *BBS1* causes the splice defect most probably by interfering with U1 binding to the transcript. To increase its binding affinity to the transcript and thereby improve recognition of the affected exon, U1 was adapted to the mutation. Treatment of patient-derived fibroblasts with the adapted form of U1 increased the amount of correctly spliced *BBS1* transcripts and completely abolished skipping of exon 5. These results could help to establish a gene therapeutic treatment to correct splice defects in patients.

1. General Introduction

1.1. General structure and function of the eye

The eye is a sensory organ for visual perception converting light impulses into neuronal signals. In general, these signals are hierarchically transferred to different areas of the brain ending in the visual cortex. This area is part of the occipital lobe which is responsible for image processing making us capable to see images of the external environment.

The eye is situated in the orbital bone cavity of the skull. A light beam has to cross different parts of the eye before it hits photoreceptor neurons of the retina where phototransduction takes place. At first, the light passes through the cornea, a translucent membrane built up by evenly arranged collagen fibers that covers the pupil and iris. Together with the cornea, the crystalline lens refracts light to ensure sharp images at the level of photoreceptor outer segments (Figure 1A). The cornea is connected with the sclera that surrounds the rest of the eye ball including optical nerve fibers. The next layer which is directly attached to the sclera is the choroid, a vascularized and pigmented tissue that supplies adjacent cells with nutritions. This energy supply is mainly relevant for photoreceptors and cells of the retinal pigment epithelium (RPE) (Blanks, 2001). Cells of the RPE carry microvilli which interdigitate part of photoreceptor outer segments and perform phagocytosis of shed outer segments (Thumann and Hinton, 2001). Furthermore components in RPE cells are involved in restoration of the visual pigment chromophore (Lamb and Pugh, Jr., 2004) as described in chapter 1.1.3. on page 8.

1.1.1. Structure and function of the retina

Before light enters the retina it has to cross the vitreus body, a transparent mass of collagen and water which fills the space between the lens and the retina. During its way through the retina light encounters different, histologic layers composed of either cell body nuclei (nuclear layers) or synaptic interconnections (plexiform layers) (Figure 1B). The first layer penetrated by light is the ganglion cell layer (GCL) which consists of bodies of retinal ganglion cell neurons (G), whose axons center to form the optic nerve. Fibers of the optic nerve project to neurons of the laterate geniculate nuclei, the primary processing center of vision in the brain. The dendrites of ganglion

cells connect with synapses from bipolar (B) and amacrine (A) cells which form the inner plexiform layer (IPL). Bipolar cells are selectively connected to rod (R) or cone (C) photoreceptors and transmit neuronal signals from photoreceptors to ganglion cells. The inner nuclear layer (INL) is built up by cell bodies of bipolar, amacrine, horizontal (H) and Müller cells (M). Amacrine and horizontal cells are considered to be local-circuit neurons which modulate and transform visual information (Blanks, 2001). Müller cells are a specialized type of glia cells, whose processes build synaptic junctions to neurons of the INL and the outer nuclear layer (ONL). Müller cells contribute to many essential retinal functions (Newman, 2001). The ONL is composed exclusively of cell bodies from cone and rod photoreceptors. Dendrites of photoreceptor neurons build synapses with horizontal and bipolar cells in the outer plexiform layer (OPL) (Blanks, 2001).

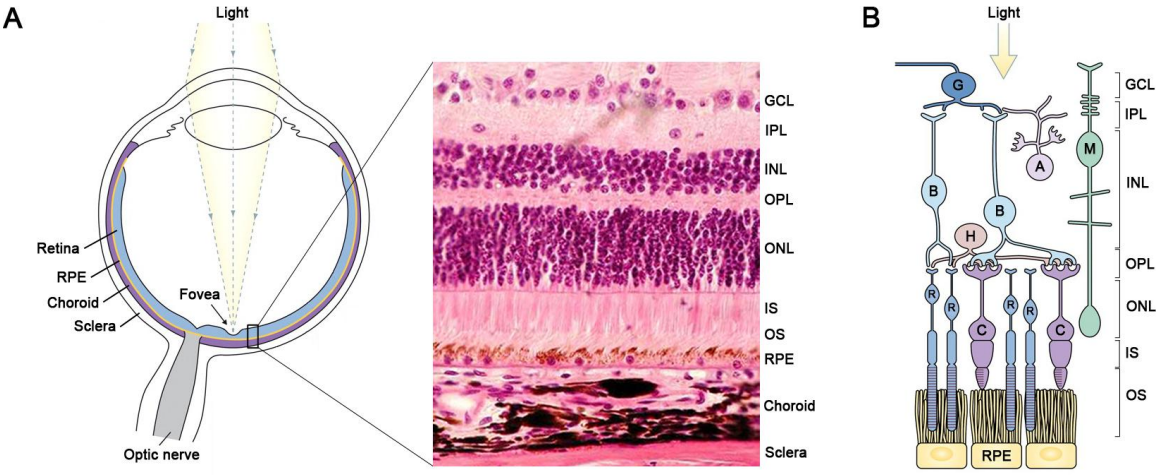

Figure 1 Cell types and histologic layers of the healthy human retina. **A** Schematic display of the human eye showing different functional components. A beam of light falls directly to the fovea, the region of highest visual acuity located close to the optical nerve head margin. A histological section through the retina comprising the ganglion cell layer (GCL), inner plexiform layer (IPL), inner nuclear layer (INL), outer plexiform layer (OPL), photoreceptors inner (IS) and outer segments (OS). Apical microvilli of retinal pigment epithelium (RPE) cells encircle the distal half of photoreceptor OS. The retina is surrounded by the choroid vasculature which is itself enclosed by the sclera, the eye's most external layer. **B** Graphical illustration of cell types and synaptic processes building the different retinal layers: G, ganglion cell; M, Müller cell; A, amacrine cell; B, bipolar cell; H, horizontal cell; R, rods; C, cones. Modified from Sung and Chuang (2010) and http://biology.clc.uc.edu/fankhauser/Labs/Anatomy_&_Physiology/A&P202/Special_Senses/Eye/eye_jpegs/retina_PC271517.JPG

1.1.2. Rod and Cone photoreceptors

The human retina is composed of two different types of sensory neurons termed rod and cone photoreceptors. Originally, photoreceptor classification was based on the morphologic appearance of outer segments in microscopic images. Rod outer segments have a more cylindrical shape, whereas the shape of cones taper in width

from inner to outer segments (Figure 2). Nevertheless, it seems that functional properties such as photosensitivity are much more useful for classification of photoreceptors. In average 4.6 million cones and 92 million rods are present on the human retina. Both cones and rods are unevenly distributed. Cones are highly concentrated in the macular region. Within the macula, cones center to the highest density in the fovea centralis, a region which lays on the optical axis of the eye ball and features best visional acuity (Figure 1A). The density of cones decreases drastically from the fovea to the periphery. Except for the rod-free fovea, rods show a nearly equal distribution across the retina with a slight decrease to the periphery (Blanks, 2001).

A photoreceptor cell can be subdivided into an outer segment (OS) that contains the visual pigment and an inner segment (IS) that contains the metabolic machinery of the cell and the nucleus (Figure 2B). Inner and outer segments are connected through a modified primary cilium, referred to as the connecting cilium, which represents the only link between the two compartments (Blanks, 2001). Active transport of new membrane lipids and proteins to the OS is performed along the microtubule-based cytoskeleton of the cilium, called the axoneme (Kennedy and Malicki, 2009). Structure and function of the connecting cilium will be further described in chapter 1.1.4. on page 11.

Rod photoreceptors are the most predominant cell type in the human retina and are responsible for night vision (scotopic) by absorbing mainly blue-green light. A rod OS (ROS) is composed of about 1000 flattened, lamellar-shaped membrane discs which are stacked perpendicular to the axis of the OS (Figure 3A). These discs are enclosed by the plasma membrane. Although membrane discs of rods are not directly fused with the plasma membrane, it appears that different proteins bridge them to the membrane. The mechanism underlying disc morphogenesis in the ROS remains poorly understood. At least two models have been postulated. In one model, formation of new discs is explained by evaginations of the ciliary plasma membrane at the base of the ROS and development of a disc rim by fusing the lower membrane of an already existing with the upper membrane of the adjacent, nascent evagination. In the other model, discs of rods form by regulated fusion of membrane vesicles directly in the ROS (Kennedy and Malicki, 2009). The disc membranes mainly contain rhodopsin (RHO) which accounts for 95% of their total protein load (Sung and

Chuang, 2010). RHO together with its chromophore is the visual pigment of rods and is most sensitive to light at a wavelength of about 500 nm.

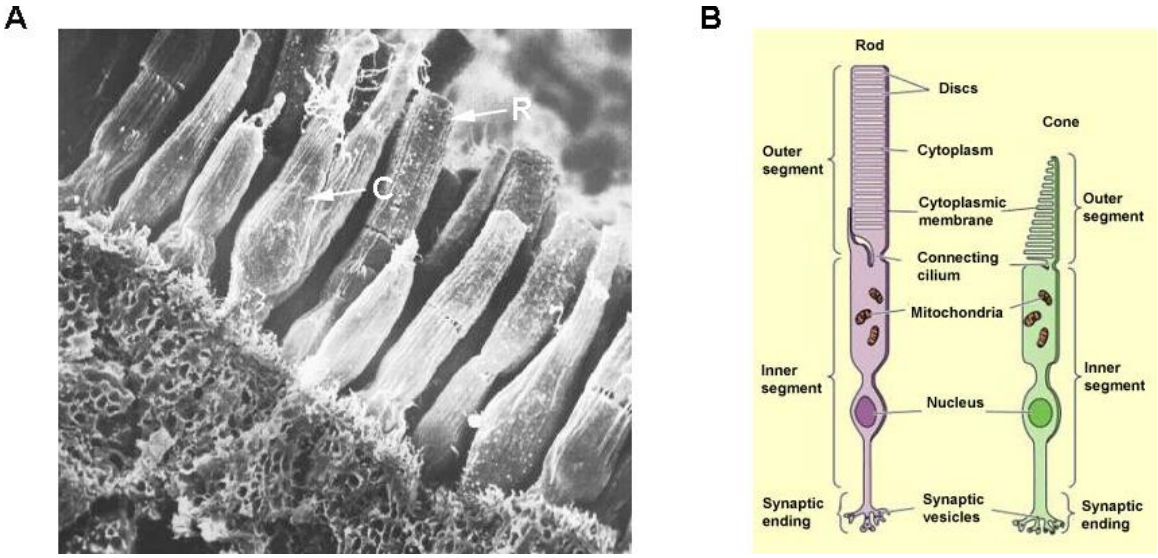

Figure 2 Cone and rod photoreceptors are the light sensing neurons of the retina. **A** Scanning electron micrograph of cone (C) and rod (R) photoreceptors in the human retina. Image adapted from http://www.faqs.org/health/Sick-V1/Color-Blindness-Causes.html.
B Schematic drawing of the cellular components of rods and cones. Picture taken from http://thebrain.mcgill.ca/flash/d/d_02/d_02_m/d_02_m_vis/d_02_m_vis.html.

There are three different types of cones in the human retina that are activated depending on the wavelength of the light stimulus. Each cone type contains a wavelength-specific visual pigment that is encoded by a certain variant of the opsin gene. The different opsin variants have evolved through gene duplication and genetic divergence from a common ancestral gene. L-cones are most sensitive to red light at wavelengths near 560 nm, M-cones to green light at around 530 nm and S-cones to blue light at 420 nm. L-cones are twice as abundant as M-cones in human. Both cone types are most concentrated in the fovea whereas S-cones are located more towards the periphery. The later accounts for only 5% of the total cone population. Cone outer segments (COS) are shorter than ROS. Disc membranes of cones develop by the evagination of the ciliary membrane and remain continuously connected to the axoneme of the connecting cilium that extends the entire length of the COS (Figure 3B) (Mustafi et al., 2009). Likewise in rods, the visual pigment of cones is located in the disc membranes of the COS.

In summary, the high density of opsins together with the orderly arrangement of disc membranes in photoreceptor OS provide most efficient visual sensitivity and spatial control over phototransduction (Kennedy and Malicki, 2009; Sung and Chuang, 2010).

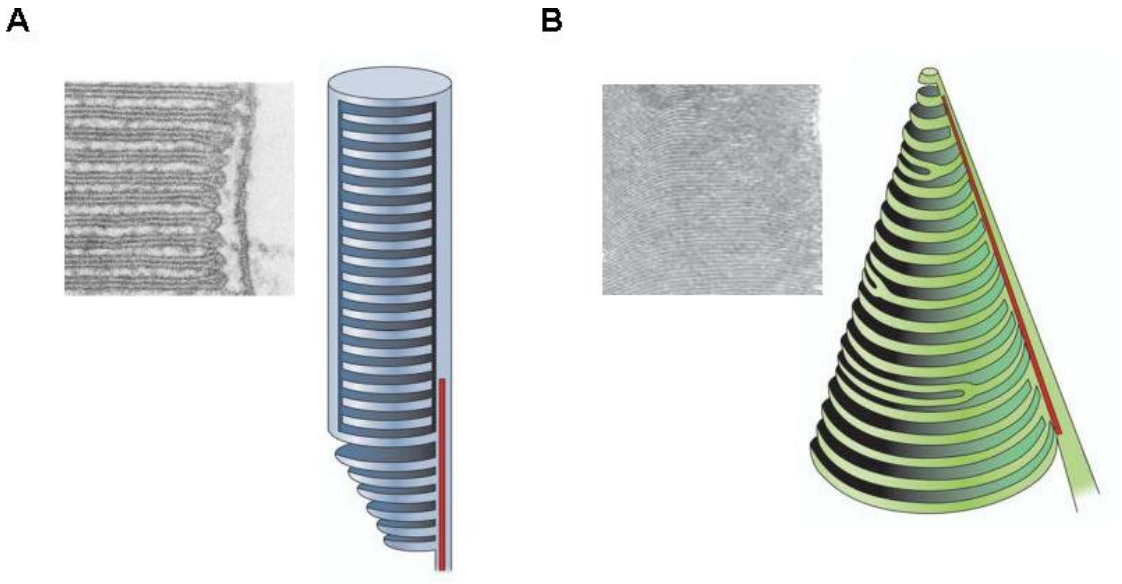

Figure 3 Structure of photoreceptor outer segments. **A** Electron microscopic image and schematic drawing of stacked membrane discs in rod outer segments which are not connected to the connecting cilium (red line) and plasma membrane. **B** Electron micrograph of evaginated membrane discs in the cone outer segment which retain associated to the connecting cilium. In contrast to rods, the ciliary axoneme of cones (red line) extends the entire length of the outer segment. Pictures are adapted from Kennedy and Malicki (2009) and Mustafi (2009).

1.1.3. The phototransduction cascade

The photopigment responsible for light sensing and signal transduction in rods and cones consists of a protein part and a retinal-derived chromophore. In humans, the protein part is encoded by the rhodopsin (*RHO*) gene or by three different cone opsin genes. In all visual pigments the chromophore 11-*cis*-retinal is covalently bound to a Lysine in the protein binding pocket and confers light sensitivity to the pigment (Nickle and Robinson, 2007). For simplicity, the term opsin is used in the following to refer to all types of chromophore-bound, light-sensitive visual pigments. Opsins are members of the G-protein-coupled receptor (GPCR) protein family. GPCRs are defined by their seven-transmembrane spanning domain and the ability to activate GTP-binding proteins (G-proteins). Opsins are activated throught light-induced isomerization of 11-*cis* retinal to all-*trans* retinal leading to a conformational change in the protein. It is assumed that substitutions of amino acids that are in close contact to the chromophore interfere with its double bound system. This can result in higher need of energy for chromophore isomerization and explains the differences in light sensitivity between opsins (Nickle and Robinson, 2007).

The phototransduction cascade in vertebrate rods is well understood (Figure 4). In darkness, there is a high concentration of cyclic GMP (cGMP) in the cytoplasm of

ROS which is produced by a constitutively active guanylate cyclase (GC) integrated into the disc membrane. The thereby synthesized cGMP can bind to cyclic-nucleotide-gated (CNG) cation channels on the plasma membrane of ROS. On the condition that cGMP is bound, these channels are permeable to monovalent and divalent cations, such as for instance Ca^{2+}. Influx of Ca^{2+} is balanced by an equal Ca^{2+} efflux via a Na^{+}/Ca^{2+}, K^{+} exchanger (NCKX) keeping the photoreceptor in a depolarized state. Likewise, the level of cytoplasmic cGMP is held in a steady state in the dark by the activity of a membrane-attached phosphodiesterase (PDE), which hydrolyses cGMP (Yau and Hardie, 2009).

The activity of PDE is further increased upon a light stimulus as described in the following. Light-induced activation of rhodopsin leads to its association with the G-protein transducin (G_t) which causes an exchange of bound GDP with GTP in the α subunit of G_t ($G_{t\alpha}$). After this step, $G_{t\alpha}$ dissociates from transducin $\beta\gamma$ subunits ($G_{t\beta\gamma}$) and associates with the γ subunit of PDE (PDE_{γ}), which blocks hydrolytic activity of PDE α and β subunits. When bound to $G_{t\alpha,}$ the inhibitory effect of PDE_{γ} on $PDE_{\alpha\beta}$ subunits is removed and cGMP can be hydrolyzed leading to lower cytosolic cGMP concentrations. This decrease lead to a rapid dissociation of cGMP bound to CNG channels and closes the cannels. The closure of CNG channels stop cation influx (e.g. Ca^{2+}) but not efflux by NCKX. Consequently, photoreceptors are hyperpolarized what reduces or stops their release of glutamate neurotransmitter at the synapse (Yau and Hardie, 2009). The reduced glutamate-release from photoreceptors activates bipolar cells that further process and transmit the signal to other retinal neurons. Finally, neuronal signals are sent to the brain for higher-order processing.

The processes that deactivate the phosphotransduction cascade are complex and not completely understood (Figure 4). Active rhodopsin can be deactivated through phosphorylation by a rhodopsin kinase (GRK1) and subsequent binding of arrestin (Arr). $G_{t\alpha}$ is deactivated by itself because of its intrinsic GTPase activity, which can be facilitated by the GTPase activating-protein (GAP) complex. Inactivation of phototransduction can also be achieved through multiple negative-feedback mechanisms mediated by Ca^{2+} levels. A decrease in Ca^{2+} has three effects. First, activity of GC is increased.

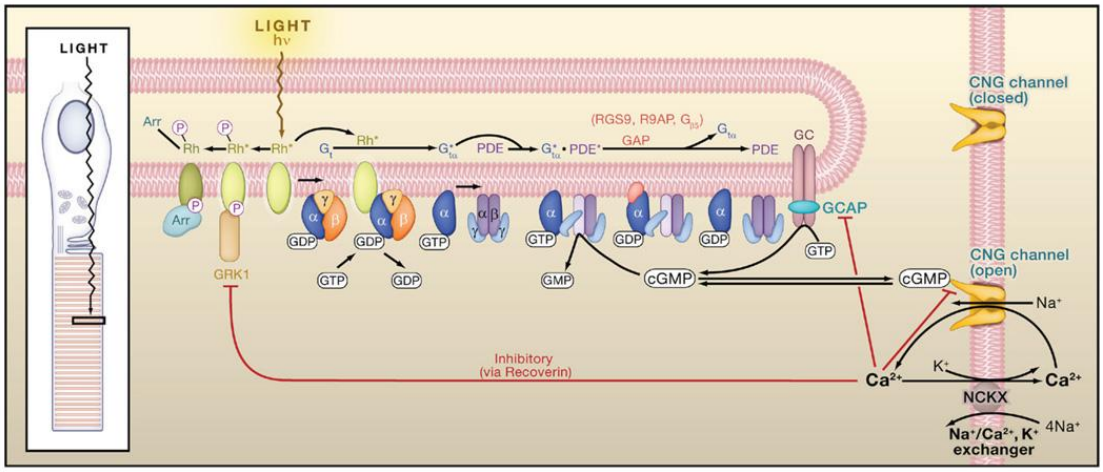

Figure 4 Phototransduction cascade in a rod photoreceptor outer segment. Different components involved in the process are shown: activated rhodopsin (Rh*), G-protein (G_t), phosphodiesterase (PDE), guanylat cyclase (GC), cyclic-nucleotide-gated (CNG) cation channels Na^+/Ca^{2+}, K^+ exchanger (NCKX). Mechanisms for deactivation of phototransduction are indicated in red and includes activities of G protein-coupled-receptor-kinase 1 (GRK1), arrestin (Arr) and guanylate cyclase-activating proteins (GCAP). Figure is taken from Yau and Hardie (2009).

Elevation of GC activity requires two guanylate cyclase-activating proteins, termed GCAP1 and GCAP2, which are negatively modulated by Ca^{2+}. Second, the activity of GRK1 is negatively influence by the Ca^{2+} binding protein recoverin leading to higher amounts of inactive rhodopsin when Ca^{2+} is low. Third, low amounts of Ca^{2+} result in higher affinity of CNG channels to cGMP what increases the frequency of these channels to be in the open state (Yau and Hardie, 2009). Together, all these mechanisms ensure deactivation of phototransduction and a fast response to the next light stimulus. Furthermore, it has been found that transducin, arrestin and recoverin change their localization in photoreceptor segments upon stimulation to bright light: Transducin translocates to the IS and recoverin towards the synapse whereas arrestin moves to the OS of photoreceptors. These light-driven translocations may contribute to the process by which photoreceptors adjust their sensitivity to ambient light intensities (Calvert et al., 2006).

In order to prepare rhodopsin to activate another phototransduction event, light-induced isomerization of all-*trans* retinal has to be restored into 11-*cis* retinal. Thereby, the isomerized retinoid undergoes a long series of reactions referred to as the retinoid cycle. In rods, the enzymatic steps of the retinoid cycle are accomplished in ROS and the adjacent RPE (Figure 5) (Yau and Hardie, 2009). The covalent bond between rhodopsin and all-*trans* retinal (RAL) is hydrolyzed and reduced to all-*trans* retinol (ROL; vitamin A) in the ROS. Vitamin A then exits the photoreceptor and

enters the RPE cell. Within the RPE, vitamin A is converted into 11-*cis* retinal after several subsequent reactions preformed by different enzymes including RPE65. Finally, the restored chromophore is transported back to the ROS where it associates with rhodopsin (Lamb and Pugh, Jr., 2004).

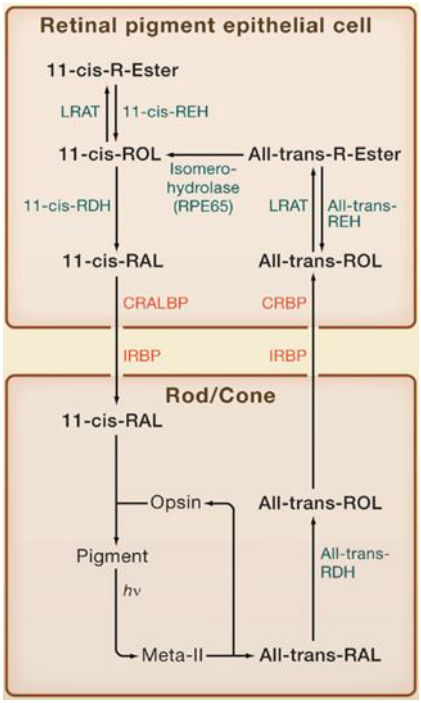

Figure 5 Restoration of isomerized retinoid from rods or cones which is accomplished by enzymes in photoreceptor OS and RPE cells. A photon (*h*ν□) produces the isomerized chromophore intermediate (Meta-II) which is enzymatically recycled from all-*trans* retinal (RAL) via all-*trans* retinol (ROL, vitamin A) to 11-*cis* retinal (RAL). These steps are performed mainly by the activities of all-*trans* retinol dehydrogenase (RDH), the extracellular carrier interphotoreceptor retinoid-binding protein (IRBP), RPE intracellular carriers (cellular retinol binding (CRBP) and retinaldehyde binding protein (CRALBP)), retinyl isomerohydrolase RPE65, and all-*cis* RDH. Figure is adapted from Yau and Hardie (2009).

1.1.4. The photoreceptor connecting cilium

The eukaryotic cilium is a cell organelle whose structure is based on centriole-derived microtubule projections. It is wrapped by the plasma membrane, called ciliary membrane. The microtubule cytoskeleton of the cilium is termed the ciliary axoneme. Mammalian ciliary axonemes can appear in two different configurations. Motile cilia usually have nine doublet microtubules surrounding a single central doublet (9+2 configuration) with axonemal dynein arms, whereas nonmotile cilia miss the doublet microtubules in the center (9+0 configuration) and are devoid of dynein (Figure 6A). In general, nonmotile cilia are found singly on almost every cell of the human body (Satir and Christensen, 2007). Because of their widespread distribution they are now defined as primary cilia. It has been demonstrated for many cases that primary cilia carry out different sensory functions.

The photoreceptor OS is a highly elaborated structure, which has been derived from a primary cilium. During differentiation of rod photoreceptors, the ROS is formed from a primary cilium located on post-mitotic retinal progenitor cells. After huge structural

modifications of the distal part of the ROS, there is only a segment of the cilium left that bridges the IS with the OS. This structure is called the connecting cilium (CC) (Pazour and Rosenbaum, 2002). The CC represents the only link between the two compartments of photoreceptor cells (Figure 6B) and is assumed to act as a ciliary necklace having similar properties as the passage formed by the nuclear pore complex (Satir and Christensen, 2007). Consequently, all lipids and proteins which are synthesized in the IS, but needed in photoreceptor OS, must be actively transported through the CC. The need for opsin in the OS is immense. It has been estimated that 2000 opsin molecules have to be transported through the CC within a minute (Pazour and Rosenbaum, 2002).

The transport of lipids and proteins along the CC is mediated by a process called intraflagellar transport (IFT). Initially, IFT was found to play a crucial role in assembly and disassembly of cilia and flagella. The main components of the IFT protein machinery that actively transports cargo along the ciliary axoneme are members of the kinesin and dynein superfamily. These microtuble-based motors move either to the plus (anterograde) or to the minus end (retrograde) of the axoneme (Figure 6C). The kinesin II complex moves anterogradely from the basal body to the cilia tip and is composed at least of KIF3A, KIF3B and the non-motor subunit kinesin-associated protein (KAP) (Rosenbaum and Witman, 2002). Recent findings identified homodimeric kinesin OSM-3/KIF17 as an additional anterograde molecular motor. The retrograde transport is mediated by a cytoplasmic dynein heavy chain subunit, known as dynein 2 (Dhc2) in mammals. Other components of the retrograde IFT motor are dynein light intermediate and the dynein light chain (Silverman and Leroux, 2009). These molecular motors transport large protein complexes, called IFT particles, which are suggested to assist transport of target proteins (Pazour and Rosenbaum, 2002). Studies in a conditional KIF3A knock out and mice affected by a hypomorphic mutation in the IFT particle gene Tg737 (IFT88) showed accumulation of rhodopsin in IS and retinal degeneration at later stages (Marszalek et al., 2000; Pazour et al., 2002). These results provided first evidence that IFT is important for development, maintenance and function of photoreceptors and for precise localization of rhodopsin to the OS. Further support for a rhodopsin transport by IFT was aquired recently by pull down assays demonstrating the interaction of rhodopsin with components of IFT particle. In the same study, the existence of a IFT cargo complex containing GC was also suggested (Bhowmick et al., 2009).

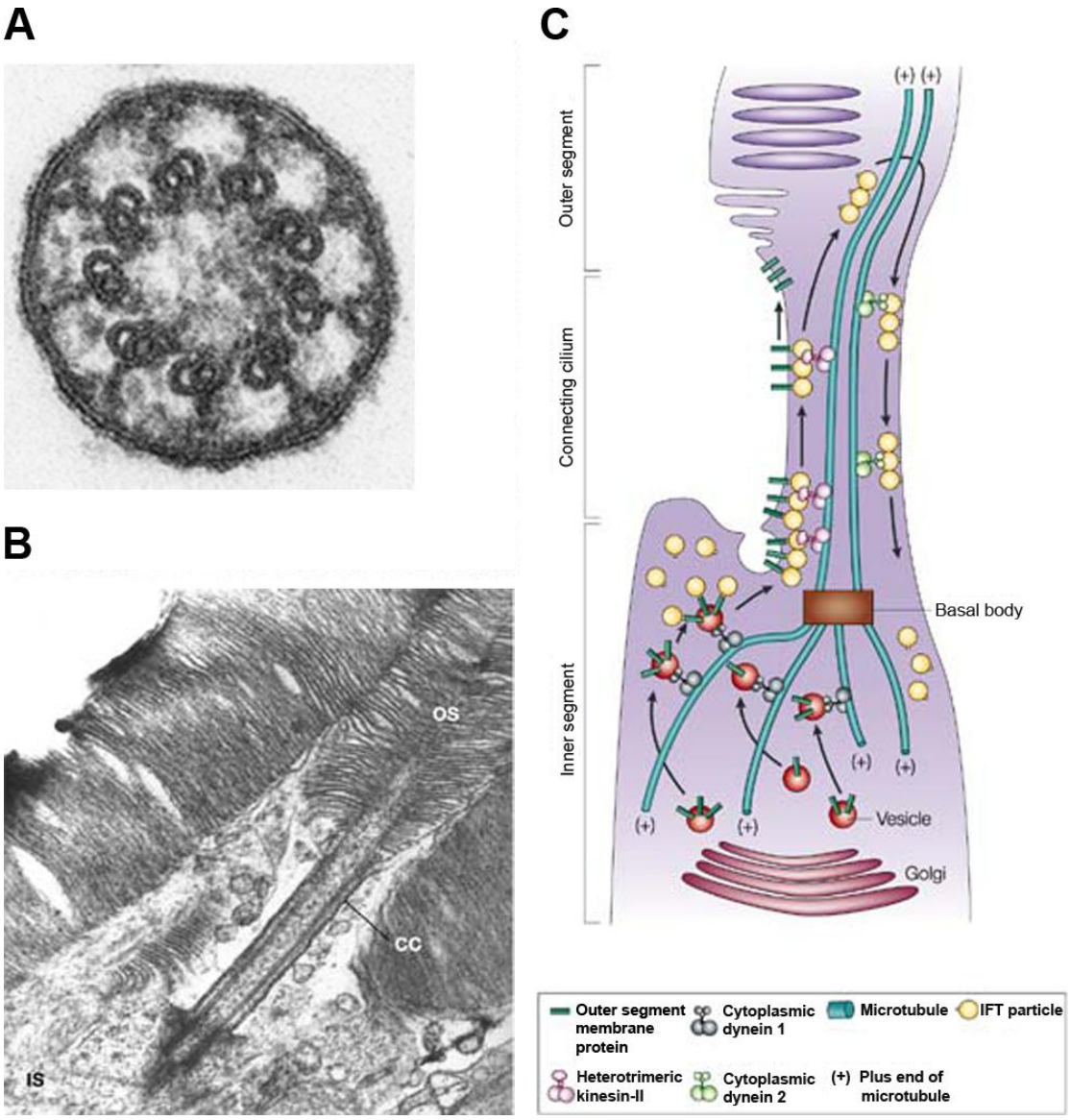

Figure 6 Structure and transport along the connecting cilium in the vertebrate rod photoreceptor. **A** Electron microscopic image of a cross section through the axoneme of a primary cilium featuring the 9+0 configuration. **B** Electron micrograph showing inner segment (IS), outer segment (OS) and the connecting cilium (CC). **C** Interflagellar transport (IFT) among the connecting cilium. Images are adapted from Rosenbaum and Witman (2002) and Insinna and Besharse (2008).

1.2. Inherited diseases affecting photoreceptors

Photoreceptors are highly organized structures, especially in the OS and are specialized to react upon a light stimulus. The correct development and maintenance of these dynamic structures is a prerequisite to perform their tasks. It is plausible, that photoreceptors are highly susceptible to mutations in genes involved in e.g. phototransduction or structure formation. Indeed, a significant fraction of human inherited disorders results in retinal degeneration.

In many cases, the cause for the disease is directly found in the photoreceptors. These ocular diseases can be classified into three major groups depending whether mainly rods, cones or both cell types are affected (Berger et al., 2010). For some of the disorders, the ocular manifestation is part of a syndromic phenotype showing also dysfunctions of other tissues. This makes it necessary to further subdivide the disorders into non-syndromic or syndromic types. A prominent example for a non-syndromic, non-progressive disease which mainly causes defects in the rod visual system is congenital stationary night blindness (CNGB). In contrast, retinitis pigmentosa (RP) shows a progressive loss of rod photoreceptors. Disruption of the cone visual system includes stationary and progressive forms. Stationary forms of cone dystrophies are represented by complete and incomplete achromatopsia which are usually congenital. Progressive loss of cones is described for cone dystrophies (CODs) , cone rod dystrophies (CORDs) and monogenic or age-related macular degenerations (Berger et al., 2010).

1.2.1. Retinitis pigmentosa

Retinitis pigmentosa (RP; OMIM 268000) is a group of inherited retinal dystrophies that show progressive loss of primarily rod photoreceptors and subsequent retinal pigment deposits. The disease is clinically and genetically heterogeneous. In the early stage of non-syndromic RP, night blindness is the main symptom which is present within the first decade or during the second decade of life. At this stage of the disease visual acuity and fundus examinations appear to be normal. At the mid stage, rod photoreceptors start to degenerate at the periphery resulting in the presence of bone spicule-shaped pigment deposits in the mid periphery of the retina (Figure 7A). At this stage patients may notice the beginning of vision loss in the peripheral visual field leading to tunnel-vision. At later stages, complete loss of peripheral vision disables patients to move autonomously. In the fundus of patients, pigment deposits can be

detected in many retinal areas, as well as clear reduction of retinal vessels thickness (Figure 7B). At late stages, cone photoreceptors may die, which lead to loss of central vision and can cause complete blindness (Hamel, 2006).

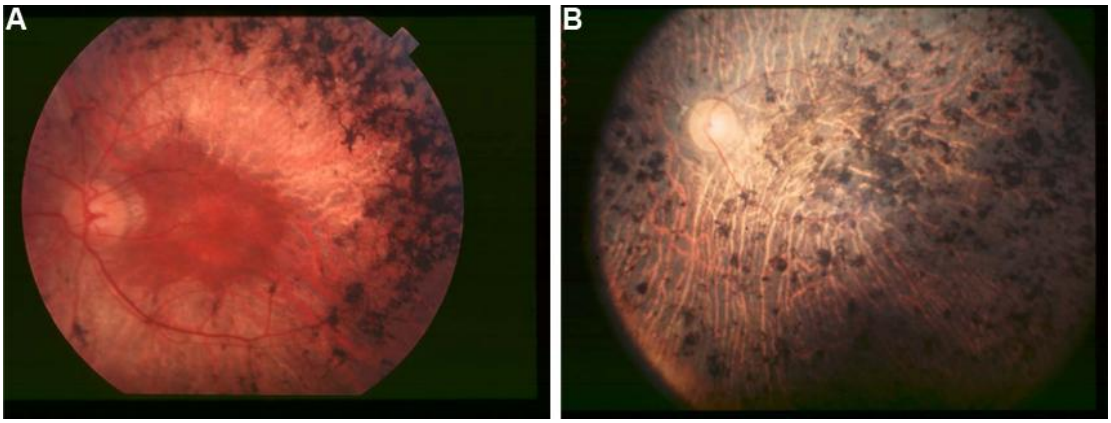

Figure 7 Funduscopic images of an RP patient. **A** Image at mid stage of the disease showing mid-peripheral pigment deposits. **B** At the final stage of the disease, pigment deposits are abundantly distributed over the whole retina and the retinal vessel system is largely attenuated. Pictures are taken from Hamel (2006).

The prevalence of RP is approximately 1 in 4000 individuals. More than 40 RP-associated genes have been identified. These genes may be involved in phototransduction, retinal metabolism, development and maintenance of cellular structures, and mRNA splicing (Berger et al., 2010). It has been described that in non-syndromic RP 30-40% of all cases are autosomal dominant (adRP), 50-60% are autosomal recessive (arRP) and 5-15% are X-linked (XlRP) (Hartong et al., 2006). Furthermore, a digenic inheritance mode has been reported in which a heterozygous mutation in the retinal outer segment membrane protein 1 (*ROM1*) together with a heterozygous mutation in peripherin 2 (*PRPH2*) cause the RP phenotype (Kajiwara et al., 1994). Mutations in RHO were the first to be associated with the disease and account for more than 25% of all adRP cases. Among the different inheritance modes, XlRP is the most severe form. Here, most of the mutations were found in the retinitis pigmentosa GTPase regulator gene (*RPGR*) which account for more than 70% of all XlRP cases (Hartong et al., 2006).

RP can also be part of a syndromic phenotype affecting other tissues. A prominent example is Usher syndrome, in which RP is associated with neurosensory deafness. Another example is Bardet-Biedl syndrome (BBS) which will be described in detail further below in this chapter. In addition, many other syndromes include RP as an ocular manifestation (Hamel, 2006). Descriptions of inherited retinal diseases are

summarized in RetNet (http://www.sph.uth.tmc.edu/Retnet/) or http://www.ncbi.nlm.nih.gov/sites/ GeneTests.

1.2.2. The retinitis pigmentosa GTPase regulator

The retinitis pigmentosa GTPase regulator (*RPGR*) gene contains 19 constitutive exons and was initially found to be disrupted in XlRP (Meindl et al., 1996; Roepman et al., 1996a; Roepman et al., 1996b). To date, a minor fraction of mutations could be identified in exons 1-14, whereas the majority of mutations were detected in an alternatively spliced exon designated ORF15 (Vervoort et al., 2000).

A minor portion of *RPGR* mutations cause a broader phenotypic spectrum than typical XlRP. For some XlRP families it has been reported that females are also affected (Mears et al., 2000; Rozet et al., 2002; Banin et al., 2007; Pelletier et al., 2007; Neidhardt et al., 2008). In other cases mutations in *RPGR* can lead to ocular phenotypes which are clearly distinct from RP. For instance mutations in *RPGR* exon ORF15 can cause CORD (Mears et al., 2000; Demirci et al., 2002; Walia et al., 2008), COD (Pelletier et al., 2007), atrophic macular degeneration (Ayyagari et al., 2002) or RP and Coats'-like exudative vasculopathy (Demirci et al., 2006). Furthermore, non-ocular manifestations in syndromic phenotypes with RP have also been described. This includes primary ciliary dyskinesia (Moore et al., 2006) or hearing loss and infections of respiratory tract (Iannaccone et al., 2003; Zito et al., 2003). In summary, these findings implicate that the function of *RPGR* might not only be important for the retina, but is also needed in other tissues. It further raises the possibility that other factors may modify the phenotypic expression of the disease in patients with *RPGR* mutations.

The *RPGR* transcript is widely expressed in human tissues including retina, brain, lung, kidney and testis. Interestingly, many alternative transcript isoforms have been identified (Figure 8) demonstrating skipping of constitutive exons 14 and 15 together or usage of alternative exons 9a, 15a or 15b or parts of ORF15 (Kirschner et al., 1999; Vervoort et al., 2000; Neidhardt et al., 2007). However, the physiological functions of these alternative transcript isoforms are not completely understood.

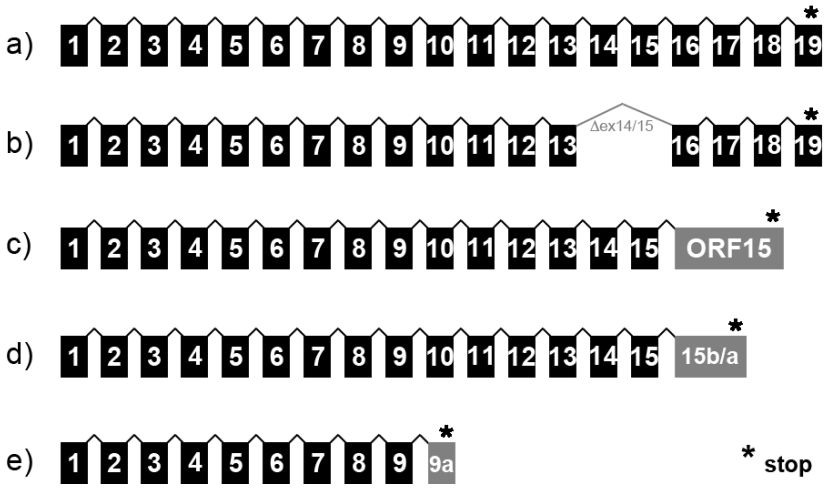

Figure 8 Schematic drawings of known *RPGR* transcript isoforms. Constitutive exons are labeled in black and alternatively used exons in gray. All alternative exons contain a stop codon (*) which truncates the protein. Thus, only the translated open reading frame of these transcripts is displayed. **a)** constitutive isoform (exons 1 to 19); **b)** transcript variant skipping exons 14 and 15; **c)** isoform containing exon ORF15; inclusion of either **d)** 15b or 15a or **e)** exon 9a.

Part of the RPGR protein encoded by exons 2 to 11 shows homology to a common domain found in the regulator of chromosome condensation (RCC1) and was designated RCC1-like domain (Meindl et al., 1996; Roepman et al., 1996b). RCC1 is a guanine nucleotide exchange factor (GEF) for Ran GTPases whose form has the structure of a seven-bladed propeller (Renault et al., 2001). Although, the RCC1-like domain in RPGR exhibits homology to GEFs, no such activity has been identified so far. However, a ciliary function has been proposed because of its colocalization to this cell organelle. It has been demonstrated that RPGR protein isoforms mainly locate in the connecting cilium and basal body of photoreceptors and to the tip and axoneme of sperm flagella (Shu et al., 2005; Khanna et al., 2005). Furthermore, male infertility was found in RPGR overexpressing mice (Brunner et al., 2008). Together these results might implicate that RPGR has an essential function in the cilium. Further evidence that RPGR is involved in cilia-specific processes has been acquired through binding studies which revealed interaction to other cilia-associated proteins e.g. RPGRIP, NPHP5, IFT88, CEP290, RPGRIPL and RAB8A (Boylan and Wright, 2000; Roepman et al., 2000; Otto et al., 2005; Chang et al., 2006; Khanna et al., 2009; Murga-Zamalloa et al., 2010).

1.2.3. Bardet-Biedl syndrome

Bardet-Biedl syndrome (BBS; OMIM 209900) is a multisystemic disorder, primarily caused by dysfunctions of cilia. The prevalence of BBS is about 1 in 120'000 individuals for all live births in North America and Europe (Blacque and Leroux, 2006). The main symptoms found in BBS patients are retinal degeneration, polydactyly, mental retardation, truncal obesity, genital and renal anomalies. Secondary features are also associated with the disease including speech disorders, developmental delay, hearing loss and situs inversus (Tobin and Beales, 2007). BBS is clinically diagnosed on the condition that either 4 primary or three primary and two secondary features are present in the patient (Beales et al., 1999). To date, mutations in 15 genes have been identified to be disease-causing (Zaghloul and Katsanis, 2009; Kim et al., 2010). These mutations account for 80% of all BBS cases and most of them are recessively inherited. Nevertheless, complex multiallelic inheritance has also been described for BBS (Katsanis et al., 2001; Beales et al., 2003; Fauser et al., 2003). Additionally, the disease phenotype in patients with BBS can be highly variable. For instance, it has been demonstrated that the gain of a third mutant allele at a second locus in BBS patients from the same family, increased severity of the disease compared to those having only two mutations at the same locus (Badano et al., 2003; Fan et al., 2004). Furthermore, mutations in BBS genes have been reported to lead to a non-syndromic RP phenotype (Aldahmesh et al., 2009; Riazuddin et al., 2010). In summary, these findings indicate that the total mutational load in these genes is mainly responsible for the variable phenotypic expression diagnosed in BBS.

Initially, Bardet-Biedl syndrome proteins 4 (BBS4) and 8 (BBS8) were found to localize to centriolar satellites and to the basal body of ciliated cells (Ansley et al., 2003; Kim et al., 2004). Interestingly, BBS4 can interact with the pericentriolar material 1 protein (PCM1) (Kim et al., 2004), which is important for centrosome integrity, microtubule organization (Dammermann and Merdes, 2002) and ciliogenesis (Mikule et al., 2007). Specific staining of BBS8 in mice revealed association to ciliary structures in spermatids, bronchial epithelial cells and to the photoreceptor connecting cilium (Ansley et al., 2003). In summary, these findings suggested that BBS4 and BBS8 function at the primary cilium. Moreover, BBS4 and BBS8 were found in a protein complex named the BBSome together with BBS1, BBS2, BBS5, BBS7, and BBS9 (Nachury et al., 2007). The complex might be transported through centriolar satellites to the basal body where it associates with the

ciliary membrane and interacts via BBS1 with the GEF Rabin8. Rabin8 activates the Rab8 GTPase which associates with post-Golgi vesicles and enters the primary cilium upon GTP loading (Nachury et al., 2007). It has been found that docking and fusion of rhodopsin containing membrane vesicles with the ciliary membrane depend on the function of Rab8 (Moritz et al., 2001). Supportively, loss of BBS proteins leads to rhodopsin mislocalization in mice (Nishimura et al., 2004; Mykytyn et al., 2004). It seems very likely that the BBSome is involved in rhodopsin transport to the connecting cilium. Furthermore, two different studies demonstrated that the BBSome is required for correct ciliary localization of leptin and G-coupled receptors (Berbari et al., 2008; Seo et al., 2009). Together, all these data suggest that the BBSome plays an important role in the vesicular trafficking of membrane proteins to the primary cilium. Consequently, disruptions in this vesicular transport process could affect the function of several tissues causing the different phenotypes associated with BBS.

1.3. Splicing of pre-mRNA transcripts

A typical eukaryotic gene contains protein coding sequences, called exons and non-coding sequences, called introns, which are arrayed alternately along the gene. Introns account for more than 90% of the primary transcript in humans (Wang and Burge, 2008). After transcription of the gene, introns have to be removed and exons joined together to produce a functional mRNA. Consensus sequences at 5'end, near to and at the 3' end of introns are required for the precise defininition of exon-intron boundaries (Figure 9A). These classical splice sites encompass the splice donor site (SD), the branch point sequence (BPS), the polypyrimidine tract and the splice acceptor site (SA). The chemical reactions essential for intron removal are two phosphoryl-transfer steps (Figure 9B). In the first step the 2' hydroxyl group of an Adenosine in the BPS attacks the phosphodiester bond between the nucleotides at the exon-intron boundary in the SD. This first transesterification reaction generates a free hydroxyl group at the 5' exon. This free 3' hydroxyl group at the 5' exon then attacks the phosphodiester at the exon intron boundary of the SA, which results in exon ligation and excision of the intron (Collins and Guthrie, 2000). These chemical reactions can occur spontaneously without additional need for energy and protein components. This has become evident when a type of intron was identified that could self-splice in vitro by absolutely identical transesterification reactions (Michel and Ferat, 1995).

Correct recognition of splice sites within a multitude of similar sequences and the establishment of the active splice complex which is a prerequisite to perform the two transesterification reactions, poses a challenge for the splicing machinery. Interactions of many RNA and protein components within a complex, designated the spliceosome, are needed to control the process of splicing. The spliceosomal components act through a multitude of RNA-RNA, RNA-protein and protein-protein interactions. Most important interactions between the degenerated sequences in classical splice sites and components of the spliceosome are weak. This implicates the necessity of *trans*-acting splicing factors to increase exon definition by binding to other sequences in the pre-mRNA (Wahl et al., 2009). In addition to these factors, many proteins have been identified that regulate the usage of specific splice sites. The mechanisms by which these regulatory proteins act on the pre-mRNA to influence splicing will be summarized in the next chapter about alternative splicing. In this chapter, the focus will be on the basic splicing process.

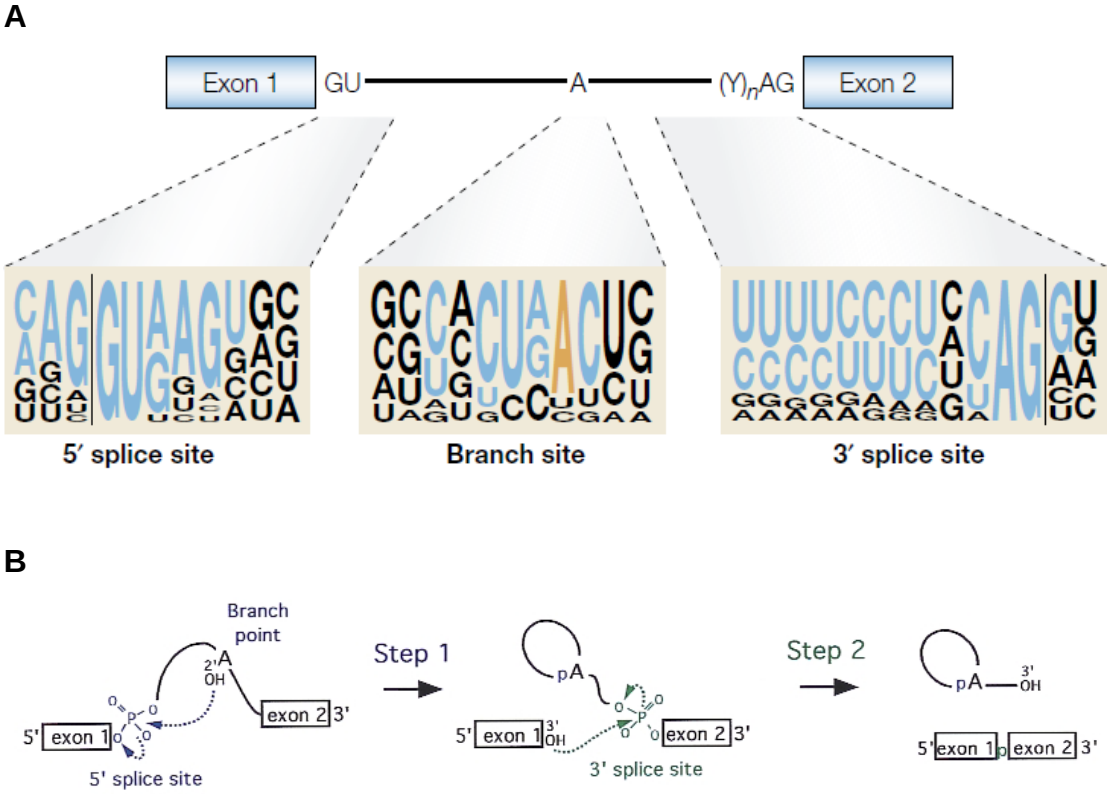

Figure 9. Classical splicing signals and chemical transesterification reactions involved in pre-mRNA splicing. **A** Degenerated sequence motifs found at the splice donor (5' splice site), branch site and splice acceptor (3' splice site) of human gene transcripts evaluated by the alignment of conserved sequences from 1'683 human introns. The size of a nucleotide at a given position is proportional to its conservation. Nucleotides which are part of the classical consensus are shown in blue, except for the branch point A nucleotide, which is coloured in orange. **B** Two step transesterification reactions resulting in excision of the intron form the pre-mRNA. Illustrations are taken from Collins and Guthrie (2000) and Cartegni (2002).

The splicing machinery features a highly dynamic structure, where different factors enter or exit during the splicing process. Furthermore, conformational changes in several spliceosomal subunits can be observed, which require chemical energy in the form of ATP and GTP. Together, this all ensures the time-controlled and accurate process of pre-mRNA splicing (Wahl et al., 2009). In general, the spliceosome comprises five main building blocks of uridine-rich small nuclear ribonucleoproteins (UsnRNP) termed U1, U2, U4/U6 and U5 snRNP which assemble stepwise on the pre-mRNA. An UsnRNP contains a snRNA (or two in case of U4/U6) and complex-specific proteins. All snRNPs, except U6, contain seven Sm proteins which bind to the highly conserved Sm sequence in the snRNA (Will and Luhrmann, 2001). Spliceosome assembly starts with binding of the U1 snRNP to the SD which is mediated through base-pairing interactions of the 5'end of the U1 snRNA to the 9 nucleotides spanning SD (Lund and Kjems, 2002). At the same time, the branch point binding protein (BBP) and the U2 auxiliary factor (U2AF) bind to the BPS, the polypyrimidine tract and the SA. These processes lead to the formation of the spliceosomal E complex. ATP-dependent base-pairing of the U2 snRNP with the BPS then causes dissociation of BBP building the A complex. Subsequently, the heterotrimeric complex preassembled from U4/U6 and U5 snRNPs, termed U4/U6.U5 tri-snRNP is recruited to form the B complex. After dissociation of U1 and U4 this complex becomes activated and the spliceosome undergoes the first catalytic step of splicing which generates the C complex. After spliceosomal rearrangements and performance of the second catalytic step, spliceosomal components dissociate from the mRNA (Wahl et al., 2009). The mRNA is then transported through the nuclear pore into the cytoplasm where it serves as template for protein synthesis.

1.3.1. Alternative splicing

Human proteins can exist in many different isoforms which mainly arise from alternative splicing of the same pre-mRNA transcript (Black, 2000). Alternative splicing is regulated often in a tissue- or developmental stage-dependent fashion and thus contributes to the complexity of multi-cellular organisms.

It is now clear that more than 90% of all human genes are alternatively spliced (Wang et al., 2008). Alternative transcript isoforms may arise through five major mechanisms in most eukaryotes, but their utilization are species dependent (Figure 10). In human and mice, skipping of constitutive exons accounts for 38% of all alternative splicing

events. Another mechanism involves the usage of alternative SDs or SAs and is responsible for 18% and 8%, respectively. Furthermore, retention of the intron can be detected in 3% of alternatively spliced transcripts. The remaining 33% may include mutually exclusive events, the usage of alternative transcription start sites and multiple polyadenylation sites (Ast, 2004).

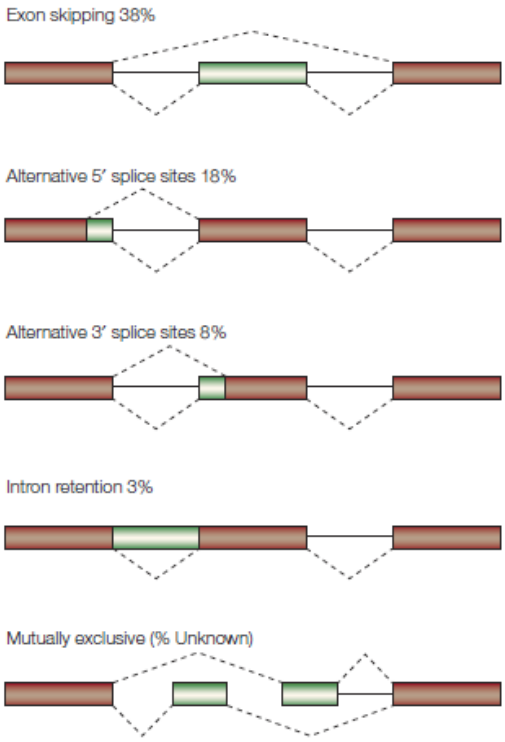

Figure 10 Alternative splicing of the pre-mRNA results in 5 major classes of spliced products. Constitutively used exons are labeled in red. Regions in the pre-mRNA transcript which are alternatively spliced are shown in green. Dashed lines represent different splice events whereas solid lines represent introns. The frequency of each splicing event in accordance to all alternative splicing events is given in percentages. Figure taken from Ast (2004).

Recognition of exons and introns is performed by the interaction of spliceosomal subunits with classical splice sites, as described above in detail. In mammals, the SD and SA are predominantly recognized in pairs across exons by a process called exon definition. However, the core splicing signals at the SD, SA and BPS are degenerated making interactions between the spliceosome and these core splice signals weak. It is assumed that these sequences account for only half of the information needed to define the boarders of the exon (Wang and Burge, 2008). As a consequence, there must be other splicing factors that guide the spliceosome to its target. These factors act in *trans* by binding to *cis*-regulatory elements and mainly control spliceosome assembly. The splicing regulatory elements (SRE) in exons are classified into either negative or positive regulators called, exonic splicing enhancer (ESE) or silencer (ESS). If they are found in introns they are named intronic splicing enhancer (ISE) or silencer (ISS). ESEs are predominantly found in constitutive exons and bound by serine/arginine (SR) proteins through their RNA recognition motiv. SR proteins

enhance splicing of its exon by facilitating spliceosome assembly. On the other hand, ESSs often recruit proteins from the class of heterogenous nuclear ribonucleoproteins (hnRNPs). Proteins in this group contain one or more RNA-binding domains and or glycine-rich motifs that can block the splicing process. The hnRNPs inhibit splicing either by blocking essential interactions of spliceosomal subunits or by occupying classical splice sites. In a few cases intronic SREs have also been identified, but many of them remain to be discovered (Wang and Burge, 2008). Because intronic regions that flank alternatively spliced exons are more conserved compared to constitutive exons, it is presumed that intronic *cis*-regulatory elements are more important for the regulation of alternative exon usage (Ast, 2004). Splicing enhancers and silencers often act additively by increasing their effect with the amount of additional copies (Wang and Burge, 2008). All together, the integration of all signals from classical splice sites and SREs will finally determine whether the exon is skipped or included into the transcript.

1.3.2. Splicing and disease

Mutations in classical splice sites reduce interactions of spliceosomal components with the pre-mRNA. As a consequence, the lower binding affinity of general splicing factors leads to impaired exon definition and finally to aberrant splicing of the transcript. Initially, it has been estimated that about 15% of all disease causing point mutations lay in classical splice sites. Many other mutations have been identified so far that are not within classical splice sites, but also disrupt the splicing process. Together, it has been proposed to date that 60% of all point mutations have their major pathogenic effect through impaired pre-mRNA splicing (Wang and Cooper, 2007). Interestingly, mutations identified in the Versican (VCAN) gene cause Wagner disease, by inducing missplicing of the transcript (Miyamoto et al., 2005; Kloeckener-Gruissem et al., 2006; Mukhopadhyay et al., 2006; Ronan et al., 2009).

Mutations affecting splicing of gene transcripts can be classified into different groups depending on their localization and effect on splicing. Mutations that affect the gene in which they are localized are termed *cis*-acting mutations. These mutations can either affect the usage of constitutive or alternative exons. Impaired exon recognition through *cis*-acting mutations in classical splice sites can cause exon skipping, intron retention or activation of a pre-existing cryptic splice site, which is distal to the mutation. Many of these aberrantly spliced products contain a premature termination

codon (PTC) as a consequence of a shift in the open reading frame (Faustino and Cooper, 2003). Transcripts possessing a PTC are usually degraded through an RNA quality control mechanism termed nonsense-mediated mRNA decay (NMD). In mammals, this control mechanism is tightly bound to the splicing events in the pre-mRNA and is most efficient when the PTC resides more than 50-55 nucleotides upstream of the next exon-intron junction (Lejeune and Maquat, 2005). Because classical splice site mutations usually lead to transcript degradation by NMD, it is assumed that these mutations gain their pathogenic effect mainly through loss of the gene product. In contrast, it seems that *cis*-acting mutations affecting the usage of alternative splice sites are pathogenic because they shift the ratio of expressed transcript isoforms (Faustino and Cooper, 2003). Changes in splice patterns can have deleterious effects on the function of a gene which often leads to diseases. Especially, neurons seem to be highly susceptible to alterations in the expression of alternative isoforms (Dredge et al., 2001).

In contrast to defects in *cis*-acting splice sites, mutations in *trans* have also been identified and are considered to affect expression of a large number of different genes, rather than only one (Cooper et al., 2009). *Trans*-acting splicing factors that can be affected by mutations include components of the basal splicing machinery or genes that promote correct maturation of these components. A prominent example for mutations leading to a dysfunction of the basal splicing machinery is found in spinal muscular atrophy (SMA). Patients with SMA show degeneration of motor neurons. Deletions in the survival motor neuron 1 gene (*SMN1*) lead to a reduction of functional SMN proteins and are considered to be the primary cause for SMA. The SMN protein is part of a multimeric complex essential for spliceosomal snRNP assembly (Yong et al., 2004). In mice, SMN deficiency reveals global defects in pre-mRNA splicing which are most probably due to the impaired functions of immature snRNPs. These findings might help to further elucidate the pathogenic mechanisms in patients with SMA (Zhang et al., 2008). A second class of *trans*-acting splicing factors is involved in regulation of alternative splicing only (Faustino and Cooper, 2003). For instance, It has been found that the small nucleolar RNA HBII-52 regulates alternative splicing of the serotonin receptor 5-HT_{2C}R and its expression is lost in patients with Prader-Willi Syndrome (PWS). Alterations in splicing of the serotonin receptor have been detected as a consequence of the lack of HBII-52 which may lead to the disease (Kishore and Stamm, 2006). Recently, novel transcript targets of HBII-

52 have been identified that, when aberrantly spliced, may contribute to the pathogenesis in PWS patients (Kishore et al., 2010).

In addition, defects in the basal splicing machinery are also involved in the pathogenesis of autosomal dominant RP. Mutations in the common splicing factors *PRPF31*, *PRPF8*, *PRPF3* and *PAP1* have been identified in RP patients. The proteins are all components of the basal splicing machinery and are crucial for the formation of the U4/U6.U5 tri-snRNP and for general assembly of several spliceosomal subunits. PRPF31 is part of the U4/U6 snRNP and is directly involved in the formation of the tri-snRNP by binding to the U4 snRNA. Furthermore, it is assumed to mediate the recruitment of the tri-snRNP into the spliceosome. Like PRPF31, PRPF3 is also a component of the U4/U6 snRNP and may recruit other factors necessary for correct assembly. A subunit of the tri-snRNP is PAP1, which interacts with other splicing factors that perform the early steps of spliceosome assembly (Mordes et al., 2006). PRPF8 is a core protein of the U5 snRNP and presumed to control spliceosome activity during the splice process (Wahl et al., 2009).

It still remains an open question why mutations in these widely expressed splicing factors lead to a tissue-specific disease, such as RP. In lymphoblasts from patients with *PRPF31* null alleles, no specific effect on splicing was observed. In contrast, splice defects in different photoreceptor-specific transcripts were observed due to mutations in *PRPF31* (Yuan et al., 2005; Mordes et al., 2007). These findings support a model where the impaired functioning of spliceosomal components cannot sustain the high demand of photoreceptors for correctly spliced transcripts. As a consequence, lower amounts of these transcripts, derived for instance from the *RHO* gene, may subsequently promote cell death (Mordes et al., 2006).

1.3.3. Therapeutic approaches to treat splice defects

Defects in pre-mRNA splicing not only decrease the amount of functional transcripts, but can also lead to aberrant splicing products or a shift in the ratio of alternative transcript isoforms. All these defects may cause the disease by acting through distinct pathogenic mechanisms. In order to fully restore the splicing pattern, these findings implicate the necessity to increase normal transcript levels and to remove the presence of potentially toxic splicing products. Many different approaches have been established where the mutant pre-mRNA is the direct target of the therapeutic intervention (Figure 11).

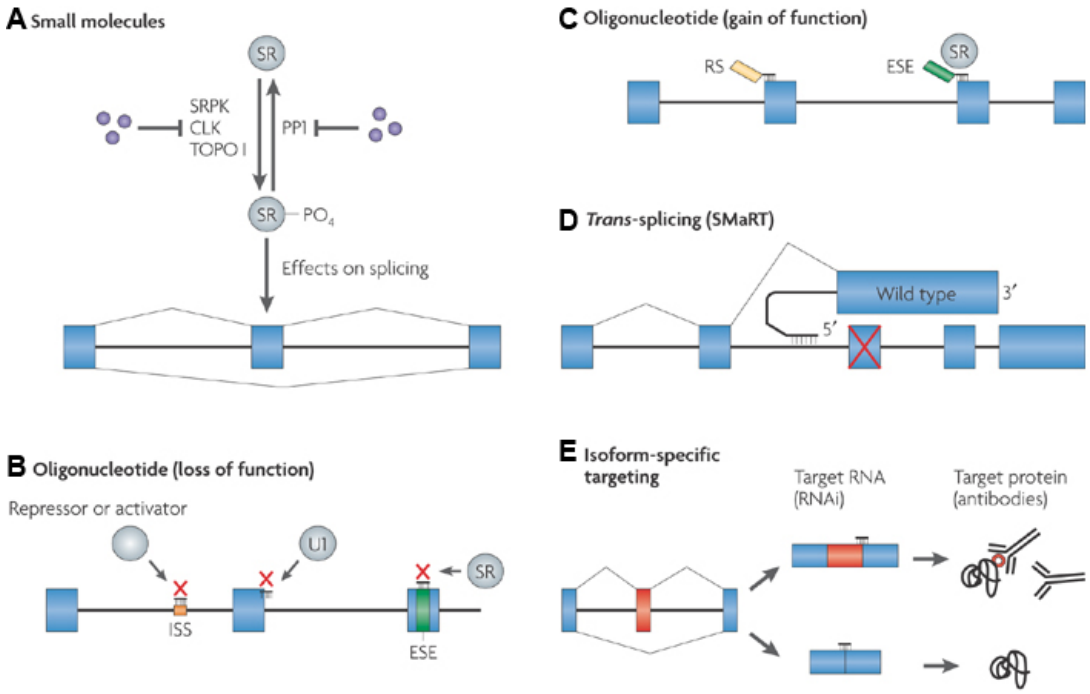

Figure 11 Overview of different therapeutic interventions to treat defects in pre-mRNA splicing. **A-E** Five approaches have been established using either: RNAs, antibodies or small molecules as the therapeutic agent. In spliceosome-mediated RNA *trans*-splicing (SMaRT) a mutated exon can be replaced by splicing with an artifical RNA template containing the wild-type cDNA sequence. Figure is adapted from Wang and Cooper (2007).

The amount of inclusion of a specific exon into the transcript can be modulated for instance by small pharmacological reagents that influence the activity state of certain splicing regulatory factors (Figure 11A). Another strategy for the treatment of splice defects is the usage of specific antisense oligonucleotides (AOs). These chemically modified nucleotides are designed with the aim to hybridize with a specific splice site on the transcript, where they can block binding of splicing factors. In most of the cases this will lead to skipping of the targeted exon, which is most favorable for loss of function approaches (Figure 11B). In gain of function approaches (Figure 11C) the AOs can be linked to an ESE which recruits SR proteins that enhance exon inclusion (Wang and Cooper, 2007). Although the AO approach appears to be successful in many model systems, the transcript accessibility may be difficult in some cases. The application of AO linked to a specific snRNA as U7 or U1 is an alternative approach. These snRNA-fused AOs assemble into mature snRNPs which often increase their nuclear localization, stability and hybridization to the mutant mRNA. Another approach that aims to reduce aberrantly spliced transcript variants or thereby derived aberrant proteins, uses RNA interference (RNAi) or specific antibodies, respectively (Figure 11E). The approach with RNAi appeared to be highly accurate in terms of

targeting specific splice isoforms. Several strategies have been established that either use synthetic double stranded small interfering RNAs, short hairpin RNAs or artificial micro RNAs (Cooper et al., 2009). Restoration of correctly spliced transcripts can also be achieved through combined splicing of two RNA molecules in *trans*, termed *trans*-splicing (Figure 11D) (Rodriguez-Martin et al., 2009; Fiskaa and Birgisdottir, 2010).
The group of Dr. John Neidhardt at the University of Zurich and other groups have established a therapeutic approach that uses a modified U1 snRNA. It has been previously shown that mutations in the splice donor site reduce interaction of the U1 snRNA at this position and thus lead to impaired recognition of the affected exon (Zhuang and Weiner, 1986). The strategy involves the adaptation of the U1 snRNA to the mutated splice site in order to restore normal binding affinities. Thereby, highly reduced levels of normal *RHO* transcripts which were induced by a splice donor site mutation, could be restored to more than 90% in minigene assays (Tanner et al., 2009). Recently, the adaptation of the U1 snRNA was used to restore normal splicing of endogenously expressed transcripts in patient fibroblasts (Hartmann et al., 2010; Glaus et al., 2011).

1.4. References General Introduction

1. Aldahmesh,M.A., Safieh,L.A., Alkuraya,H., Al-Rajhi,A., Shamseldin,H., Hashem,M., Alzahrani,F., Khan,A.O., Alqahtani,F., Rahbeeni,Z., Alowain,M., Khalak,H., Al-Hazzaa,S., Meyer,B.F., and Alkuraya,F.S. (2009). Molecular characterization of retinitis pigmentosa in Saudi Arabia. Mol. Vis. *15*, 2464-2469.

2. Ansley,S.J., Badano,J.L., Blacque,O.E., Hill,J., Hoskins,B.E., Leitch,C.C., Kim,J.C., Ross,A.J., Eichers,E.R., Teslovich,T.M., Mah,A.K., Johnsen,R.C., Cavender,J.C., Lewis,R.A., Leroux,M.R., Beales,P.L., and Katsanis,N. (2003). Basal body dysfunction is a likely cause of pleiotropic Bardet-Biedl syndrome. Nature *425*, 628-633.

3. Ast,G. (2004). How did alternative splicing evolve? Nat. Rev. Genet. *5*, 773-782.

4. Ayyagari,R., Demirci,F.Y., Liu,J., Bingham,E.L., Stringham,H., Kakuk,L.E., Boehnke,M., Gorin,M.B., Richards,J.E., and Sieving,P.A. (2002). X-linked recessive atrophic macular degeneration from RPGR mutation. Genomics *80*, 166-171.

5. Badano,J.L., Kim,J.C., Hoskins,B.E., Lewis,R.A., Ansley,S.J., Cutler,D.J., Castellan,C., Beales,P.L., Leroux,M.R., and Katsanis,N. (2003). Heterozygous mutations in BBS1, BBS2 and BBS6 have a potential epistatic effect on Bardet-Biedl patients with two mutations at a second BBS locus. Hum. Mol. Genet. *12*, 1651-1659.

6. Banin,E., Mizrahi-Meissonnier,L., Neis,R., Silverstein,S., Magyar,I., Abeliovich,D., Roepman,R., Berger,W., Rosenberg,T., and Sharon,D. (2007). A non-ancestral RPGR missense mutation in families with either recessive or semi-dominant X-linked retinitis pigmentosa. Am. J. Med. Genet. A *143A*, 1150-1158.

7. Beales,P.L., Badano,J.L., Ross,A.J., Ansley,S.J., Hoskins,B.E., Kirsten,B., Mein,C.A., Froguel,P., Scambler,P.J., Lewis,R.A., Lupski,J.R., and Katsanis,N. (2003). Genetic interaction of BBS1 mutations with alleles at other BBS loci can result in non-Mendelian Bardet-Biedl syndrome. Am. J. Hum. Genet. *72*, 1187-1199.

8. Beales,P.L., Elcioglu,N., Woolf,A.S., Parker,D., and Flinter,F.A. (1999). New criteria for improved diagnosis of Bardet-Biedl syndrome: results of a population survey. J. Med. Genet. *36*, 437-446.

9. Berbari,N.F., Lewis,J.S., Bishop,G.A., Askwith,C.C., and Mykytyn,K. (2008). Bardet-Biedl syndrome proteins are required for the localization of G protein-coupled receptors to primary cilia. Proc. Natl. Acad. Sci. U. S. A *105*, 4242-4246.

10. Berger,W., Kloeckener-Gruissem,B., and Neidhardt,J. (2010). The molecular basis of human retinal and vitreoretinal diseases. Prog. Retin. Eye Res. *29*, 335-375.

11. Bhowmick,R., Li,M., Sun,J., Baker,S.A., Insinna,C., and Besharse,J.C. (2009). Photoreceptor IFT complexes containing chaperones, guanylyl cyclase 1 and rhodopsin. Traffic. *10*, 648-663.

12. Black,D.L. (2000). Protein diversity from alternative splicing: a challenge for bioinformatics and post-genome biology. Cell *103*, 367-370.

13. Blacque,O.E. and Leroux,M.R. (2006). Bardet-Biedl syndrome: an emerging pathomechanism of intracellular transport. Cell Mol. Life Sci. *63*, 2145-2161.

14. Blanks,J.C. (2001). Morphology and Topography of the Retina. In RETINA, S.J.Ryan, ed. Mosby), pp. 32-49.

15. Boylan,J.P. and Wright,A.F. (2000). Identification of a novel protein interacting with RPGR. Hum. Mol. Genet. *9*, 2085-2093.

16. Brunner,S., Colman,D., Travis,A.J., Luhmann,U.F., Shi,W., Feil,S., Imsand,C., Nelson,J., Grimm,C., Rulicke,T., Fundele,R., Neidhardt,J., and Berger,W. (2008). Overexpression of RPGR leads to male infertility in mice due to defects in flagellar assembly. Biol. Reprod. *79*, 608-617.

17. Calvert,P.D., Strissel,K.J., Schiesser,W.E., Pugh,E.N., Jr., and Arshavsky,V.Y. (2006). Light-driven translocation of signaling proteins in vertebrate photoreceptors. Trends Cell Biol. *16*, 560-568.

18. Cartegni,L., Chew,S.L., and Krainer,A.R. (2002). Listening to silence and understanding nonsense: exonic mutations that affect splicing. Nat. Rev. Genet. *3*, 285-298.

19. Chang,B., Khanna,H., Hawes,N., Jimeno,D., He,S., Lillo,C., Parapuram,S.K., Cheng,H., Scott,A., Hurd,R.E., Sayer,J.A., Otto,E.A., Attanasio,M., O'Toole,J.F., Jin,G., Shou,C., Hildebrandt,F., Williams,D.S., Heckenlively,J.R., and Swaroop,A. (2006). In-frame deletion in a novel centrosomal/ciliary protein CEP290/NPHP6 perturbs its interaction with RPGR and results in early-onset retinal degeneration in the rd16 mouse. Hum. Mol. Genet. *15*, 1847-1857.

20. Collins,C.A. and Guthrie,C. (2000). The question remains: is the spliceosome a ribozyme? Nat. Struct. Biol. *7*, 850-854.

21. Cooper,T.A., Wan,L., and Dreyfuss,G. (2009). RNA and disease. Cell *136*, 777-793.

22. Dammermann,A. and Merdes,A. (2002). Assembly of centrosomal proteins and microtubule organization depends on PCM-1. J. Cell Biol. *159*, 255-266.

23. Demirci,F.Y., Rigatti,B.W., Mah,T.S., and Gorin,M.B. (2006). A novel RPGR exon ORF15 mutation in a family with X-linked retinitis pigmentosa and Coats'-like exudative vasculopathy. Am. J. Ophthalmol. *141*, 208-210.

24. Demirci,F.Y., Rigatti,B.W., Wen,G., Radak,A.L., Mah,T.S., Baic,C.L., Traboulsi,E.I., Alitalo,T., Ramser,J., and Gorin,M.B. (2002). X-linked cone-rod dystrophy (locus COD1): identification of mutations in RPGR exon ORF15. Am. J. Hum. Genet. *70*, 1049-1053.

25. Dredge,B.K., Polydorides,A.D., and Darnell,R.B. (2001). The splice of life: alternative splicing and neurological disease. Nat. Rev. Neurosci. *2*, 43-50.

26. Fan,Y., Esmail,M.A., Ansley,S.J., Blacque,O.E., Boroevich,K., Ross,A.J., Moore,S.J., Badano,J.L., May-Simera,H., Compton,D.S., Green,J.S., Lewis,R.A., van Haelst,M.M., Parfrey,P.S., Baillie,D.L., Beales,P.L., Katsanis,N., Davidson,W.S., and Leroux,M.R. (2004). Mutations in a member of the Ras superfamily of small GTP-binding proteins causes Bardet-Biedl syndrome. Nat. Genet. *36*, 989-993.

27. Fauser,S., Munz,M., and Besch,D. (2003). Further support for digenic inheritance in Bardet-Biedl syndrome. J. Med. Genet. *40*, e104.

28. Faustino,N.A. and Cooper,T.A. (2003). Pre-mRNA splicing and human disease. Genes Dev. *17*, 419-437.

29. Fiskaa,T. and Birgisdottir,A.B. (2010). RNA reprogramming and repair based on trans-splicing group I ribozymes. N. Biotechnol. *27*, 194-203.

30. Glaus,E., Schmid,F., Da,C.R., Berger,W., and Neidhardt,J. (2011). Gene Therapeutic Approach Using Mutation-adapted U1 snRNA to Correct a RPGR Splice Defect in Patient-derived Cells. Mol. Ther.

31. Hamel,C. (2006). Retinitis pigmentosa. Orphanet. J. Rare. Dis. *1*, 40.

32. Hartmann,L., Neveling,K., Borkens,S., Schneider,H., Freund,M., Grassman,E., Theiss,S., Wawer,A., Burdach,S., Auerbach,A.D., Schindler,D., Hanenberg,H., and Schaal,H. (2010). Correct mRNA Processing at a Mutant TT Splice Donor in FANCC Ameliorates the Clinical Phenotype in Patients and Is Enhanced by Delivery of Suppressor U1 snRNAs. Am. J. Hum. Genet. *87*, 480-493.

33. Hartong,D.T., Berson,E.L., and Dryja,T.P. (2006). Retinitis pigmentosa. Lancet *368*, 1795-1809.

34. Iannaccone,A., Breuer,D.K., Wang,X.F., Kuo,S.F., Normando,E.M., Filippova,E., Baldi,A., Hiriyanna,S., MacDonald,C.B., Baldi,F., Cosgrove,D., Morton,C.C., Swaroop,A., and Jablonski,M.M. (2003). Clinical and immunohistochemical evidence for an X linked retinitis pigmentosa syndrome with recurrent infections and hearing loss in association with an RPGR mutation. J. Med. Genet. *40*, e118.

35. Insinna,C. and Besharse,J.C. (2008). Intraflagellar transport and the sensory outer segment of vertebrate photoreceptors. Dev. Dyn. *237*, 1982-1992.

36. Kajiwara,K., Berson,E.L., and Dryja,T.P. (1994). Digenic retinitis pigmentosa due to mutations at the unlinked peripherin/RDS and ROM1 loci. Science *264*, 1604-1608.

37. Katsanis,N., Ansley,S.J., Badano,J.L., Eichers,E.R., Lewis,R.A., Hoskins,B.E., Scambler,P.J., Davidson,W.S., Beales,P.L., and Lupski,J.R. (2001). Triallelic inheritance in Bardet-Biedl syndrome, a Mendelian recessive disorder. Science *293*, 2256-2259.

38. Kennedy,B. and Malicki,J. (2009). What drives cell morphogenesis: a look inside the vertebrate photoreceptor. Dev. Dyn. *238*, 2115-2138.

39. Khanna,H., Davis,E.E., Murga-Zamalloa,C.A., Estrada-Cuzcano,A., Lopez,I., den Hollander,A.I., Zonneveld,M.N., Othman,M.I., Waseem,N., Chakarova,C.F., Maubaret,C., Diaz-Font,A., MacDonald,I., Muzny,D.M., Wheeler,D.A., Morgan,M., Lewis,L.R., Logan,C.V., Tan,P.L., Beer,M.A., Inglehearn,C.F., Lewis,R.A., Jacobson,S.G., Bergmann,C., Beales,P.L., Attie-Bitach,T., Johnson,C.A., Otto,E.A., Bhattacharya,S.S., Hildebrandt,F., Gibbs,R.A., Koenekoop,R.K., Swaroop,A., and Katsanis,N. (2009). A common allele in RPGRIP1L is a modifier of retinal degeneration in ciliopathies. Nat. Genet. *41*, 739-745.

40. Khanna,H., Hurd,T.W., Lillo,C., Shu,X., Parapuram,S.K., He,S., Akimoto,M., Wright,A.F., Margolis,B., Williams,D.S., and Swaroop,A. (2005). RPGR-ORF15, which is mutated in retinitis pigmentosa, associates with SMC1, SMC3, and microtubule transport proteins. J. Biol. Chem. *280*, 33580-33587.

41. Kim,J.C., Badano,J.L., Sibold,S., Esmail,M.A., Hill,J., Hoskins,B.E., Leitch,C.C., Venner,K., Ansley,S.J., Ross,A.J., Leroux,M.R., Katsanis,N., and Beales,P.L. (2004). The Bardet-Biedl protein BBS4 targets cargo to the pericentriolar region and is required for microtubule anchoring and cell cycle progression. Nat. Genet. *36*, 462-470.

42. Kim,S.K., Shindo,A., Park,T.J., Oh,E.C., Ghosh,S., Gray,R.S., Lewis,R.A., Johnson,C.A., Attie-Bittach,T., Katsanis,N., and Wallingford,J.B. (2010). Planar cell polarity acts through septins to control collective cell movement and ciliogenesis. Science *329*, 1337-1340.

43. Kirschner,R., Rosenberg,T., Schultz-Heienbrok,R., Lenzner,S., Feil,S., Roepman,R., Cremers,F.P., Ropers,H.H., and Berger,W. (1999). RPGR transcription studies in mouse and human tissues reveal a retina-specific isoform that is disrupted in a patient with X-linked retinitis pigmentosa. Hum. Mol. Genet. *8*, 1571-1578.

44. Kishore,S., Khanna,A., Zhang,Z., Hui,J., Balwierz,P.J., Stefan,M., Beach,C., Nicholls,R.D., Zavolan,M., and Stamm,S. (2010). The snoRNA MBII-52 (SNORD 115) is processed into smaller RNAs and regulates alternative splicing. Hum. Mol. Genet. *19*, 1153-1164.

45. Kishore,S. and Stamm,S. (2006). The snoRNA HBII-52 regulates alternative splicing of the serotonin receptor 2C. Science *311*, 230-232.

46. Kloeckener-Gruissem,B., Bartholdi,D., Abdou,M.T., Zimmermann,D.R., and Berger,W. (2006). Identification of the genetic defect in the original Wagner syndrome family. Mol. Vis. *12*, 350-355.

47. Lamb,T.D. and Pugh,E.N., Jr. (2004). Dark adaptation and the retinoid cycle of vision. Prog. Retin. Eye Res. *23*, 307-380.

48. Lejeune,F. and Maquat,L.E. (2005). Mechanistic links between nonsense-mediated mRNA decay and pre-mRNA splicing in mammalian cells. Curr. Opin. Cell Biol. *17*, 309-315.

49. Lund,M. and Kjems,J. (2002). Defining a 5' splice site by functional selection in the presence and absence of U1 snRNA 5' end. RNA. *8*, 166-179.

50. Marszalek,J.R., Liu,X., Roberts,E.A., Chui,D., Marth,J.D., Williams,D.S., and Goldstein,L.S. (2000). Genetic evidence for selective transport of opsin and arrestin by kinesin-II in mammalian photoreceptors. Cell *102*, 175-187.

51. Mears,A.J., Hiriyanna,S., Vervoort,R., Yashar,B., Gieser,L., Fahrner,S., Daiger,S.P., Heckenlively,J.R., Sieving,P.A., Wright,A.F., and Swaroop,A. (2000). Remapping of the RP15 locus for X-linked cone-rod degeneration to Xp11.4-p21.1, and identification of a de novo insertion in the RPGR exon ORF15. Am. J. Hum. Genet. *67*, 1000-1003.

52. Meindl,A., Dry,K., Herrmann,K., Manson,F., Ciccodicola,A., Edgar,A., Carvalho,M.R., Achatz,H., Hellebrand,H., Lennon,A., Migliaccio,C., Porter,K., Zrenner,E., Bird,A., Jay,M., Lorenz,B., Wittwer,B., D'Urso,M., Meitinger,T., and Wright,A. (1996). A gene (RPGR) with homology to the RCC1 guanine nucleotide exchange factor is mutated in X-linked retinitis pigmentosa (RP3). Nat. Genet. *13*, 35-42.

53. Michel,F. and Ferat,J.L. (1995). Structure and activities of group II introns. Annu. Rev. Biochem. *64*, 435-461.

54. Mikule,K., Delaval,B., Kaldis,P., Jurcyzk,A., Hergert,P., and Doxsey,S. (2007). Loss of centrosome integrity induces p38-p53-p21-dependent G1-S arrest. Nat. Cell Biol. *9*, 160-170.

55. Miyamoto,T., Inoue,H., Sakamoto,Y., Kudo,E., Naito,T., Mikawa,T., Mikawa,Y., Isashiki,Y., Osabe,D., Shinohara,S., Shiota,H., and Itakura,M. (2005). Identification of a novel splice site mutation of the CSPG2 gene in a Japanese family with Wagner syndrome. Invest Ophthalmol. Vis. Sci. *46*, 2726-2735.

56. Moore,A., Escudier,E., Roger,G., Tamalet,A., Pelosse,B., Marlin,S., Clement,A., Geremek,M., Delaisi,B., Bridoux,A.M., Coste,A., Witt,M., Duriez,B., and Amselem,S. (2006). RPGR is mutated in patients with a complex X linked phenotype combining primary ciliary dyskinesia and retinitis pigmentosa. J. Med. Genet. *43*, 326-333.

57. Mordes,D., Luo,X., Kar,A., Kuo,D., Xu,L., Fushimi,K., Yu,G., Sternberg,P., Jr., and Wu,J.Y. (2006). Pre-mRNA splicing and retinitis pigmentosa. Mol. Vis. *12*, 1259-1271.

58. Mordes,D., Yuan,L., Xu,L., Kawada,M., Molday,R.S., and Wu,J.Y. (2007). Identification of photoreceptor genes affected by PRPF31 mutations associated with autosomal dominant retinitis pigmentosa. Neurobiol. Dis. *26*, 291-300.

59. Moritz,O.L., Tam,B.M., Hurd,L.L., Peranen,J., Deretic,D., and Papermaster,D.S. (2001). Mutant rab8 Impairs docking and fusion of rhodopsin-bearing post-Golgi membranes and causes cell death of transgenic Xenopus rods. Mol. Biol. Cell *12*, 2341-2351.

60. Mukhopadhyay,A., Nikopoulos,K., Maugeri,A., de Brouwer,A.P., van Nouhuys,C.E., Boon,C.J., Perveen,R., Zegers,H.A., Wittebol-Post,D., van den Biesen,P.R., van der Velde-Visser SD, Brunner,H.G., Black,G.C., Hoyng,C.B., and Cremers,F.P. (2006). Erosive vitreoretinopathy and wagner disease are caused by intronic mutations in CSPG2/Versican that result in an imbalance of splice variants. Invest Ophthalmol. Vis. Sci. *47*, 3565-3572.

61. Murga-Zamalloa,C.A., Atkins,S.J., Peranen,J., Swaroop,A., and Khanna,H. (2010). Interaction of retinitis pigmentosa GTPase regulator (RPGR) with RAB8A GTPase: implications for cilia dysfunction and photoreceptor degeneration. Hum. Mol. Genet. *19*, 3591-3598.

62. Mustafi,D., Engel,A.H., and Palczewski,K. (2009). Structure of cone photoreceptors. Prog. Retin. Eye Res. *28*, 289-302.

63. Mykytyn,K., Mullins,R.F., Andrews,M., Chiang,A.P., Swiderski,R.E., Yang,B., Braun,T., Casavant,T., Stone,E.M., and Sheffield,V.C. (2004). Bardet-Biedl syndrome type 4 (BBS4)-null mice implicate Bbs4 in flagella formation but not global cilia assembly. Proc. Natl. Acad. Sci. U. S. A *101*, 8664-8669.

64. Nachury,M.V., Loktev,A.V., Zhang,Q., Westlake,C.J., Peranen,J., Merdes,A., Slusarski,D.C., Scheller,R.H., Bazan,J.F., Sheffield,V.C., and Jackson,P.K. (2007). A core complex of BBS proteins cooperates with the GTPase Rab8 to promote ciliary membrane biogenesis. Cell *129*, 1201-1213.

65. Neidhardt,J., Glaus,E., Barthelmes,D., Zeitz,C., Fleischhauer,J., and Berger,W. (2007). Identification and characterization of a novel RPGR isoform in human retina. Hum. Mutat. *28*, 797-807.

66. Neidhardt,J., Glaus,E., Lorenz,B., Netzer,C., Li,Y., Schambeck,M., Wittmer,M., Feil,S., Kirschner-Schwabe,R., Rosenberg,T., Cremers,F.P., Bergen,A.A., Barthelmes,D., Baraki,H., Schmid,F., Tanner,G., Fleischhauer,J., Orth,U., Becker,C., Wegscheider,E., Nurnberg,G., Nurnberg,P., Bolz,H.J., Gal,A., and Berger,W. (2008). Identification of novel mutations in X-linked retinitis pigmentosa families and implications for diagnostic testing. Mol. Vis. *14*, 1081-1093.

67. Newman,E.A. (2001). Glia of the Retina. In RETINA, S.J.Ryan, ed. Mosby), pp. 89-103.

68. Nickle,B. and Robinson,P.R. (2007). The opsins of the vertebrate retina: insights from structural, biochemical, and evolutionary studies. Cell Mol. Life Sci. *64*, 2917-2932.

69. Nishimura,D.Y., Fath,M., Mullins,R.F., Searby,C., Andrews,M., Davis,R., Andorf,J.L., Mykytyn,K., Swiderski,R.E., Yang,B., Carmi,R., Stone,E.M., and Sheffield,V.C. (2004). Bbs2-null mice have neurosensory deficits, a defect in social dominance, and retinopathy associated with mislocalization of rhodopsin. Proc. Natl. Acad. Sci. U. S. A *101*, 16588-16593.

70. Otto,E.A., Loeys,B., Khanna,H., Hellemans,J., Sudbrak,R., Fan,S., Muerb,U., O'Toole,J.F., Helou,J., Attanasio,M., Utsch,B., Sayer,J.A., Lillo,C., Jimeno,D., Coucke,P., De,P.A., Reinhardt,R., Klages,S., Tsuda,M., Kawakami,I., Kusakabe,T., Omran,H., Imm,A., Tippens,M., Raymond,P.A., Hill,J., Beales,P., He,S., Kispert,A., Margolis,B., Williams,D.S., Swaroop,A., and Hildebrandt,F. (2005). Nephrocystin-5, a ciliary IQ domain protein, is mutated in Senior-Loken syndrome and interacts with RPGR and calmodulin. Nat. Genet. *37*, 282-288.

71. Pazour,G.J., Baker,S.A., Deane,J.A., Cole,D.G., Dickert,B.L., Rosenbaum,J.L., Witman,G.B., and Besharse,J.C. (2002). The intraflagellar transport protein, IFT88, is essential for vertebrate photoreceptor assembly and maintenance. J. Cell Biol. *157*, 103-113.

72. Pazour,G.J. and Rosenbaum,J.L. (2002). Intraflagellar transport and cilia-dependent diseases. Trends Cell Biol. *12*, 551-555.

73. Pelletier,V., Jambou,M., Delphin,N., Zinovieva,E., Stum,M., Gigarel,N., Dollfus,H., Hamel,C., Toutain,A., Dufier,J.L., Roche,O., Munnich,A., Bonnefont,J.P., Kaplan,J., and Rozet,J.M. (2007). Comprehensive survey of mutations in RP2 and RPGR in patients affected with distinct retinal dystrophies: genotype-phenotype correlations and impact on genetic counseling. Hum. Mutat. *28*, 81-91.

74. Renault,L., Kuhlmann,J., Henkel,A., and Wittinghofer,A. (2001). Structural basis for guanine nucleotide exchange on Ran by the regulator of chromosome condensation (RCC1). Cell *105*, 245-255.

75. Riazuddin,S.A., Iqbal,M., Wang,Y., Masuda,T., Chen,Y., Bowne,S., Sullivan,L.S., Waseem,N.H., Bhattacharya,S., Daiger,S.P., Zhang,K., Khan,S.N., Riazuddin,S., Hejtmancik,J.F., Sieving,P.A., Zack,D.J., and Katsanis,N. (2010). A splice-site mutation in a retina-specific exon of BBS8 causes nonsyndromic retinitis pigmentosa. Am. J. Hum. Genet. *86*, 805-812.

76. Rodriguez-Martin,T., Anthony,K., Garcia-Blanco,M.A., Mansfield,S.G., Anderton,B.H., and Gallo,J.M. (2009). Correction of tau mis-splicing caused by FTDP-17 MAPT mutations by spliceosome-mediated RNA trans-splicing. Hum. Mol. Genet. *18*, 3266-3273.

77. Roepman,R., Bauer,D., Rosenberg,T., van Duijnhoven,G., van,d., V, Platzer,M., Rosenthal,A., Ropers,H.H., Cremers,F.P., and Berger,W. (1996a). Identification of a gene disrupted by a microdeletion in a patient with X-linked retinitis pigmentosa (XLRP). Hum. Mol. Genet. *5*, 827-833.

78. Roepman,R., Bernoud-Hubac,N., Schick,D.E., Maugeri,A., Berger,W., Ropers,H.H., Cremers,F.P., and Ferreira,P.A. (2000). The retinitis pigmentosa GTPase regulator (RPGR) interacts with novel transport-like proteins in the outer segments of rod photoreceptors. Hum. Mol. Genet. *9*, 2095-2105.

79. Roepman,R., van Duijnhoven,G., Rosenberg,T., Pinckers,A.J., Bleeker-Wagemakers,L.M., Bergen,A.A., Post,J., Beck,A., Reinhardt,R., Ropers,H.H., Cremers,F.P., and Berger,W. (1996b). Positional cloning of the gene for X-linked retinitis pigmentosa 3: homology with the guanine-nucleotide-exchange factor RCC1. Hum. Mol. Genet. *5*, 1035-1041.

80. Ronan,S.M., Tran-Viet,K.N., Burner,E.L., Metlapally,R., Toth,C.A., and Young,T.L. (2009). Mutational hot spot potential of a novel base pair mutation of the CSPG2 gene in a family with Wagner syndrome. Arch. Ophthalmol. *127*, 1511-1519.

81. Rosenbaum,J.L. and Witman,G.B. (2002). Intraflagellar transport. Nat. Rev. Mol. Cell Biol. *3*, 813-825.

82. Rozet,J.M., Perrault,I., Gigarel,N., Souied,E., Ghazi,I., Gerber,S., Dufier,J.L., Munnich,A., and Kaplan,J. (2002). Dominant X linked retinitis pigmentosa is frequently accounted for by truncating mutations in exon ORF15 of the RPGR gene. J. Med. Genet. *39*, 284-285.

83. Satir,P. and Christensen,S.T. (2007). Overview of structure and function of mammalian cilia. Annu. Rev. Physiol *69*, 377-400.

84. Seo,S., Guo,D.F., Bugge,K., Morgan,D.A., Rahmouni,K., and Sheffield,V.C. (2009). Requirement of Bardet-Biedl syndrome proteins for leptin receptor signaling. Hum. Mol. Genet. *18*, 1323-1331.

85. Shu,X., Fry,A.M., Tulloch,B., Manson,F.D., Crabb,J.W., Khanna,H., Faragher,A.J., Lennon,A., He,S., Trojan,P., Giessl,A., Wolfrum,U., Vervoort,R., Swaroop,A., and Wright,A.F. (2005). RPGR ORF15 isoform co-localizes with RPGRIP1 at centrioles and basal bodies and interacts with nucleophosmin. Hum. Mol. Genet. *14*, 1183-1197.

86. Silverman,M.A. and Leroux,M.R. (2009). Intraflagellar transport and the generation of dynamic, structurally and functionally diverse cilia. Trends Cell Biol. *19*, 306-316.

87. Sung,C.H. and Chuang,J.Z. (2010). The cell biology of vision. J. Cell Biol. *190*, 953-963.

88. Tanner,G., Glaus,E., Barthelmes,D., Ader,M., Fleischhauer,J., Pagani,F., Berger,W., and Neidhardt,J. (2009). Therapeutic strategy to rescue mutation-

induced exon skipping in rhodopsin by adaptation of U1 snRNA. Hum. Mutat. *30*, 255-263.

89. Thumann,G. and Hinton,D.R. (2001). Cell Biology of the Retinal Pigment Epithelium. In RETINA, S.J.Ryan, ed. Mosby), pp. 104-121.

90. Tobin,J.L. and Beales,P.L. (2007). Bardet-Biedl syndrome: beyond the cilium. Pediatr. Nephrol. *22*, 926-936.

91. Vervoort,R., Lennon,A., Bird,A.C., Tulloch,B., Axton,R., Miano,M.G., Meindl,A., Meitinger,T., Ciccodicola,A., and Wright,A.F. (2000). Mutational hot spot within a new RPGR exon in X-linked retinitis pigmentosa. Nat. Genet. *25*, 462-466.

92. Wahl,M.C., Will,C.L., and Luhrmann,R. (2009). The spliceosome: design principles of a dynamic RNP machine. Cell *136*, 701-718.

93. Walia,S., Fishman,G.A., Swaroop,A., Branham,K.E., Lindeman,M., Othman,M., and Weleber,R.G. (2008). Discordant phenotypes in fraternal twins having an identical mutation in exon ORF15 of the RPGR gene. Arch. Ophthalmol. *126*, 379-384.

94. Wang,E.T., Sandberg,R., Luo,S., Khrebtukova,I., Zhang,L., Mayr,C., Kingsmore,S.F., Schroth,G.P., and Burge,C.B. (2008). Alternative isoform regulation in human tissue transcriptomes. Nature *456*, 470-476.

95. Wang,G.S. and Cooper,T.A. (2007). Splicing in disease: disruption of the splicing code and the decoding machinery. Nat. Rev. Genet. *8*, 749-761.

96. Wang,Z. and Burge,C.B. (2008). Splicing regulation: from a parts list of regulatory elements to an integrated splicing code. RNA. *14*, 802-813.

97. Will,C.L. and Luhrmann,R. (2001). Spliceosomal UsnRNP biogenesis, structure and function. Curr. Opin. Cell Biol. *13*, 290-301.

98. Yau,K.W. and Hardie,R.C. (2009). Phototransduction motifs and variations. Cell *139*, 246-264.

99. Yong,J., Wan,L., and Dreyfuss,G. (2004). Why do cells need an assembly machine for RNA-protein complexes? Trends Cell Biol. *14*, 226-232.

100. Yuan,L., Kawada,M., Havlioglu,N., Tang,H., and Wu,J.Y. (2005). Mutations in PRPF31 inhibit pre-mRNA splicing of rhodopsin gene and cause apoptosis of retinal cells. J. Neurosci. *25*, 748-757.

101. Zaghloul,N.A. and Katsanis,N. (2009). Mechanistic insights into Bardet-Biedl syndrome, a model ciliopathy. J. Clin. Invest *119*, 428-437.

102. Zhang,Z., Lotti,F., Dittmar,K., Younis,I., Wan,L., Kasim,M., and Dreyfuss,G. (2008). SMN deficiency causes tissue-specific perturbations in the repertoire of snRNAs and widespread defects in splicing. Cell *133*, 585-600.

103. Zhuang,Y. and Weiner,A.M. (1986). A compensatory base change in U1 snRNA suppresses a 5' splice site mutation. Cell *46*, 827-835.

104. Zito,I., Downes,S.M., Patel,R.J., Cheetham,M.E., Ebenezer,N.D., Jenkins,S.A., Bhattacharya,S.S., Webster,A.R., Holder,G.E., Bird,A.C., Bamiou,D.E., and Hardcastle,A.J. (2003). RPGR mutation associated with retinitis pigmentosa, impaired hearing, and sinorespiratory infections. J. Med. Genet. *40*, 609-615.

2. Aims of the thesis

1. Based on the findings that *RPGR* frequently undergoes alternative splicing and that mutations can cause variable phenotypes, we aimed to understand the contribution of *RPGR* splicing to the pathogenesis of several, clinically distinct phenotypes.

2. To analyze whether a therapeutic approach using an adapted U1 snRNA can correct endogenously expressed transcripts, we designed experiments to restore a splice defect induced by a *BBS1* splice donor site mutation in patient-derived fibroblasts.

3. Because the usage of an adapted U1 snRNA could interfere with mRNA splicing of other genes than the target, we investigated possible side effects caused by this treatment.

4. Given that an increase in the amount of correctly spliced *BBS1* transcripts could improve properties of cilia in fibroblasts from the patients, we aimed to identify genes which expression is regulated by the ciliary function of BBS1.

3. Results

3.1. Mutation- and tissue-specific alterations of *RPGR* transcripts

Fabian Schmid[1], Esther Glaus[1], Frans P.M. Cremers[2], Barbara Kloeckener-Gruissem[1,3], Wolfgang Berger[1], John Neidhardt[1*]

[1]Division of Medical Molecular Genetics and Gene Diagnostics, Institute of Medical Genetics, University of Zurich, Zurich, Switzerland

[2]Department of Human Genetics, Radboud University Nijmegen Medical Centre, Nijmegen, The Netherlands

[3]Department of Biology, ETH Zurich, Switzerland

* Corresponding author

Manuscript published in *IOVS*, March 2010, Vol 51, No 3, pp. 1628-1635

3.1.1. Abstract

The majority of patients with X chromosome-linked Retinitis pigmentosa (XlRP) carry mutations in the *RPGR* gene. We studied whether patients with *RPGR* mutations show additional splice defects that may interfere with *RPGR* properties.

Patient-derived cell lines with *RPGR* mutations were raised in suspension. To verify mutations, direct sequencing of PCR products was performed. Patient-specific alterations in *RPGR* splicing were analyzed by RT-PCR and confirmed by sequencing. Tissue-specific expression levels of *RPGR* splice variants were quantified by real-time PCR using pools of different human donor tissues.

We have analyzed splicing of *RPGR* in seven RP patient-derived lymphoblastoid cell lines carrying hemizygous *RPGR* mutations. In three patient cell lines, we identified and characterized splice defects that were present in addition to a mutation. These splice defects were likely to interfere with normal *RPGR* properties. Furthermore, we identified four novel *RPGR* transcripts, either containing a new exon termed 11a or skipping the constitutive exons 12, 14 or 15. Novel and known *RPGR* isoforms were found to be differentially regulated in several human tissues. In human retina, approximately 10% of *RPGR* transcripts are alternatively spliced between exons 9 and 15.

Our findings show that splicing of *RPGR* is precisely regulated in a tissue-dependent fashion and suggest that mutations in *RPGR* frequently interfere with the expression of alternative transcript isoforms. These results implicate the importance of *RPGR* transcript analysis in patients with RP. We further discuss *RPGR* splicing as a modifier of different disease phenotypes described in patients with XlRP.

3.1.2. Introduction

Retinitis pigmentosa (RP) is a clinically and genetically heterogeneous eye disorder leading to the degeneration of photoreceptors in the human retina. Most patients with RP exhibit difficulties in dark adaptation and night blindness in adolescence and loss of midperipheral vision in young adulthood. In general, the rod photoreceptors degenerate first, causing a loss of peripheral vision. During progression of the disease, cone photoreceptors may also die, which ultimately leads to loss of central vision and complete blindness (Hartong et al., 2006). The disease prevalence is about 1 in 3000 to 4000 people affecting more than 1.5 million worldwide. More than 35 RP-associated genes have been identified so far. Most of them have been reported to be involved in phototransduction, basic metabolic pathways, maintenance of photoreceptor morphology, transcripional regulation, or pre-mRNA splicing as reviewed by Kennan (2005).

The inheritance pattern of RP can either be autosomal recessive (arRP), autosomal dominant (adRP) or X-linked (XlRP). The latter is considered to cause the clinically severest form of RP. Approximately 60 to 70% of all X-linked families show mutations in the retinitis pigmentosa GTPase regulator (*RPGR*) gene (Breuer et al., 2002; Iannaccone et al., 2003). Here, the majority of mutations were found in the alternatively spliced exon ORF15, whereas exons 1 to 15 carry a minor portion of all *RPGR* mutations (Vervoort and Wright, 2002; Sharon et al., 2003; Pelletier et al., 2007; Neidhardt et al., 2008; Shu et al., 2008). A few mutations in exon 1 to 15 of *RPGR* have been associated with additional nonocular manifestations. In a family with XlRP described previously, two members displayed a complex phenotype combining primary ciliary dyskinesia (PCD) and retinitis pigmentosa. In this case, aberrant splicing of *RPGR* was found in nasal epithelial cells due to a 57 bp deletion in exon 6 (Moore et al., 2006). Additionally, a syndromic phenotype including RP, hearing defects and severe sinorespiratory infections has been associated with mutations either in *RPGR* exon 6 (Iannaccone et al., 2003) or exon 8 (Zito et al., 2003). These reports indicate that the function of the widely expressed *RPGR* is important not only for the retina but also for other tissues.

RPGR transcripts have been identified in several human tissues (e.g. retina, brain, lung, kidney, and testis) (Meindl et al., 1996; Roepman et al., 1996a; Kirschner et al., 1999). Moreover, transcript isoforms of *RPGR* have been described and occasionally found to be expressed in a tissue- or cell-type-specific manner. One of these

transcripts includes the alternative exon 15a (Kirschner et al., 1999) and another contains exon 15b (Vervoort et al., 2000). *RPGR* isoforms may also show skipping of constitutive exons (e.g. exon 14 and 15) (Kirschner et al., 1999). Transcripts containing the alternative exon 9a produce a truncated protein that is predominantly expressed in human cone photoreceptors (Neidhardt et al., 2007).

The effect of many *RPGR* mutations on protein structure has been predicted (Meindl et al., 1996; Roepman et al., 1996a; Roepman et al., 1996b; Kirschner et al., 1999; Vervoort et al., 2000; Vervoort and Wright, 2002; Neidhardt et al., 2008). However, as has been described for other genes, a large fraction of exonic mutations also leads to splice defects by disruption of constitutive and regulatory splice-relevant sequences (Wang and Cooper, 2007). Because mutation-induced alterations of splice patterns in *RPGR* may contribute to the pathogenic mechanism for RP (Fujita et al., 1997; Bauer et al., 1998; Dry et al., 1999; Demirci et al., 2004; Neidhardt et al., 2007), we analyzed the effect of different *RPGR* mutations on splicing. Four novel *RPGR* isoforms were identified that showed differential expression in several tissues. Our results suggest that *RPGR* splicing is part of the pathogenic mechanism underlying the complex disease of RP. This further raises the possibility that alterations in *RPGR* splicing act as modifiers of the disease expression.

3.1.3. Materials and Methods

Cell culture

Splicing of *RPGR* was analyzed in seven EBV-transformed lymphoblastoid cell lines (LCLs) which have been derived from blood of male patients with RP (Table 1) and an unaffected male control. Informed consent was obtained from each patient and unaffected control in this study. Additional family members were not available for further tests. LCLs were grown in RPMI 1640 medium (LabForce, Nunningen, Switzerland), 10 % FBS (LabForce), 1.1 % Penicillin-Streptomycin (LabForce), 1.3 % L-Gutamine (LabForce) at 37°C, 5% CO_2 by using 75 cm^2 cell culture flasks (Techno Plastic Products [TPP], Trasadingen, Switzerland). Between $8x10^6$ and $4x10^7$ cells were pelleted by centrifugation at 4°C with 2000 x g for 10 minutes. The pellets were washed with 1x DPBS (LabForce), snap frozen and stored at -80°C before extraction of DNA or RNA. To inhibit nonsense-mediated mRNA decay (NMD), $1x10^6$ cells/ml were incubated in 30µg/ml cycloheximide (Sigma-Aldrich, Schnelldorf, Germany) at 37°C, 5% CO_2 in 25cm^2 cell culture flasks (TPP) for 4h as previously described (Chatr-Aryamontri et al., 2004).

RNA extraction, cDNA synthesis and RT-PCRs

To extract total RNA from LCLs, the cells were disrupted using either QIAshredder columns (Qiagen, Hombrechtikon, Switzerland) or a rotor-stator homogenizer (Ultra-Turrax T8, IKA Analysetechnik GmbH, Germany). Subsequently, RNA was isolated with RNeasy Mini or Midi kits (Qiagen) according to the manufacturer's instructions. RNA quality was verified by the Agilent 2100 Bioanalyzer and the amount was determined by the NanoDrop photometer (ND-1000, Litau, Switzerland). One thousand ng of total RNA were randomly primed before reverse transcription by reverse transcriptase (Superscript III; Invitrogen, Basel, Switzerland) according to the manufacturer's protocol. To verify correct splicing of the *RPGR* transcripts, RT-PCR reactions were performed with 50 ng cDNA, as described previously (Neidhardt et al., 2007). Primers used in the RT-PCR assays are shown in Supplementary Table S1. RT-PCR products were confirmed by sequencing. Each RT-PCR experiment was replicated three times using RNA from independently grown LCL cells.

Quantitative real-time PCR of alternative *RPGR* transcript variants

Quantifications of *RPGR* transcript levels were performed by quantitative real-time PCR on HT 7900 TaqMan using Assay by Design MGB FAM-TAMRA labeled probes (Applied Biosystems, Rotkreuz, Switzerland). To study the expression of *RPGR* transcript isoforms in several tissues, total RNA from pools of different human donor tissues (brain: n=5, kidney: n=5, lung: n=3, retina: n=25 and testis: n=39) was purchased from Becton Dickinson (BD, Allschwil, Switzerland) or BioCat (Heidelberg, Germany). Three to four cDNA batches were independently generated and analyzed from each tissue.

We designed TaqMan probes to quantify exon/exon boundaries for each alternative *RPGR* transcript isoforms as well as a corresponding probe for the constitutive transcript. Probes specific to the constitutive transcript of *RPGR* were used as endogenous controls. Their comparability was tested following the manufacturer's instructions. Each quantification reaction was technically replicated at least 4 times and gave results with amplification curves starting between 25 and 30 cycles. Using equal amounts of cDNA per sample, Ct values of the constitutive transcript did not differ significantly between tissues (errors represent confidence intervals of 95%): retina 26.3 (+/- 0.86), brain 25.75 (+/- 1.45), lung 25.9 (+/- 0.37), kidney 26.53 (+/- 1.23), and testis 25.6 (+/- 1.49). The outcome was anayzed using the SDS 2.2 software (ABI). The expression levels of the tested tissues or LCLs were normalized to human retina or an unaffected male control, respectively. Confidence intervals (CIs) of 95% were calculated from 3 to 4 independently generated samples.

DNA purification and sequencing

RT-PCR products were gel-extracted using the QIAquick Gel Extraction Kit (Qiagen). Gel-purified DNA was either cloned into the pCRII-TOPO vector (Topo TA Cloning Kit Dual Promoter, Invitrogen) according to the manufacturer's instructions or sequenced directly. DNA from LCLs was extracted as previously described (Neidhardt et al., 2006). To identify or verify mutations in patient cell lines, exons of *RPGR* were amplified by PCR using HotFirePol and sequenced directly (Sequencing analyzer, model 3100, ABI). Mutations were designated according to the nomenclature provided by the human genome variation society (www.hgvs.org). The numbering of mutations refers to the human *RPGR* reference sequence NM_001034853 for cDNA or reference assembly NC_000023.9 (range: 38013367 to

38071732) for genomic DNA from the NCBI database. The potential effect of exonic mutations on exonic splicing enhancer (ESE) binding sites was analyzed using ESEfinder 3.0 (http://rulai.cshl.edu/cgi-bin/tools/ESE3/esefinder.cgi?process=home).

3.1.4 Results

We followed the hypothesis that splice defects frequently occur in addition to mutations found in *RPGR*. To detect splice defects, we established RT-PCR assays that allow analysis of *RPGR* transcripts and screened lymphoblastoid cell lines (LCLs) derived from seven male patients with RP affected by known hemizygous *RPGR* mutations (Table 1). The LCLs used were not preselected for possible splice defects.

Splice site mutation in *RPGR* intron 1

In patient cell line LCL 2616, RT-PCR amplification of exons 1 through 5 yielded no product (Fig. 1). In contrast, using primers that bind to exons 2 and 5 resulted in a fragment, although weaker compared to that of the unaffected control and other cell lines. Furthermore, RT-PCRs with primer combinations specific to downstream located exons confirmed that LCL 2616 shows reduced *RPGR* transcript amounts (Fig.1). These analyses suggested the presence of a mutation affecting normal transcript processing in this patient cell line. Indeed, a mutation at the first base of intron 1 (c.28+1G>A; Table 1) was present in LCL 2616. This mutation is expected to result in a splice defect. Although extensively assayed, we were not able to amplify splice products between exon 1 and 2. These results suggest defective splicing of *RPGR* because of the mutation c.28+1G>A leading to a reduced amount of transcripts. It further raises the possibility that translation of RPGR may start from exon 3, where the next in-frame start codon is located.

The novel *RPGR* exon 11a

We performed RT-PCR analyses of *RPGR* transcripts containing exons 11 through 15 in all patient cell lines listed in table 1. In LCL 4767 we detected an additional amplicon of approximately 700 bp in length by conventional RT-PCR (Fig. 2A). Sequencing revealed that this fragment includes a novel exon spliced between exons 11 and 12. It was thus termed exon 11a. It contains 160 nucleotides and starts 1’139 bp downstream of the splice donor site of exon 11 (Fig. 2B). The resultant new coding sequence contains a stop codon.

These results suggested elevated expression levels of *RPGR* transcripts containing exon 11a (*RPGR*$^{+Ex11a}$) in LCL 4767. We confirmed this observation by quantitative RT-PCR and detected a four-fold increased expression of *RPGR*$^{+Ex11a}$ only in this

patient cell line (Fig. 2C). These results document a splice alteration specific to LCL 4767.

The previously identified missense mutation in exon 5 (c.289T>G, p.Phe130Cys, Table 1) in this patient (Roepman et al., 1996a) is most likely not causing the overexpression of exon 11a because of the distance between the two affected exons. Therefore we searched for additional sequence alterations in exon 11a and identified a G>A transition at position 36 (g.31259G>A), 15 bp upstream of the stop codon of exon 11a (fig. 2D, table 1). The sequence alteration was not annotated as a single nucleotide polymorphism (SNP) in databases (UCSC, ENSEMBL, NCBI) and was not found in 300 ethnically matched control alleles (Caucasians), suggesting a pathogenic nature of this variant.

Application of the ESEfinder program to this sequence alteration predicted a novel binding site for the splice factor SC35 only in the mutated exon 11a (Fig. 2D). Enhanced binding of SC35 to exon 11a may thus explain the significantly elevated levels of *RPGR*$^{+Ex11a}$ transcripts specifically found in patient 4767.

RPGR exon 12, 14 or 15 skipping

RT-PCR analysis of *RPGR* transcripts including exons 11 through 19, revealed two major isoforms either containing all known exons or simultaneously skipping exons 14 and 15 (Fig. 3A). The control samples showed an additional band at 1000 bp (Fig. 3A). Cloning and sequencing of this band documented that this amplicon is a mixture of two so far unknown *RPGR* isoforms that either skip only exon 14 (*RPGR*^{skipEx14}) or 15 (*RPGR*^{skipEx15}).

Comparing all patient-derived cell lines, LCL 2550 showed an alteration from the control splice pattern in conventional RT-PCR analyses. We detected two additional fragments, both migrating 92 bp below the two major products. As confirmed by sequencing, these novel transcripts lack exon 12 of *RPGR* (*RPGR*^{skipEx12}, Fig. 3A).

Patient 2550 carries a deletion of 4 bp in exon 11 (c.1402_1405delCCAG, p.Arg468fs, Table 1) (Roepman et al., 1996a). This deletion affects positions -12 to -9 upstream of the last nucleotide of exon 11, an exonic region spatially unrelated to the splice donor site. Importantly, the deletion causes a frame-shift that leads to a premature termination codon (PTC) in exon 12 (Fig. 3C). Because transcripts containing a PTC are susceptible to nonsense-mediated mRNA decay (NMD) (Maquat, 1995), we searched for such potential effects. To inhibit NMD, we treated

cells with cycloheximide (CHX) and compared them with untreated cells. We found only in LCL 2550 that inhibition of NMD affects splicing and restores the amplification pattern identified in the control cell line (Fig. 3B). These findings show that the 4 bp deletion in exon 11 causes a PTC in exon 12 which activates partial degradation by NMD. Interestingly, LCL 2550 showed a transcript combining exon 12 skipping (deletion of 92 bp) and deleting 4 bp in exon 11. This combination restores the open reading frame in the *RPGR* transcript (Fig. 3C). Thus, a protein migh be translated which lacks amino acids coded by exon 12.

Tissue-specific expression analysis of *RPGR* isoforms

Our studies identified the four novel *RPGR* transcripts $RPGR^{+Ex11a}$, $RPGR^{skipEx12}$, $RPGR^{skipEx14}$ and $RPGR^{skipEx15}$. To verify whether they are also generated in human tissues other than lymphoblastoid cell lines, transcript analysis was performed by quantitative RT-PCR using cDNA from pools of different human tissues, including retina, brain, lung, kidney and testis. In addition, we tested whether the expression of previously reported *RPGR* isoforms also shows tissue-specific variation. This included $RPGR^{+Ex9a}$, which has recently been found to be expressed predominantely in cone photoreceptors of the human retina (Neidhardt et al., 2007) and transcripts simultaneously skipping exons 14 and 15 ($RPGR^{skipEx14/15}$) (Kirschner et al., 1999).The assessment of isoform quantities was performed in comparison to the constitutive transcript of *RPGR*.

Our data show that the abundance of each of the alternative *RPGR* isoforms varied between 0.8% ($RPGR^{skipEx12}$) and 2.7% ($RPGR^{skipEx14/15}$) within retina (Fig. 4). In summary, we document that in human retina approximately 10% of *RPGR* transcripts are alternatively spliced between exons 9 and 15 (Fig. 4).

The amount of each alternative isoform also varied among different tissues (Fig. 5). Highest levels of $RPGR^{+Ex11a}$ were observed in the retina, while other tissues contained significantly lower amounts (Fig. 5A). Furthermore, we detected highest expression of $RPGR^{skipEx12}$ in lung and kidney and found 10 to 12 fold lower amounts of this isoform in retina, brain and testis (Fig. 5B). Similarly, $RPGR^{+Ex9a}$ transcripts were expressed higher in lung and kidney than in retina (Fig. 5E). Highest expression of the novel *RPGR* variant $RPGR^{skipEx14}$ was found in brain (Fig. 5C), whereas $RPGR^{skipEx15}$ expression was lowest in retina (Fig. 5D). Isoform $RPGR^{skipEx14/15}$

exhibited the largest variation: it was 20 times higher expressed in brain than in retina (Fig. 5F).

Taken together, these findings show that the expression of alternative *RPGR* transcripts varies significantly among and within tissues. This indicates distinct tissue-specific *RPGR* splicing which may confer specialized function of the different isoforms.

3.1.5. Discussion

Alternative splicing of pre-mRNA transcripts is considered to be an important mechanism to increase protein variability from a single gene (Black, 2000). This process also acts on human *RPGR* and generates alternative transcript isoforms, the expression of which is spatially and temporally regulated (Kirschner et al., 1999; Vervoort et al., 2000; Neidhardt et al., 2007).

In this article, we describe four novel transcript isoforms of *RPGR* termed *RPGR*$^{+Ex11a}$, *RPGR*^{skipEx12}, *RPGR*^{skipEx14} and *RPGR*^{skipEx15}. We showed that all are expressed in a tissue-dependent fashion, which suggests functional consequences. The highest expression levels of both *RPGR*^{skipEx14} and *RPGR*$^{skipEx14/15}$ were detected in brain. Consequently, misregulation of transcripts lacking exon 14 or exons 14/15 might disturb their function in brain. To date, no mutation in *RPGR* has been described that shows a phenotypic manifestation in this tissue. However, only a few patients are known to contain mutations in exon 14 or 15 (compare to http://rpgr.hgu.mrc.ac.uk). A detailed clinical characterization of the brain functions in these patients might add valuable information on the phenotypic spectrum caused by mutations in *RPGR*.

Our data suggest that *RPGR* transcripts are differentially spliced among tissues. They further show that the novel isoforms described herein are expressed at lower levels compared to the constitutive transcript of *RPGR*. Nevertheless, a significant portion of *RPGR* transcripts are alternatively spliced between exon 9 and 15 in the retina. Since tissues are heterogenous with respect to cell type, one possible explanation for our observation is that either only a fraction of cells within a given tissue expresses a distinct isoform or that expression is cell type specific. Similar observations have been published for *RPGR* containing exon 9a (Neidhardt et al., 2007). The corresponding protein of the exon 9a-containing transcript was predominantly present in cones of the retina suggesting a specialized function of this isoforms in a subfraction of photorecptors. It is a matter of future studies to evaluate whether the novel *RPGR* isoforms described herein are also expressed by a specific cell type within distinct tissues.

Regulation of alternative and tissue-specific splicing is thought to be controlled by proteins that stimulate or repress exon recognition. In general, such factors are called exonic or intronic splicing enhancers (ESEs or ISEs) and silencers (ESSs or ISSs). Some of these factors are expressed only in certain tissues and regulate splicing of

specific sets of pre-mRNAs (Maniatis and Tasic, 2002). A well known example is the mammalian splicing factor NOVA-1, which is involved in the control of alternative pre-mRNA splicing in neurons. This protein binds specific intronic sequences of pre-mRNA targets through its K-homology (KH) domains. NOVA-1 is reported to enhance the inclusion of specific alternative exons into target transcripts and is expressed in distinct populations of neurons in the brain (Dredge et al., 2001). Taking this into account, we envision that factors with similar functions might regulate the expression of alternative *RPGR* transcript isoforms within tissues.

A different mechanism of gene regulation acts through NMD which constitutes a posttranscriptional regulatory process. We found that NMD reduces the amount of a mutated *RPGR* transcript which contains a PTC. Of note, NMD may also act on non-mutated transcripts (Mendell et al., 2004; Rehwinkel et al., 2005; Wittmann et al., 2006). In addition, it has been documented that it can be active in a tissue specific-manner (Bateman et al., 2003; Linde et al., 2007; Weischenfeldt et al., 2008). These observations provide a possible explanation why *RPGR* isoforms were found to be expressed at elevated levels among tissues.

Interestingly, most *RPGR* isoforms truncate the deduced protein downstream of the Regulator of Chromosome Condensation 1-like domain (RCC1). The RCC1-like domain of *RPGR* includes exons 2 through 11 (Kirschner et al., 1999; Vervoort and Wright, 2002; Neidhardt et al., 2007). This domain has been shown to bind four different interaction partners: RPGR interacting protein 1 (RPGRIP1), prenyl-binding protein delta as well as structural maintenance of chromosomes 1 and 3 proteins (Linari et al., 1999; Boylan and Wright, 2000; Roepman et al., 2000; Khanna et al., 2005). Different RPGR protein isoforms have been shown to be associated with a multiprotein complex, which is thought to be involved in intraphotoreceptor protein transport through the connecting cilium (He et al., 2008). We have previously shown that exon 9a containing *RPGR* transcripts give rise to a truncated protein which binds distinct isoforms of RPGRIP1 (Neidhardt et al., 2007). On the assumption that the other transcript variants described herein are also translated, our data support a model that predicts binding of distinct RPGR isoforms to different sets of interaction partners to form various functionally unique protein complexes. Mutations that modify distinct *RPGR* isoforms would influence the formation of these complexes. Supportively, cases have been reported where *RPGR* mutations in the RCC1-like

domain (affecting exons 6 and 8) are associated with non-ocular manifestations (Iannaccone et al., 2003; Zito et al., 2003; Moore et al., 2006). These reports further support our hypothesis that RPGR isoform-specific protein complexes fulfill tissue-specific functions.

The disease phenotype in patients affected by *RPGR* mutations can be highly variable even within one family. These observations imply the existence of modifiers that influence the severity of the disease. Here, we showed that not only does a mutation in *RPGR* affect the predicted amino acid sequence of the protein, but may also results in missplicing or altered regulation of specific transcripts. Since alternative splicing is precisely regulated in a tissue-specific and developmental stage-dependent manner, changes in this process may cause or modify disease symptoms (Nissim-Rafinia and Kerem, 2002). Taking this into account, our results suggest that defects in *RPGR* splicing could modify the disease phenotype of RP. Several examples for splicing-induced modifications of a disease have been reported (Garcia-Blanco et al., 2004).

We have identified alterations in splicing of *RPGR* in three out of seven RP patient cell lines. Our findings implicate the importance of including the analyis of *RPGR* splicing in patients with retinal degenerations and associated phenotypes. Furthermore, patient-derived cell lines showed splice alterations in *RPGR* isoforms which are differentially regulated among distinct human tissues. Thus, a change in the expression of these isoforms could not only affect the retina, but also disrupt their function in other tissues.

In patient cell line 2550, we detected elevated levels of $RPGR^{skipEx12}$ transcripts. The deletion of 4 bp in combination with exon 12 skipping abolishes the deleterious effects of the frame-shift. Therefore, these trancripts can now escape degradation by NMD and may be expressed as a truncated RPGR protein in the patient. The splice defect is likely to take place in most tissues indicating that not only the retina is affected. Interestingly, there is evidence that patient 2550 suffers from a mild hearing impairment. The audiogram showed a dip with high frequency pure tones (personal communication: Thomas Rosenberg). Although speculatory, the nonocular manifestation of auditory problems might be the result of the expression of this aberrant protein isoform. Supportively, it has been observed in a different patient (patient ID 2557) that an 6.4 kb deletion within *RPGR* (Roepman et al., 1996b), in addition to a single bp deletion at the 3' end of exon ORF15 (c.3395delA) (Neidhardt et al., 2008) may affect the audiogram (Rosenberg et al., 1997). Nevertheless, an age-

related effect on hearing in these patients cannot be excluded. It would further be of interest to clarify whether the respiratory function of patient 2550 impaired, because our expression data suggest that *RPGR*^{skipEx12} transcripts might be relevant in lung.

We showed that patient 4767 expresses increased levels of *RPGR*$^{+Ex11a}$, likely because of a sequence alteration in exon 11a. This novel mutation is predicted to change the activity of a splice enhancer site of SC35, which might control the frequency of exon 11a inclusion into the transcript. SC35, a ubiquitously expressed splice factor, has been shown to increase the integration of a target exon by mediating specific interactions with components of the spliceosome (Fu and Maniatis, 1992). Mutations that increase the binding affinity for an exonic splicing enhancer have already been associated with other human diseases, e.g. frontotemporal dementia with Parkinsonism-chromosome 17 type (FTDP-17) (D'Souza and Schellenberg, 2000) and a cardiac phenotype of Fabry disease (Ishii et al., 2002). We demonstrated that the expression of exon 11a was significantly increased only in cell line 4767. Toxic effects leading to premature death of photoreceptors might be caused by overexpression of a distinct *RPGR* isoform, a mechanism similar as proposed by us for *RPGR*$^{+Ex9a}$ (Neidhardt et al., 2007). Furthermore, the overexpression of *RPGR* in mice also leads to a severe phenotype in sperm flagella resulting in male infertility (Brunner et al., 2008).

Interestingly, the family pedigree of patient 4767 shows over a period of six generations an inheritance pattern by which female carriers are also affected (data not shown). We cannot exclude that this mode of inheritance is caused by skewed X-inactivation in affected females. However, this mechanism has never been found to influence the phenotype of female carriers of *RPGR* mutations (Banin et al., 2007; Neidhardt et al., 2008; Walia et al., 2008) and thus, is unlikely to be a common mechanism explaining symptomatic female carriers. In the patient described herein, either a cumulative or a separate effect of the two identified sequence alternation in exons 5 and 11a might be the cause of the disease.

Taken together, the results reported here provide new insights into alternative splicing of *RPGR* and will help to elucidate its role in distinct tissues. Moreover, *RPGR* splice defects provide a pathogenic mechanism newly associated with *RPGR*, which implies that classical and syndromic RP patients should be analyzed for alterations in *RPGR* splicing.

3.1.6 Acknowledgements

We are grateful to Silke Feil for cell culture support. Additional thank goes to Christina Reinhard and Heymut Omran for providing us with a control cell line. We thank the ‘Velux Foundation’, ‘Olga Mayenfisch Foundation’ and ‘Forschungskredit der Universität Zürich’ for financial support (to J.N.).

3.1.7. References

1. Banin,E., Mizrahi-Meissonnier,L., Neis,R., Silverstein,S., Magyar,I., Abeliovich,D., Roepman,R., Berger,W., Rosenberg,T., and Sharon,D. (2007). A non-ancestral RPGR missense mutation in families with either recessive or semi-dominant X-linked retinitis pigmentosa. Am. J. Med. Genet. A *143A*, 1150-1158.

2. Bateman,J.F., Freddi,S., Nattrass,G., and Savarirayan,R. (2003). Tissue-specific RNA surveillance? Nonsense-mediated mRNA decay causes collagen X haploinsufficiency in Schmid metaphyseal chondrodysplasia cartilage. Hum. Mol. Genet. *12*, 217-225.

3. Bauer,S., Fujita,R., Buraczynska,M., Abrahamson,M., Ehinger,B., Wu,W., Falls,T.J., Andreasson,S., and Swaroop,A. (1998). Phenotype of an X-linked retinitis pigmentosa family with a novel splice defect in the RPGR gene. Invest Ophthalmol. Vis. Sci. *39*, 2470-2474.

4. Black,D.L. (2000). Protein diversity from alternative splicing: a challenge for bioinformatics and post-genome biology. Cell *103*, 367-370.

5. Boylan,J.P. and Wright,A.F. (2000). Identification of a novel protein interacting with RPGR. Hum. Mol. Genet. *9*, 2085-2093.

6. Breuer,D.K., Yashar,B.M., Filippova,E., Hiriyanna,S., Lyons,R.H., Mears,A.J., Asaye,B., Acar,C., Vervoort,R., Wright,A.F., Musarella,M.A., Wheeler,P., MacDonald,I., Iannaccone,A., Birch,D., Hoffman,D.R., Fishman,G.A., Heckenlively,J.R., Jacobson,S.G., Sieving,P.A., and Swaroop,A. (2002). A comprehensive mutation analysis of RP2 and RPGR in a North American cohort of families with X-linked retinitis pigmentosa. Am. J. Hum. Genet. *70*, 1545-1554.

7. Brunner,S., Colman,D., Travis,A.J., Luhmann,U.F., Shi,W., Feil,S., Imsand,C., Nelson,J., Grimm,C., Rulicke,T., Fundele,R., Neidhardt,J., and Berger,W. (2008). Overexpression of RPGR Leads to Male Infertility in Mice Due to Defects in Flagellar Assembly. Biol. Reprod.

8. Chatr-Aryamontri,A., Angelini,M., Garelli,E., Tchernia,G., Ramenghi,U., Dianzani,I., and Loreni,F. (2004). Nonsense-mediated and nonstop decay of ribosomal protein S19 mRNA in Diamond-Blackfan anemia. Hum. Mutat. *24*, 526-533.

9. D'Souza,I. and Schellenberg,G.D. (2000). Determinants of 4-repeat tau expression. Coordination between enhancing and inhibitory splicing sequences for exon 10 inclusion. J. Biol. Chem. *275*, 17700-17709.

10. Demirci,F.Y., Radak,A.L., Rigatti,B.W., Mah,T.S., and Gorin,M.B. (2004). A presumed missense mutation of RPGR causes abnormal RNA splicing with exon skipping. Am. J. Ophthalmol. *138*, 504-505.

11. Dredge,B.K., Polydorides,A.D., and Darnell,R.B. (2001). The splice of life: alternative splicing and neurological disease. Nat. Rev. Neurosci. *2*, 43-50.

12. Dry,K.L., Manson,F.D., Lennon,A., Bergen,A.A., Van Dorp,D.B., and Wright,A.F. (1999). Identification of a 5' splice site mutation in the RPGR gene in a family with X-linked retinitis pigmentosa (RP3). Hum. Mutat. *13*, 141-145.

13. Fu,X.D. and Maniatis,T. (1992). The 35-kDa mammalian splicing factor SC35 mediates specific interactions between U1 and U2 small nuclear ribonucleoprotein particles at the 3' splice site. Proc. Natl. Acad. Sci. U. S. A *89*, 1725-1729.

14. Fujita,R., Buraczynska,M., Gieser,L., Wu,W., Forsythe,P., Abrahamson,M., Jacobson,S.G., Sieving,P.A., Andreasson,S., and Swaroop,A. (1997). Analysis of the RPGR gene in 11 pedigrees with the retinitis pigmentosa type 3 genotype: paucity of mutations in the coding region but splice defects in two families. Am. J. Hum. Genet. *61*, 571-580.

15. Garcia-Blanco,M.A., Baraniak,A.P., and Lasda,E.L. (2004). Alternative splicing in disease and therapy. Nat. Biotechnol. *22*, 535-546.

16. Hartong,D.T., Berson,E.L., and Dryja,T.P. (2006). Retinitis pigmentosa. Lancet *368*, 1795-1809.

17. He,S., Parapuram,S.K., Hurd,T.W., Behnam,B., Margolis,B., Swaroop,A., and Khanna,H. (2008). Retinitis Pigmentosa GTPase Regulator (RPGR) protein isoforms in mammalian retina: insights into X-linked Retinitis Pigmentosa and associated ciliopathies. Vision Res. *48*, 366-376.

18. Iannaccone,A., Breuer,D.K., Wang,X.F., Kuo,S.F., Normando,E.M., Filippova,E., Baldi,A., Hiriyanna,S., MacDonald,C.B., Baldi,F., Cosgrove,D., Morton,C.C., Swaroop,A., and Jablonski,M.M. (2003). Clinical and immunohistochemical evidence for an X linked retinitis pigmentosa syndrome with recurrent infections and hearing loss in association with an RPGR mutation. J. Med. Genet. *40*, e118.

19. Ishii,S., Nakao,S., Minamikawa-Tachino,R., Desnick,R.J., and Fan,J.Q. (2002). Alternative splicing in the alpha-galactosidase A gene: increased exon inclusion results in the Fabry cardiac phenotype. Am. J. Hum. Genet. *70*, 994-1002.

20. Kennan,A., Aherne,A., and Humphries,P. (2005). Light in retinitis pigmentosa. Trends Genet. *21*, 103-110.

21. Khanna,H., Hurd,T.W., Lillo,C., Shu,X., Parapuram,S.K., He,S., Akimoto,M., Wright,A.F., Margolis,B., Williams,D.S., and Swaroop,A. (2005). RPGR-ORF15, which is mutated in retinitis pigmentosa, associates with SMC1, SMC3, and microtubule transport proteins. J. Biol. Chem. *280*, 33580-33587.

22. Kirschner,R., Rosenberg,T., Schultz-Heienbrok,R., Lenzner,S., Feil,S., Roepman,R., Cremers,F.P., Ropers,H.H., and Berger,W. (1999). RPGR transcription studies in mouse and human tissues reveal a retina-specific isoform

that is disrupted in a patient with X-linked retinitis pigmentosa. Hum. Mol. Genet. *8*, 1571-1578.

23. Linari,M., Ueffing,M., Manson,F., Wright,A., Meitinger,T., and Becker,J. (1999). The retinitis pigmentosa GTPase regulator, RPGR, interacts with the delta subunit of rod cyclic GMP phosphodiesterase. Proc. Natl. Acad. Sci. U. S. A *96*, 1315-1320.

24. Linde,L., Boelz,S., Neu-Yilik,G., Kulozik,A.E., and Kerem,B. (2007). The efficiency of nonsense-mediated mRNA decay is an inherent character and varies among different cells. Eur. J. Hum. Genet. *15*, 1156-1162.

25. Maniatis,T. and Tasic,B. (2002). Alternative pre-mRNA splicing and proteome expansion in metazoans. Nature *418*, 236-243.

26. Maquat,L.E. (1995). When cells stop making sense: effects of nonsense codons on RNA metabolism in vertebrate cells. RNA. *1*, 453-465.

27. Meindl,A., Dry,K., Herrmann,K., Manson,F., Ciccodicola,A., Edgar,A., Carvalho,M.R., Achatz,H., Hellebrand,H., Lennon,A., Migliaccio,C., Porter,K., Zrenner,E., Bird,A., Jay,M., Lorenz,B., Wittwer,B., D'Urso,M., Meitinger,T., and Wright,A. (1996). A gene (RPGR) with homology to the RCC1 guanine nucleotide exchange factor is mutated in X-linked retinitis pigmentosa (RP3). Nat. Genet. *13*, 35-42.

28. Mendell,J.T., Sharifi,N.A., Meyers,J.L., Martinez-Murillo,F., and Dietz,H.C. (2004). Nonsense surveillance regulates expression of diverse classes of mammalian transcripts and mutes genomic noise. Nat. Genet. *36*, 1073-1078.

29. Moore,A., Escudier,E., Roger,G., Tamalet,A., Pelosse,B., Marlin,S., Clement,A., Geremek,M., Delaisi,B., Bridoux,A.M., Coste,A., Witt,M., Duriez,B., and Amselem,S. (2006). RPGR is mutated in patients with a complex X linked phenotype combining primary ciliary dyskinesia and retinitis pigmentosa. J. Med. Genet. *43*, 326-333.

30. Neidhardt,J., Barthelmes,D., Farahmand,F., Fleischhauer,J.C., and Berger,W. (2006). Different amino acid substitutions at the same position in rhodopsin lead to distinct phenotypes. Invest Ophthalmol. Vis. Sci. *47*, 1630-1635.

31. Neidhardt,J., Glaus,E., Barthelmes,D., Zeitz,C., Fleischhauer,J., and Berger,W. (2007). Identification and characterization of a novel RPGR isoform in human retina. Hum. Mutat. *28*, 797-807.

32. Neidhardt,J., Glaus,E., Lorenz,B., Netzer,C., Li,Y., Schambeck,M., Wittmer,M., Feil,S., Kirschner-Schwabe,R., Rosenberg,T., Cremers,F.P., Bergen,A.A., Barthelmes,D., Baraki,H., Schmid,F., Tanner,G., Fleischhauer,J., Orth,U., Becker,C., Wegscheider,E., Nurnberg,G., Nurnberg,P., Bolz,H.J., Gal,A., and Berger,W. (2008). Identification of novel mutations in X-linked retinitis pigmentosa families and implications for diagnostic testing. Mol. Vis. *14*, 1081-1093.

33. Nissim-Rafinia,M. and Kerem,B. (2002). Splicing regulation as a potential genetic modifier. Trends in Genetics *18*, 123-127.

34. Pelletier,V., Jambou,M., Delphin,N., Zinovieva,E., Stum,M., Gigarel,N., Dollfus,H., Hamel,C., Toutain,A., Dufier,J.L., Roche,O., Munnich,A., Bonnefont,J.P., Kaplan,J., and Rozet,J.M. (2007). Comprehensive survey of mutations in RP2 and RPGR in patients affected with distinct retinal dystrophies: genotype-phenotype correlations and impact on genetic counseling. Hum. Mutat. *28*, 81-91.

35. Rehwinkel,J., Letunic,I., Raes,J., Bork,P., and Izaurralde,E. (2005). Nonsense-mediated mRNA decay factors act in concert to regulate common mRNA targets. RNA. *11*, 1530-1544.

36. Roepman,R., Bauer,D., Rosenberg,T., van Duijnhoven,G., van,d., V, Platzer,M., Rosenthal,A., Ropers,H.H., Cremers,F.P., and Berger,W. (1996a). Identification of a gene disrupted by a microdeletion in a patient with X-linked retinitis pigmentosa (XLRP). Hum. Mol. Genet. *5*, 827-833.

37. Roepman,R., Bernoud-Hubac,N., Schick,D.E., Maugeri,A., Berger,W., Ropers,H.H., Cremers,F.P., and Ferreira,P.A. (2000). The retinitis pigmentosa GTPase regulator (RPGR) interacts with novel transport-like proteins in the outer segments of rod photoreceptors. Hum. Mol. Genet. *9*, 2095-2105.

38. Roepman,R., van Duijnhoven,G., Rosenberg,T., Pinckers,A.J., Bleeker-Wagemakers,L.M., Bergen,A.A., Post,J., Beck,A., Reinhardt,R., Ropers,H.H., Cremers,F.P., and Berger,W. (1996b). Positional cloning of the gene for X-linked retinitis pigmentosa 3: homology with the guanine-nucleotide-exchange factor RCC1. Hum. Mol. Genet. *5*, 1035-1041.

39. Rosenberg,T., Haim,M., Hauch,A.M., and Parving,A. (1997). The prevalence of Usher syndrome and other retinal dystrophy-hearing impairment associations. Clin. Genet. *51*, 314-321.

40. Sharon,D., Sandberg,M.A., Rabe,V.W., Stillberger,M., Dryja,T.P., and Berson,E.L. (2003). RP2 and RPGR mutations and clinical correlations in patients with X-linked retinitis pigmentosa. Am. J. Hum. Genet. *73*, 1131-1146.

41. Shu,X., McDowall,E., Brown,A.F., and Wright,A.F. (2008). The human retinitis pigmentosa GTPase regulator gene variant database. Hum. Mutat. *29*, 605-608.

42. Vervoort,R., Lennon,A., Bird,A.C., Tulloch,B., Axton,R., Miano,M.G., Meindl,A., Meitinger,T., Ciccodicola,A., and Wright,A.F. (2000). Mutational hot spot within a new RPGR exon in X-linked retinitis pigmentosa. Nat. Genet. *25*, 462-466.

43. Vervoort,R. and Wright,A.F. (2002). Mutations of RPGR in X-linked retinitis pigmentosa (RP3). Hum. Mutat. *19*, 486-500.

44. Walia,S., Fishman,G.A., Swaroop,A., Branham,K.E., Lindeman,M., Othman,M., and Weleber,R.G. (2008). Discordant phenotypes in fraternal twins

having an identical mutation in exon ORF15 of the RPGR gene. Arch. Ophthalmol. *126*, 379-384.

45. Wang,G.S. and Cooper,T.A. (2007). Splicing in disease: disruption of the splicing code and the decoding machinery. Nat. Rev. Genet. *8*, 749-761.

46. Weischenfeldt,J., Damgaard,I., Bryder,D., Theilgaard-Monch,K., Thoren,L.A., Nielsen,F.C., Jacobsen,S.E., Nerlov,C., and Porse,B.T. (2008). NMD is essential for hematopoietic stem and progenitor cells and for eliminating by-products of programmed DNA rearrangements. Genes Dev. *22*, 1381-1396.

47. Wittmann,J., Hol,E.M., and Jack,H.M. (2006). hUPF2 silencing identifies physiologic substrates of mammalian nonsense-mediated mRNA decay. Mol. Cell Biol. *26*, 1272-1287.

48. Zito,I., Downes,S.M., Patel,R.J., Cheetham,M.E., Ebenezer,N.D., Jenkins,S.A., Bhattacharya,S.S., Webster,A.R., Holder,G.E., Bird,A.C., Bamiou,D.E., and Hardcastle,A.J. (2003). RPGR mutation associated with retinitis pigmentosa, impaired hearing, and sinorespiratory infections. J. Med. Genet. *40*, 609-615.

3.1.8. Figure and Tables

Table 1. *RPGR* mutations of analyzed lymphoblastoid cell lines derived from male patients with XlRP

Patient ID	Mutation in Exon/Intron	Sequence alteration	Conseq. of Seq. alteration
2616	intron 1	c.28+1G>A	potential splice defect
4767 †	exon 5	c.389T>G	p.Phe130Cys
	exon 11a	g.31259G>A *, **	Splice defect/ p.Asp484Asn
2884	exon 7	c.706C>T	p.Glu236X
2555	exon 8	c.823G>A	p.Gly275Ser
2603	exon 8	c.823G>A	p.Gly275Ser
2549	exon 11	c.1399C>T	p.Gln467X
2550††	exon 11	c.1402_1405delCCAG	p.Arg468fs

cDNA reference sequence: NM_001034853

*genomic DNA reference sequence: NC_000023.9 (range: 38013367 to 38071732)

** Mutation is first described in this report.

† Female carriers are affected in this family.

†† Patient has a mild hearing impairment (personal communication: Thomas Rosenberg).

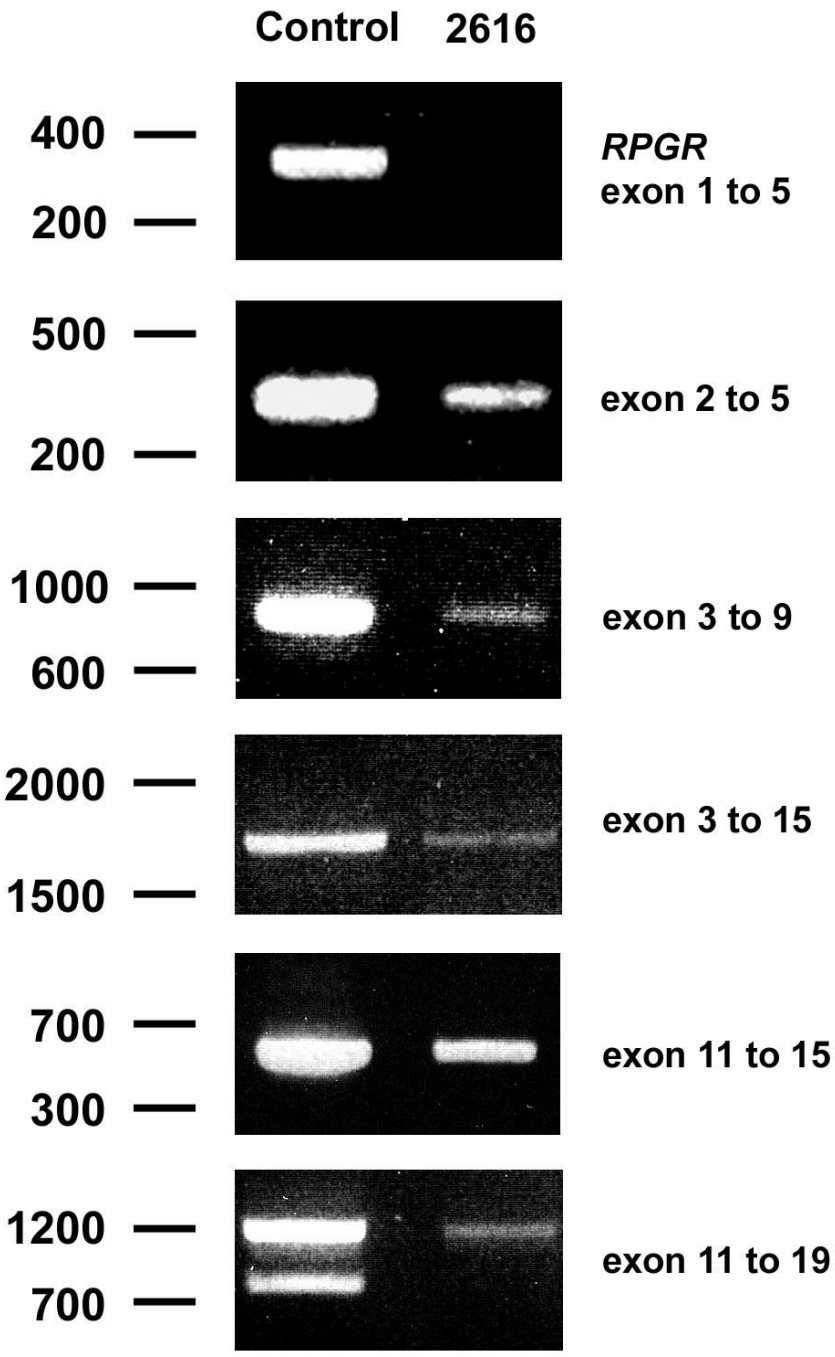

Figure 1 Characterization of a splice site mutation in LCL 2616. *RPGR* transcript analysis in the patient cell line 2616 and the unaffected control using different primer combinations that span the whole *RPGR* transcript. DNA marker sizes are given in base pairs.

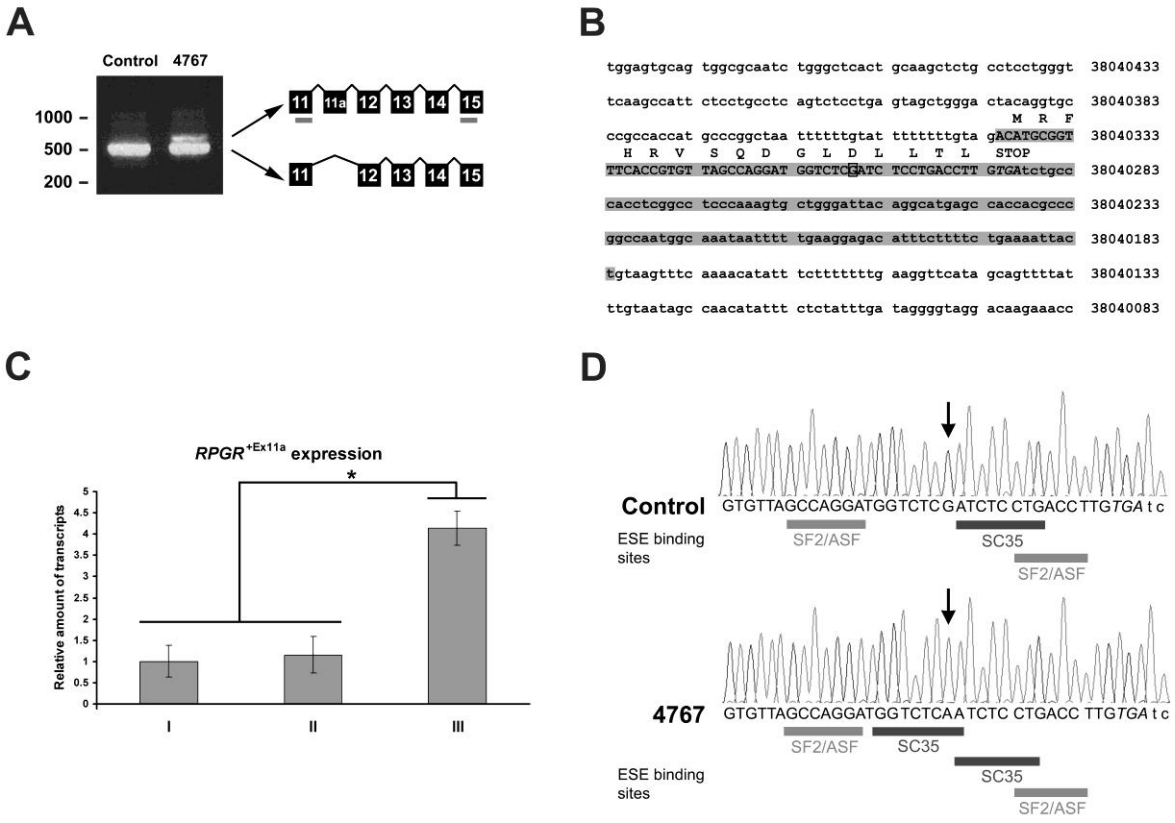

Figure 2 Overexpression of the *RPGR*$^{+Ex11a}$ transcript isoform in patient cell line 4767.
A RT-PCR amplification of *RPGR* transcripts containing exons 11 through 15. Schematic drawings illustrate the exon composition of amplified RT-PCR products. Primer binding sites are indicated as horizontal gray bars. DNA marker sizes are given in base pairs. **B** Sequence of the novel *RPGR* exon 11a and flanking intronic regions. Nucleotides in gray represent exon 11a sequences, whereas deduced amino acids are indicated as single letter code above of each nucleotide triplet. The stop codon is presented in italics and coding sequences are shown in uppercase letters. The position mutated in patient 4767 (g.31259G>A) is marked by a box. NC_000023.9 was used as reference sequence for genomic DNA (numbers at the right indicate the nucleotide position). **C** Real-time quantitative RT-PCR of exon 11a expression levels detected in the unaffected control (I), in a pool of 6 LCLs carrying hemizygous *RPGR* mutations (n=6) different from the sequence alteration in exon 11a (II) and in the patient cell line 4767(III). Error bars represent confidence intervals of 95% calculated from cDNA batches which were generated from RNA of three independently grown LCL cells. Asterisk illustrates statistical significance between measurements. **D** Electropherograms from parts of the exon 11a sequence of patient cell line 4767 and a control. Arrows indicate the postition of the mutation g.31259G>A in patient 4767. The stop codon is shown in italics. Positions of putative binding sites for exonic splicing enhancers (ESEs) SF2/ASF and SC35 are depicted as horizontal bars. The results suggest the existence of an additional SC35 binding site uniquely in the patient.

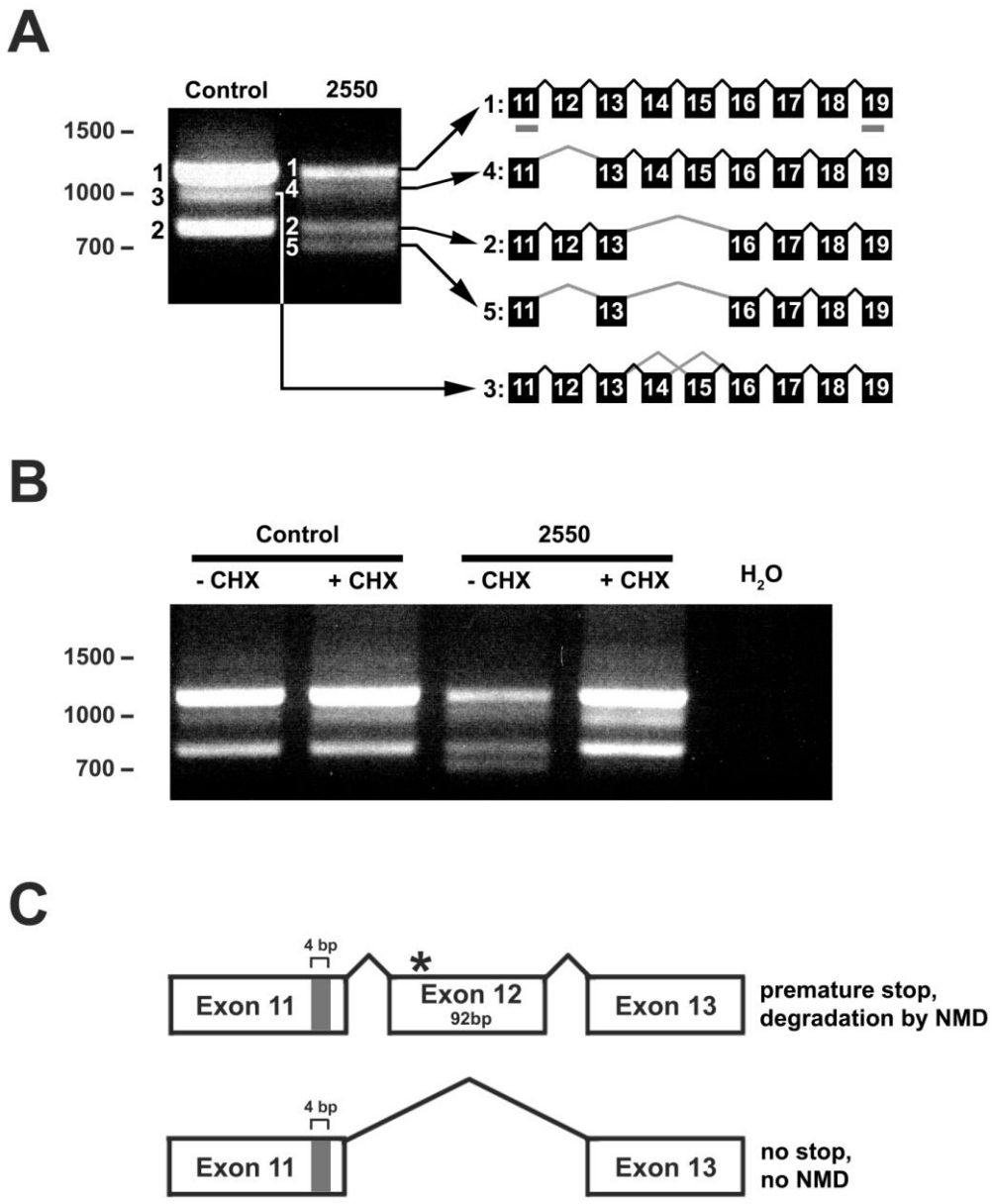

Figure 3 Upregulation of the novel *RPGR*^{skipEx12} transcript. **A** RT-PCR amplification of exons 11 to 19 of the *RPGR* transcript. Schematic drawings illustrate the sequence of amplified RT-PCR products. Each RT-PCR product is marked by a number corresponding to the respective schematic drawing. Primer binding sites in exons 11 and 19 are indicated by horizontal gray bars. Numbers at the left represent DNA marker sizes and are given in base pairs. **B** RT-PCR of *RPGR* exon 11 to 19 of patient cell line 2550 and a control, either incubated with (+) or without (-) cycloheximide (CHX) to inhibit nonsense-mediated mRNA decay (NMD). The RT-PCR reaction lacking a template is indicated as H_2O. **C** Graphical illustration of mutation-induced mechanisms in patient cell line 2550 leading to detectable levels of *RPGR*^{skipEx12} transcripts. The asterisk labels a premature termination codon (PTC) in exon 12, which is generated in patient cell line 2550 because of the 4-bp deletion in exon 11. The PTC causes reduced expression levels of transcripts including exon 12, by NMD (upper). In contrast, transcripts lacking exon 12 in combination with the 4 bp deletion escape NMD because of preservation of the open reading frame (lower).

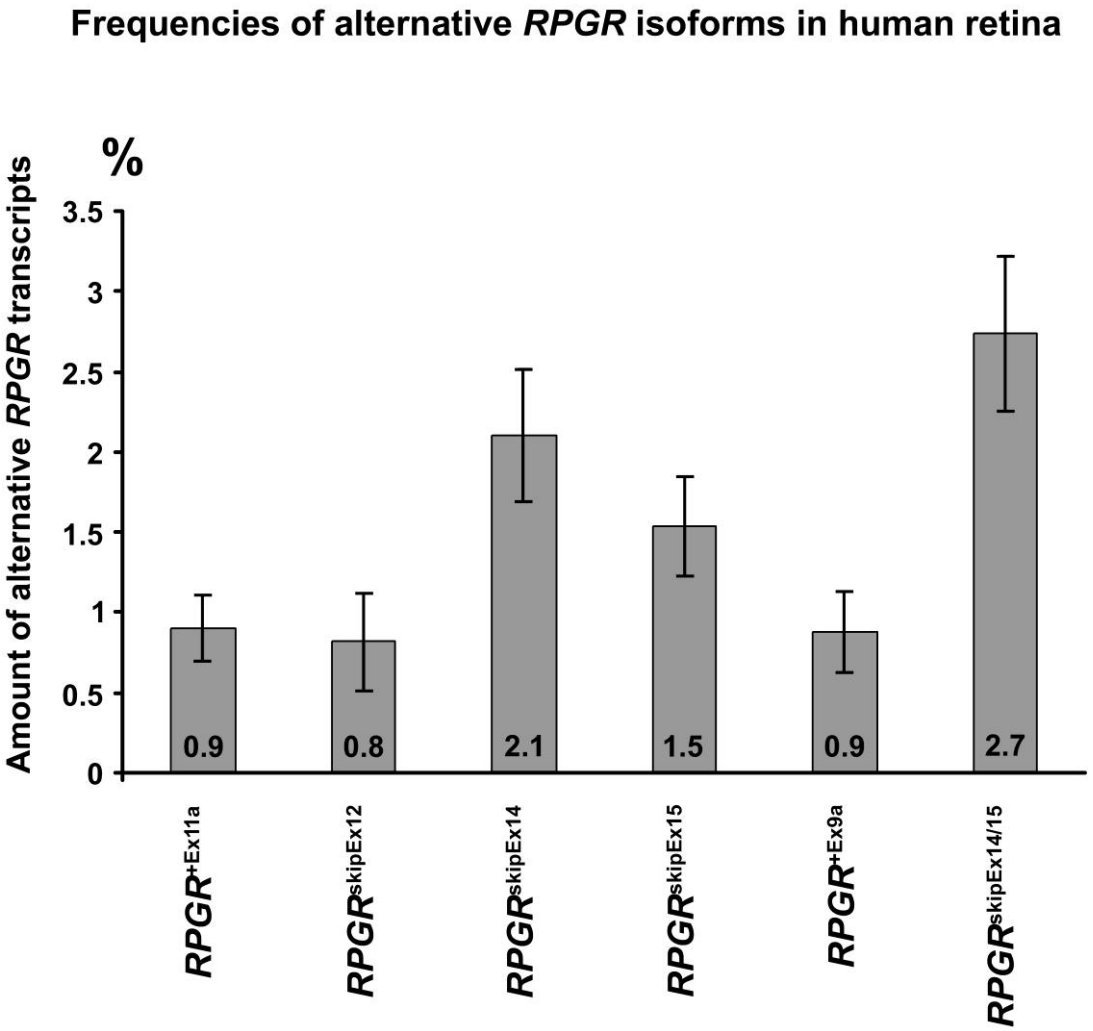

Figure 4 Relative abundance of alternative transcript isoforms of *RPGR* in human retina. Expression levels of alternative variants are displayed as percentages of the constitutive *RPGR* transcript in human retina. Numbers in bars represent mean values given in percentages. Error bars represent confidence intervals of 95% calculated from 3-4 independently generated cDNA batches.

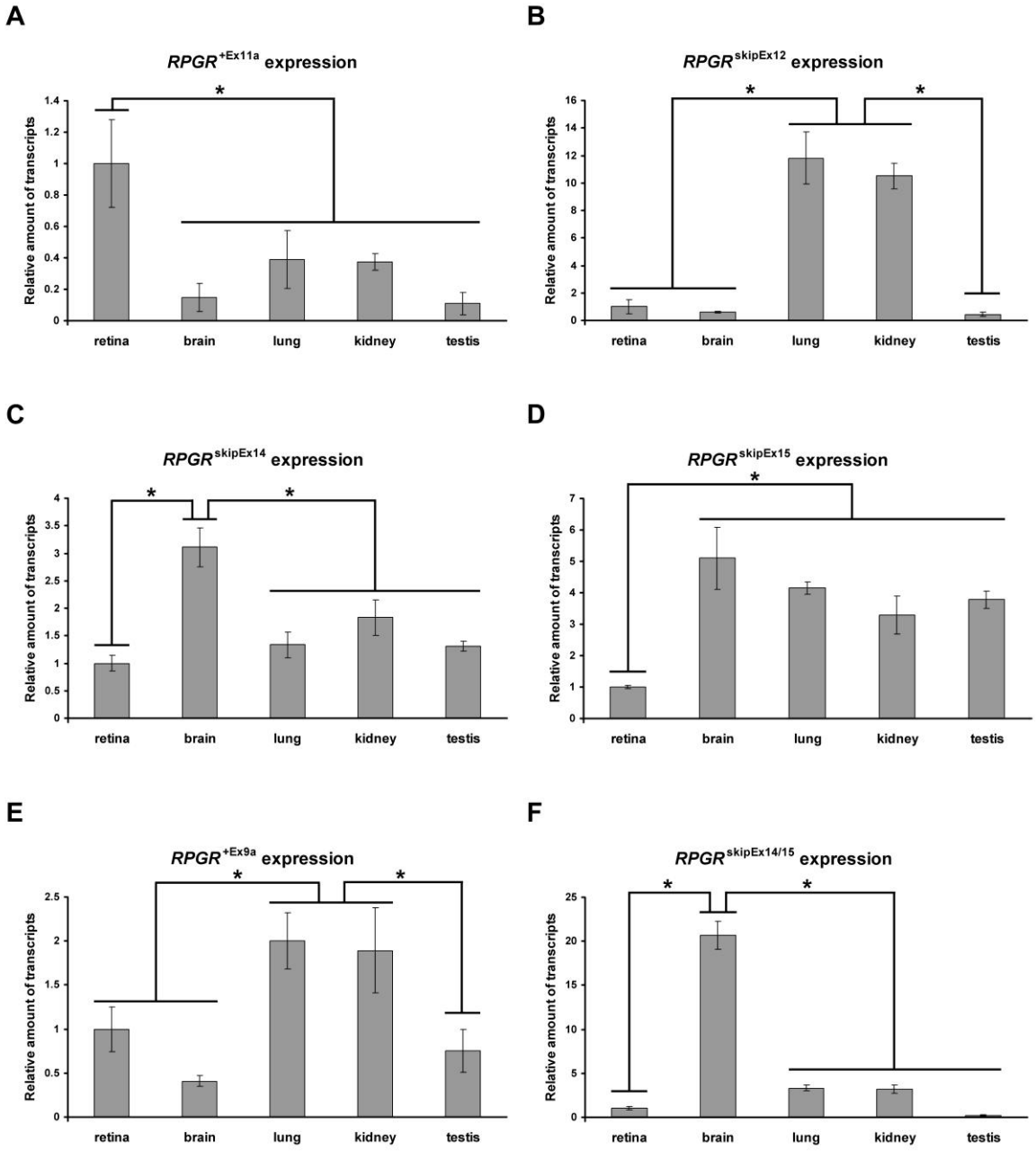

Figure 5 Multi-tissue expression analyses of novel and previously reported *RPGR* transcript isoforms. Quantitative RT-PCR to detect expression of **A** *RPGR*$^{+Ex11a}$, **B** *RPGR*^{skipEx12}, **C** *RPGR*^{skipEx14}, **D** *RPGR*^{skipEx15}, **E** *RPGR*$^{+Ex9a}$, **F** *RPGR*$^{skipEx14/15}$ from different donor tissues. For quantification of the novel *RPGR* transcript isoform we used expression of the constitutive *RPGR* transcript as endogenous control. Subsequently, relative expression levels of each isoform were compared with human retina (retinal levels were set to 1). Asterisks illustrate significance between measurements as described in the Results section. Error bars represent confidence intervals of 95% calculated from 3 to 4 independently generated cDNA batches.

Supplementary Table S1. Primer combinations used for RT-PCR assays to screen for splice defects in the *RPGR* transcript

RT-PCR product	Fw primer		Rev primer	
	Name	**Sequence (5'-3')**	**Name**	**Sequence (5'-3')**
RPGR exon 1 to 5	Eco-RP3-5UTR1	ACCGAATTCCAAACCGTCCTCTACAGCC	RP3-Ex4/5up	ATATACATTGCCTCCTTCTG
RPGR exon 2 to 5	RP3-ex2dn	CGATTCGGGTGCTGTGTTTA	RP3-Ex4/5up	ATATACATTGCCTCCTTCTG
RPGR exon 3 to 15	RP3-Ex3dn	TGGGGTCAGTTAGGATTAGG	RP3-Ex15up	TTTGCTTCTACCTCTTGCTCCTCTATTCC
RPGR exon 3 to 9	RP3-Ex3dn	TGGGGTCAGTTAGGATTAGG	RP3-Ex9up	GGTAAAATTCTCCAGTCCAAGTC
RPGR exon 11 to 15	RP3-Ex11dn	GGGACTCTTGGCCTTTCTGCTTGTT	RP3-Ex15up	TTTGCTTCTACCTCTTGCTCCTCTATTCC
RPGR exon 11 to 19	RP3-Ex11dn	GGGACTCTTGGCCTTTCTGCTTGTT	RP3-Ex19up	ATTTGTTGGTGGGATATTCTGATGATT

3.1.9 Own contribution to the manuscript “Mutation- and tissue-specific alterations of *RPGR* transcripts”

Cell culture, cycloheximide treatment, sequencing analysis, RT-PCR analysis, contributions to interpretation of the data and manuscript writing

3.2. U1 snRNA-mediated gene therapeutic correction of splice defects caused by an exceptionally mild BBS mutation

Fabian Schmid [1], Esther Glaus [1], Daniel Barthelmes [2], Manfred Fliegauf [3], Harald Gaspar [4], Gudrun Nürnberg [5], Peter Nürnberg [5], Heymut Omran [6], Wolfgang Berger [1], John Neidhardt [1*]

[1] University of Zurich, Institute of Medical Molecular Genetics, Schorenstrasse 16, 8603 Schwerzenbach, Switzerland.

[2] The University of Sydney, Save Sight Institute, 8 Macquarie Street, Sydney 2000 NSW, Australia

[3] Center of Chronic Immunodeficiency (CCI), University Medical Center Freiburg and University of Freiburg, Breisacherstrasse 117, 79106 Freiburg, Germany.

[4] Heidelberg University Hospital, Institute of Human Genetics, Im Neuenheimer Feld 344a, 69120 Heidelberg, Germany

[5] Cologne Center for Genomics (CCG) and Center for Molecular Medicine Cologne (CMMC), University of Cologne, Cologne, Germany

[6] Klinik und Poliklinik für Kinder und Jugendmedizin, University Hospital Muenster, Germany

* Corresponding author

Manuscript submitted to Human Mutation

3.2.1. Abstract

Bardet-Biedl syndrome (BBS) is a multi-system disorder caused by ciliary defects. To date, mutations in 15 genes have been associated with the disease and *BBS1* is most frequently affected in BBS patients.

We identified the splice donor site (SD) mutation c.479G>A in *BBS1* exon 5 using homozygosity mapping in a large consanguineous family. Affected family members show retinitis pigmentosa (RP) and no other primary feature of BBS. In agreement with this exceptionally mild BBS phenotype, we did not detect obvious ciliary defects in patient derived cells.

SDs are bound by the U1 small nuclear RNA (U1) which initiates exon recognition during splicing. The mutation described herein interferes with U1 binding and induces aberrant splicing of *BBS1*. To improve interaction of U1 to the mutated SD, we have increased complementarity of the U1 snRNA with the mutated SD. Lentivrial treatment of patient-derived fibroblasts with adapted U1 partially corrects aberrant splicing of endogenously expressed *BBS1* transcripts. The therapeutic effect is dose-dependent. These results suggest that the adaptation of U1 to rescue pathogenic effects of splice donor site mutations has a high potential for gene therapy.

3.2.2. Introduction

Bardet-Biedl syndrome (BBS) constitutes a rare malformation syndrome which is primarily associated with retinal dystrophy, renal disease, polydactyly, obesity, hypogenitalism, and learning disabilities. In addition, secondary phenotypical features such as developmental delay, diabetes mellitus, dental and cardiovascular abnormalities, and hepatic involvement might occur in BBS patients. The diagnosis of BBS is usually established if the patient is affected by four primary features of the disease or by three primary plus two secondary features (Beales et al., 1999). The incidence of BBS has been estimated to be 1 individual in 120'000 live births in North America and Europe, although population-dependent variations are reported (Blacque and Leroux, 2006). In general, the inheritance of the disease follows an autosomal recessive pattern, but triallelic inheritance patterns have also been described (Katsanis et al., 2001). To date, 15 genes have been associated with the disease and approximately 20% of the cases are likely to be caused by mutations in additional genes (Zaghloul and Katsanis, 2009; Kim et al., 2010; www.genetests.org).

The Bardet-Biedl Syndrome 1 gene (*BBS1*) is most frequently affected in BBS patients. *BBS1* localizes to chromosome 11q 13.1 and is composed of 17 exons which encode a protein of 593 amino acids (reference sequence NM_024649). The N-terminal part of BBS1 shares homology with other BBS-associated gene products (BBS2 and 7) and predominantly localizes to the basal body / transitional zone of ciliated cells. BBS1 has been found in a heptameric complex with BBS2, BBS5, BBS7, BBS8 and BBS9 termed the BBSome and physically interacts with the GTP exchange factor Rabin8 (Nachury et al., 2007). These results suggested that Rabin8 helps to recruit the BBSome from neighboring centriolar satellites to the centrosome and activates the Rab8 small GTPase which seems to facilitate the fusion and docking of vesicles to the ciliary membrane (Leroux, 2007). It has been demonstrated recently that the interaction of Arl6 (*BBS3*) with the BBSome constitutes a coat for membrane proteins to be directed towards the cilium (Jin et al., 2010). However, the precise molecular function of the BBSome remains to be elucidated.

The mutational spectrum of *BBS1* includes the missense mutation p.M390R (Mykytyn et al., 2002) which accounts for the majority of pathogenic sequence alterations found in this gene and causes BBS in about 20% to 30% of unrelated individuals (Mykytyn et al., 2003; Beales et al., 2003). Together with a frequent mutation in *BBS10* (p.C91fsX95) (Stoetzel et al., 2006), up to 40% of the cases can be explained. Among

other mutations, splice site mutations have been described to cause BBS. Most frequently splice site mutations interfere with exon recognition in pre-mRNA transcripts and lead to exon skipping or intron retention. Most of these mutations are not characterized in detail, but missplicing of corresponding transcripts can be assumed. In the majority of disease genes, more than 15% of point mutations affect classical splice sites (Faustino and Cooper, 2003). Furthermore, an unexpectedly high number (up to 60%) of the exonic and intronic mutations are reported to have their primary pathogenic effect on splicing rather than on the deduced protein composition (Wang and Cooper, 2007). Together, these findings emphasize the importance of splice site mutations.

A mutation in a splice donor site (SD) often interferes with U1 snRNA (U1) binding to its pre-mRNA target which leads to aberrant splicing of the transcript. The recognition of the SD, is mediated by Watson-Crick base pairing of U1 and pre-mRNA templates (Zhuang and Weiner, 1986). Together with seven Sm and other complex-specific proteins U1 constitutes the U1 small nuclear ribonucleoprotein. This splice factor is capable of recruiting other components of the spliceosome to the SD to further promote splicing of the pre-mRNA (Wahl et al., 2009).

In order to overcome the pathogenic effect of SD mutations, we have developed a therapeutic approach for genes associated with eye diseases. Our approach uses the adaptation of U1 to increase recognition of the mutated SD. This therapeutic intervention corrected up to 90% of the misspliced transcripts that showed exon skipping (Tanner et al., 2009). In this report, we describe the identification and characterization of a SD mutation in *BBS1* that leads to missplicing of the transcript. Interestingly, the affected family members show retinal degeneration but no additional primary features. Furthermore, we show that the U1-mediated intervention can correct the mutation-induced splice defect not only in the minigene assay, but also in endogenous *BBS1* transcripts of patient-derived cell lines. In summary, the U1-mediated intervention is a promising therapeutic approach to treat the pathogenic effect of SD mutations.

3.2.3. Materials and Methods

Patients and clinical evaluation

Prior to the examination, informed consent was obtained from patients and unaffected control individuals after explaining the nature, aims and consequences of the study. Peripheral blood samples of 10 family members were collected and used for DNA extraction.

The index patient (IV:10), a 33 year old woman, was referred for genetic counselling of retinitis pigmentosa (RP) or related retinal diseases. Family history revealed multiple consanguineous marriages and a Turkish origin. The general medical history of the index patient and her affected sister was taken including prior surgeries, hospital admissions, education, past and present employments, learning difficulties, diabetes, blood pressure (mmHg), bodyweight (kg) and height (cm).

Ophthalmological evaluation of the patients included funduscopy in mydriasis, slit lamp examination, Ganzfeld-electroretinography (ERG), testing of best corrected visual acuity, optical coherence tomography and Goldmann kinetic perimetry (kinetic perimetry module on the Octopus 101 visual field testing device, Haag-Streit, Köniz, Switzerland) (Neidhardt et al., 2007).

To examine whether the RP phenotype in the affected family members was associated with additional features of BBS, a range of examinations were performed besides the ophthalmological examinations. In order to evaluate kidney and liver function and the hematologic system, both blood parameters (white and red blood cell count, creatinine, glucose, carbamide, uric acid, alkaline phosphatase) and urine parameters (urine status, creatinine, protein, glucose, sodium, potassium, phosphate, 24 hours urine collection, including protein and urine clearance) were examined. Gynaecological examinations of female patients included ultrasound of the reproductive system, hormonal status and medical history of pregnancies and life births. To exclude polydactyly and other limb anomalies, a careful examination of hands and feet was performed and photographs were taken.

Linkage analysis

To map the disease locus in the consanguineous family described herein, we genotyped 7 DNA samples using the Affymetrix GeneChip Human Mapping 250K Sty Array (Affymetrix, Santa Clara, CA). This array uses the Sty I restriction enzyme. Genotypes were called by the GeneChip DNA Analysis Software (GDAS v3.0,

Affymetrix). Genders of samples were verified by counting heterozygous SNPs on the X chromosome. Relationship errors were evaluated with the help of the program Graphical Relationship Representation (Abecasis et al., 2001). The program PedCheck was applied to detect Mendelian errors (O'Connell and Weeks, 1998) and data for SNPs with such errors were removed from the data set. Non-Mendelian errors were identified by using the program MERLIN (Abecasis et al., 2002) and unlikely genotypes for related samples were deleted. Nonparametric linkage analysis using all genotypes of a chromosome simultaneously was carried out with MERLIN. Parametric linkage analysis was performed by the program ALLEGRO (Gudbjartsson et al., 2000) assuming autosomal recessive inheritance with complete penetrance, a disease allele frequency of 0.0001. Haplotypes were reconstructed with ALLEGRO and presented graphically with HaploPainter (Thiele and Nurnberg, 2005). All data handling was performed using the graphical user interface ALOHOMORA (Ruschendorf and Nurnberg, 2005).

Mutation screening and RT-PCR analysis

We performed mutation screenings of both the rod outer membrane protein 1 (*ROM1*) and *BBS1* in 10 family members of the consanguineous RP family 26223. Genomic DNA from blood samples and cell lines were extracted as described previously (Neidhardt et al., 2007). We amplified all coding exons and parts of the flanking intronic regions of *ROM1* and *BBS1* by PCR and directly sequenced the PCR products. Using SeqScape Software 2.0 (Applied Biosystems, Rotkreuz, Switzerland), *ROM1* and *BBS1* sequence profiles were compared to reference data base entries NM_000327 and NM_024649, respectively (NCBI data base; http://www.ncbi.nlm.nih.gov/). Sequence alterations are described as recommended (guidelines published by the Human Genome Variation Society http://www.hgvs.org/mutnomen).

For RT-PCR analysis, we extracted total RNA from either cultured cells or blood samples using the RNeasy Mini Kit (Qiagene, Hombrechtikon, Switzerland) or PAXgene Kit (PreAnalytiX, Hombrechtikon, Switzerland). Total RNA was transcribed to cDNA by random priming according to the manufacturer's instructions (Superscript III reverse transcriptase; Invitrogen, Basel, Switzerland). RNA from cultured cells or blood derived from individuals IV:9, IV:10, and IV:11 of the consanguineous family (index patient 26223) was analyzed by RT-PCR using either

10, 100, or 300 ng of cDNA. For amplification of *BBS1* transcripts, we used primers specific to exon 4 and 8 of *BBS1* (BBS1-ex4dn: 5' GCCCCAATTGCCTCCAA ATCCT 3' and BBS1-ex8up: 5' GCATCCTCGTCAGCCAGGTTCTTC 3'). The result of the experiment was verified by at least 3 different replicates.

BBS1 minigenes and U1 snRNA expression constructs

Minigenes were generated by PCR amplification of the *BBS1* genomic region spanning intron 4 to 7 using ProofStart polymerase (Qiagen, Hombrechtikon, Switzerland). The PCR reaction was either performed with genomic DNA from affected or unaffected individuals using primers BBS1-ex5/6/7dn (5' ATGGCCATGAGACTGGATTCAGATA 3') and BBS1-ex5/6/7up (5' GGCTGGAAGGGATATAGCAAAGAGA 3'). PCR products were subcloned into the pCRII TOPO vector (Invitrogen). XhoI and BamHI restriction sites in the pCRII TOPO vector were utilized to transfer the insert into the minigene vector pSPL3 (Church et al., 1994).

To express wild type U1 snRNA, we used the vector pG3U1 which includes the sequences coding for human U1 snRNA (Lund and Dahlberg, 1984; Pagani et al., 2002). The U1 snRNA was adapted to the *BBS1* splice donor site and/or mutation of exon 5 by site-directed mutagenesis as previously described (Tanner et al., 2009). PCR reactions were performed with specific primers for each construct (U1 mut: pGU1Mutfwd and pGU1Mutrev (Tanner et al., 2009), U1-BBS1_wt: F_U1_BBS1_adpt: 5'CGAAGATCTCATTCTCACCGGGCAGGGGAGATACC 3' and R_U1_BBS1_adpt: 5'GCCTGATCATGGTATCTCCCCTGCCCGGTGAGAA 3'; U1-BBS1_mut: F_U1_BBS1_Mut_adpt: 5' CGAAGATCTCATTCTCACTGGGC AGGGGAGATACC 3' and R_U1_BBS1_Mut_adpt: 5'GCCTGATCATGGTATCTC CCCTGCCCAGTGAGAA 3').

COS-7 cells were cultured in Dulbecco's modified Eagle's medium (DMEM) supplemented with 10% FBS, 1.3% L-glutamine and 1.1% penicillin/streptomycin (PAA) at 37°C, 5% CO_2. $2*10^5$ cells/ml were cotransfected with either 2.4 µg wt or mut minigene and 2.4 µg U1 expression construct using branched polythyleneimine (PEI) (Sigma-Aldrich, Steinheim, Germany). cDNA was amplified by PCR using the forward primer SD6 (5'TCTGAGTCACCTGGACAACC 3') which binds the splice donor exon of pSPL3 and the reverse primer BBS1-ex7up binding to *BBS1* exon 7

(5'TGCCGCTTGATGGAGTTGGACTT3'). The RT-PCR reaction was performed with 300 ng cDNA at 66°C annealing temperature and 6 mM $MgCl_2$ using Hotfire polymerase (Solis Biodyne, Tartu, Estonia). The experiment was replicated on at least 3 independent transfections.

Cell culture of patient-derived fibroblasts and immunocytochemistry

Peripheral blood lymphocytes were isolated from whole blood samples by ficoll density gradient centrifugation and transformed with Epstein-Barr virus (EBV). EBV-transformed lymphoblastoid cell lines from *BBS1* mutation carriers IV:9, IV:10 and control IV:11 of family 26223 were cultured in RPMI 1640, 10% FBS, 1.1 % penicillin/ streptomycin, 1.3 % L-glutamine (PAA, Chemie Brunschwig AG, Basel, Switzerland) at 37°C, 5% CO_2.

Human dermal fibroblasts from individual IV:9, IV:10, and IV:11 were cultured as described (Villegas and McPhaul, 2005). Briefly, skin biopsies of about 5 mm^2 were prepared under sterile conditions and transferred to fibroblast culture medium consisting of MEM with 20% FBS, 1.3% L-glutamine (PAA), 0.8% Antibiotic-Antimycotic (Invitrogen). The biopsies were cut in smaller pieces of approximately 1 mm^2 and transferred to a sterile 25 cm^2 culture flask to adhere for 15 min without medium, followed by 5 to 8 days of incubation with fibroblast culture medium at 37°C and 5% CO_2. After primary fibroblasts covered 75% of the culture flask, the cells were trypsinized and transferred to 75 cm^2 flask for maintenance and experiments.

To induce formation of monocilia in fibroblasts, we deprived cell cultures (approximately 90% confluent) from fetal calf serum for 24 hrs. Immunohistochemistry was performed with polyclonal rabbit antibodies against detyrosinated alpha tubulin (Chemicon International, Europe) and mouse monoclonal gamma tubulin (Abcam, Cambridge, UK) to stain cilia and basal bodies, respectively. Cells were fixed in 4% paraformaldehyde, blocked in 1x DPBS (PAA) containing 2% BSA, incubated with a 1:200 dilution of primary antibodies in 1x DPBS over night at 4°C, followed by washing steps and incubation with Cy3 or Alexa-Fluor 488 conjugated secondary antibody (1:200 diluted; Dianova, Hamburg, Germany; Molecular probes, Leiden, Netherlands). Respiratory epithelial cells were obtained by transnasal brush biopsy, suspended in RPMI 1640 medium without supplements and spread onto glass slides. After air-drying, slides were stored at –80°C until use.

Samples were treated with 4% paraformaldehyde, 0.2% Triton-X 100, and 5% skim milk (all in PBS) before incubation with primary antibodies (mouse anti-acetylated-D-tubulin (Sigma); rabbit-anti-BBS1, kindly provided by N. Katsanis, Baltimore) and secondary antibodies (Alexa Fluor 488, Alexa Fluor 546; Molecular Probes) at room temperature. Slides were washed with PBS after each step and DNA was stained with Hoechst 33342 (Sigma). Appropriate controls were performed omitting the primary antibodies. Confocal images were taken on a Zeiss laser scanning microscope (Axiovert 200 LSM510 META) using a 63 x 1.2 numerical aperture water immersion objective, and were processed with the Zeiss LSM software.

Viral transduction of patient-derived fibroblasts

The genomic sequence of the human U1 snRNA expression cassette (Lund and Dahlberg, 1984) was cloned into the lentiviral expression plasmid pRRLSIN.cPPT.SFFV/GFP.WPRE (Brenner and Malech, 2003; Werner et al., 2004) using HpaI restriction sites. The expression plasmid was co-transfected with packaging plasmids pSPAX2 and pMD2.G into HEK293T cells using branched PEI (Sigma-Aldrich) and culture medium containing the secreted viral shuttles was harvested twice within 3 days. Fibroblasts were directly added to fibroblast culture medium supplied with lentiviral particles and grown in 6-wells at 37°C, 5% CO_2 for 3 to 4 days.

3.2.4 Results

Linkage

We collected DNA samples from a family of Turkish origin with multiple consanguineous marriages. The family pedigree suggested an autosomal recessive inheritance pattern and showed three family members affected by RP (Figure 1). Two of the affected family members were siblings (IV:9 and IV:10) and the third was the daughter of their cousin (V:1). The parents of the two siblings IV:9 and IV:10 were cousins, whereas consanguinity was not documented for the parents of the patient V:1.

To identify the chromosomal region that carries the causative mutation, we performed SNP homozygosity mapping including family members III:6, IV:3, IV:5, IV:7, IV:9, IV:10, and V:1. Significant linkage to a 5.6 Mb interval between SNP markers SNP_A-2212956 (rs10897271) and SNP_A-2224092 (rs7943216) on chromosome 11q12.3-11q13.1 was identified and showed a multipoint parametric LOD score of 3.08 for the RP phenotype (Figure 2). Within this region on chromosome 11, over 200 genes were annotated. Among these, genes associated with RP included *ROM1* and *BBS1*. Furthermore, refinement of the homozygosity mapping suggested a smaller region flanked by SNP markers SNP_A-2153886 (rs2226866) and SNP_A-2224092 (rs7943216) (data not shown). This smaller region excluded the *ROM1* locus from the interval on chromosome 11. In accordance with this finding, mutation screening did not identify sequence alterations in *ROM1*.

Mutation analysis of *BBS1*

The *BBS1* gene consists of 17 exons, which contain an open reading frame of 1782 bp and codes for 593 amino acids. We performed mutation analysis of all exons and flanking intronic regions of *BBS1* in the index patient IV:10 and identified the homozygous sequence alteration c.479G>A (NM_024649; Figure 3). The mutation affects the splice donor site (SD) of exon 5 and was confirmed to be homozygous in all RP affected family members (IV:9, IV:10, V:1). Six non-affected family members carried the mutation on one allele (II:3, III:1, III:6, IV:3, IV:5, IV:7). The unaffected husband of the index patient (IV:11) did not carry the mutation. Thus, the *BBS1* mutation c.479G>A cosegregates with the phenotype of RP (Figure 1).

The mutation affects the last base of exon 5 which strongly indicates an effect on pre-mRNA splicing of *BBS1* (Figure 3). Moreover, it is also predicted to substitute an arginine for a glutamine at position 160 (p.R160Q).

Clinical characterization of the patients' phenotype

BBS primarily includes features of retinal dystrophies, polydactyly, obesity, renal anomalies, learning disabilities, and genital abnormalities. The affected patients described herein were referred to ophthalmologic examination without any signs of additional features besides RP.

All patients examined had normal intraocular pressure and normal anterior segment morphology. Patients IV:9 and IV:10 showed RP with nightblindness present since early childhood, extinguished ERG, concentrically constricted visual fields, reduced visual acuity, bone spicules and attenuated vessels (Table 1). Both patients had similar phenotypes, although patient IV:9 appeared to have a clincially more progressed stage of the disease. OCT examination of patients IV:9 and IV:10 revealed a reduction of retinal thickness that was more pronounced in the periphery compared to the fovea (data not shown). The patients completed their compulsory school without any problems and were employed after finishing school. Due to increasing visual problems both patients IV:9 and IV:10 could not continue working at the age of 23 and 25 respectively. In patient IV:11 no signs of the disease were detected and all results of the clinical examinations were within normal ranges. Details are summarized in Table 1.

In summary, we did not find clinical evidence for BBS in patients IV:9 and IV:10, which showed RP without signs of polydactyly, obvious kidney defects, obesity or genital abnormalities.

Mutation-induced missplicing in *BBS1*

To analyze possible consequences of the mutation c.479G>A for *BBS1* splicing, we performed RT-PCR analysis on blood, EBV-transformed lymphocytes, and cultured skin fibroblasts of three family members (IV:9, affected, homozygous mutation carrier; IV:10, affected, homozygous mutation carrier; IV:11, unaffected, no carrier). RT-PCR analysis of IV:11 using primers to exon 4 and 8 resulted in a band at the expected size of about 300 base pairs (bp). In contrast, the two affected family members IV:9 and IV:10 showed three bands at approximately 400, 300, and 200 bp

(Figure 4). All three bands occurred in cDNA from blood, EBV-transformed lymphocytes, and fibroblasts. Sequencing of the RT-PCR products confirmed that the 300 bp band contains exons 4 through 8 without any indication of missplicing. The 400 bp band includes intron 5 in addition to constitutively spliced exons, whereas the 200 bp band skips exon 5 from the normal transcript. These results show that the mutation c.479G>A leads to missplicing of *BBS1*. Unexpectedly, the correctly spliced transcript at 300 bp is also found in samples of homozygous mutation carriers, although clearly reduced (Figure 4). The inclusion of intron 5 leads to a premature stop at the first inserted codon and skipping of exon 5 results in a frameshift followed by 20 BBS1-unrelated amino acids and a stop codon in exon 7. Thus, both misspliced transcripts are predicted to lead to a truncated BBS1 protein.

Analysis of cilia in patients with the homozygous *BBS1* mutation

The molecular pathomechanism underlying BBS is associated with ciliary defects. Depletion of *BBS1* has been shown to prevent the formation of cilia in cultured cells (Nachury et al., 2007).

Based on these observations, we analyzed monocilia of cultured fibroblasts from patients IV:9, IV:10, and IV:11. Fibroblasts were deprived from serum to induce generation of a monocilium on the surface of the cells. Immunocytochemical analysis of basal bodies and monocilia did not reveal an obvious ciliary defect in cell lines from affected patients (Figure 5A-D). We further analyzed cilia of patient-derived nasal epithelial cells (Figure 5E). The immunohistochemical staining for markers of the cilium and BBS1 in the transitional zone did not show obvious differences between affected and unaffected patient samples, thus confirming the results of the fibroblast culture.

Correction of mutation-induced missplicing in a *BBS1* minigene assay

Recently, we have shown that adaptation of U1 snRNA to a mutated splice donor site can efficiently rescue mutation-induced missplicing (Tanner et al., 2009). In order to simulate the splice processes as observed in the patient, we generated minigene constructs that consist of the genomic region of *BBS1* including intron 4 through 7. The minigenes either contained the wild-type (Mini-wt) or the mutated (Mini-mut) allele of IV:11 or IV:9, respectively (Figure 6A). The minigenes were transfected into COS-7 cells following RT-PCR amplification. We found that the splice patterns of

minigenes closely resemble the patterns identified in blood or cultured cells of either the control or patients (Figure 6C). PCR amplicons were analyzed by sequencing and confirmed splice products as detected in patient samples (intron 5 retention, normal splicing and exon 5 skipping).

To correct missplicing from *BBS1* minigenes, we adapted U1 with the aim to increase complementarity to the mutated SD sequence of *BBS1* exon 5. To optimize the efficiency of the U1 intervention, four different U1 snRNA expression constructs were generated (Figure 6B): 1) wild-type U1 (U1-wt), 2) U1 only adapted to the *BBS1* mutation c.479G>A (U1-mut), 3) U1 matching all nucleotides of the reference SD of *BBS1* exon 5 (U1-BBS1_wt), 4) U1 matching all nucleotides of the mutated SD (U1-BBS1_mut). These expression constructs were cotransfected with one of the two minigenes and splicing of minigene-derived *BBS1* transcripts was analyzed by RT-PCR (Figure 6C). The splice pattern from the minigene Mini-wt was neither altered by overexpression of wild type U1, nor by any of the differently adapted U1 isoforms. In contrast, the aberrant splice pattern from minigene Mini-mut was corrected by different U1 isoforms. Especially, U1-BBS1_wt as well as U1-BBS1_mut rescued missplicing of *BBS1* most efficiently and reverted the mutation-induced splice defect into a normal splice pattern (Figure 6C). Direct sequencing of correct *BBS1* transcripts confirmed appropriate splicing of the mutated transcript.

Correction of endogenously expressed *BBS1* transcripts

The minigene assay clearly showed that the splice defect can be corrected by the expression of a modified U1 with increased binding affinity to the mutated SD in *BBS1* exon 5. In order to test whether this approach is able to correct missplicing of endogenously expressed *BBS1* transcripts of patient-derived cell lines, we transduced fibroblasts using a lentiviral shuttle. The lentivirus contained the same U1 isoforms as used for the minigene assay. As evaluated by the co-expressed EGFP, the transduction efficiencies of the virus were within ranges between 90 to 100% (Figure 7A). Endogenously spliced *BBS1* transcripts from lentivirus-treated fibroblasts were analyzed by RT-PCR.

Upon treatment with fully adapted U1 (U1-BBS1_mut), a large increase in the amount of the correctly spliced *BBS1* transcripts and a clear reduction of *BBS1* lacking exon 5 was detected (Figure 7B). A smaller increase in the amount of correctly spliced transcripts was observed by the expression of U1-BBS1_wt. In contrast, expression of

U1-wt as well as U1-mut had no detectable effect on *BBS1* splicing. Importantly, treatment of control fibroblasts IV:11 with all of our adapted U1 isoforms did not alter splicing of *BBS1*. Sequence analysis confirmed that the corrected *BBS1* transcript is accurately spliced. Taken together, these results demonstrate that treatment with the fully adapted U1 isoform efficiently abolishes exon 5 skipping and largely increases the amount of correctly spliced *BBS1* transcripts in the patient-derived cell line.

To test whether elevated levels of fully adapted U1 (U1-BBS1_mut) can improve therapeutic effects, we treated the fibroblasts with increasing amounts of the lentiviral shuttles. In fibroblasts derived from affected patients (IV:9 and IV:10), the efficiency of the treatment increased with higher concentrations of the lentivirus (Figure 7C). A similar treatment with U1-wt or mock showed no detectable effect on splicing of *BBS1*. The control cell line (IV:11) revealed unaltered *BBS1* expression and splicing under all tested conditions and thus confirms that the treatment does not interfere with normal *BBS1* splicing. Together, our data demonstrate that the adaptation of U1 to a mutated SD is a promising gene therapeutic approach to correct splice defects

.

3.2.5. Discussion

BBS can be caused by mutations in at least 15 genes (Zaghloul and Katsanis, 2009; Kim et al., 2010). We identified the mutation c.479G>A in *BBS1* in a large consanguineous family of Turkish origin. The same mutation has previously been described in a patient of Caucasian origin, who was compound heterozygous with the mutation p.M390R (Hichri et al., 2005) and diagnosed with a clear BBS phenotype. In contrast, patients of the family described herein, suffer from RP showing no additional symptoms that would clearly support the clinical diagnosis of BBS. Similarly, the occurrence of isolated RP has been recently described for mutations in *BBS3* and *BBS8* (Aldahmesh et al., 2009; Riazuddin et al., 2010). It has further been reported that patients with mutations in *BBS1* may show milder BBS phenotypes with only one or two additional symptoms (Azari et al., 2006; Gerth et al., 2008).

The mode of inheritance in BBS can be multiallelic and the expression or penetrance of the phenotype is variable depending on the total load and type of mutations (Fauser et al., 2003; Fan et al., 2004; Katsanis, 2004; Pawlik et al., 2010). A case has been published where three nonsense mutations in *BBS2* and *BBS6* genes are required to cause a phenotype, whereas two nonsense mutations in *BBS2* alone did not lead to symptoms (Katsanis et al., 2001). These reports show that the mode of inheritance and the phenotypic expression in BBS can be highly variable.

As found in RP patients described in this study, both alleles carry the *BBS1* mutation c.479G>A. This results in aberrant splicing of the *BBS1* pre-mRNA and reduces the amount of correctly spliced transcripts. A residual level of normally spliced *BBS1* transcripts is generated even in homozygous carriers of the mutation. Consequently, the c.479G>A mutation may be considered as a mild mutation, which only reduces *BBS1* levels. The remaining amount of correctly spliced *BBS1* transcripts seems to be enough to maintain BBS1 function in most tissues of the patient, but fails to ensure survival of photoreceptors. This hypothesis is supported by the disease phenotype which only shows rod photoreceptor degeneration as seen in RP. Furthermore, we did not find obvious defects in generating basal bodies or cilia in patient-derived fibroblasts or nasal epithelia cells.

Photoreceptors are considered to have high demands for transport across the connecting cilium, a specialized nonmotile cilium which serves as a transition zone between inner and outer segments. The fact that about 2000 photopigment molecules have to be delivered to outer segments within a minute might explain the high

vulnerability of photoreceptors to defects in ciliary function (Badano et al., 2006). A mislocalization of rhodopsin has been detected in *Bbs2* knock-out mice which precedes apoptosis of rod photoreceptors (Nishimura et al., 2004). Furthermore, it has recently been shown that the BBSome is involved in transport of membrane proteins to cilia (Jin et al., 2010). These findings suggest a functional link between the ciliary transport, the activity of the BBSome, and the survival of photoreceptors.

The c.479G>A-induced splice defect of exon skipping and intron retention is likely caused by impaired interaction of the U1 with the mutated SD. We modified U1 in order to increase its binding affinity to the mutated transcript. In two different cell lines, our results revealed a significant increase of correctly spliced *BBS1* transcripts and a simultaneous reduction of exon 5 skipping. From these results, we conclude that an increase in the binding affinity of U1 snRNA to its target sequence leads to an efficient correction of splice defects. This is the first time that the U1 approach has been successfully used to treat endogenously expressed transcripts in cell lines derived from eye disease patients. In conclusion, the presented technique is a promising gene therapeutic approach to treat splice defects caused by a SD site mutation. This is particularly true for autosomal recessive diseases that might only need 50% of the gene dose to avoid the expression or progression of the disease.

The eye is an optimal target tissue for gene therapeutic treatments, because of its easy accessibility, transparency and immune privilege. Several different gene therapeutic strategies have been developed to treat inherited ocular diseases (Bainbridge, 2009; Stone, 2009) and important progress has been made using gene replacement therapy in human. Especially for Leber's congenital amourosis type 2 (LCA2), which involves retinal degeneration and severe vision loss in early childhood, three independent groups published the efficiency and safety of human gene therapy trials (Bainbridge et al., 2008; Cideciyan et al., 2008; Maguire et al., 2008). LCA can be caused by mutations in the *RPE65* gene which is expressed in RPE cells and responsible for the regeneration of rod photoreceptor visual pigment. To improve vision, wild-type *RPE65* was expressed by an AAV2-based vector and delivered to the eye of the patient by intraocular injections. In all three clinical trials, patients showed improvement in retinal functions. Furthermore, there was no significant systemic delivery of the vector or immunoreactive response detected upon exposure to the AAV vector, indicating high safety of the treatment.

In addition to gene replacement strategies, therapeutic approaches with the aim to restore pathogenic effects of mutation-induced aberrant splicing have been established using RNAi-based strategies or antisense oligonucleotides (Cooper et al., 2009). Nevertheless, the technique of U1 adaptation may have advantages compared to other gene therapeutic strategies: First, splice mutations are among the most frequent pathogenic sequence alterations. Around 15% of all point mutations are estimated to alter splice sites, an observation that is almost irrespective of the disease gene (Faustino and Cooper, 2003). Second, this method has the potential to be applied to different SD mutations requiring only simple modifications of the U1 binding sequence. Third, it simultaneously restores normal transcript levels and removes potentially pathogenic splice variants.

Taken together, we show that the use of mutation-adapted U1 can efficiently correct aberrant splicing in cell lines of affected patients. To further clarify the potential of this approach for gene therapy, it will be instrumental to test animal models.

3.2.6. Acknowledgements

We are grateful to Silke Feil for technical assistance and support of cell culture. We thank Gaby Tanner for assistance during cloning of *BBS1* minigenes. Furthermore, we would like to thank Arun Pal and Marino Zerial for providing the lentiviral vector backbone. We thank Nicolas Katsanis for providing the antibody against BBS1. The study was financially supported by the Velux Foundation, the Forschungskredit of the University of Zurich, Schweizerischer Fonds zur Verhütung und Bekämpfung der Blindheit, Hartmann Müller Foundation (to J.N.).

3.2.7. References

1. Abecasis,G.R., Cherny,S.S., Cookson,W.O., and Cardon,L.R. (2001). GRR: graphical representation of relationship errors. Bioinformatics. *17*, 742-743.

2. Abecasis,G.R., Cherny,S.S., Cookson,W.O., and Cardon,L.R. (2002). Merlin--rapid analysis of dense genetic maps using sparse gene flow trees. Nat. Genet. *30*, 97-101.

3. Aldahmesh,M.A., Safieh,L.A., Alkuraya,H., Al-Rajhi,A., Shamseldin,H., Hashem,M., Alzahrani,F., Khan,A.O., Alqahtani,F., Rahbeeni,Z., Alowain,M., Khalak,H., Al-Hazzaa,S., Meyer,B.F., and Alkuraya,F.S. (2009). Molecular characterization of retinitis pigmentosa in Saudi Arabia. Mol. Vis. *15*, 2464-2469.

4. Azari,A.A., Aleman,T.S., Cideciyan,A.V., Schwartz,S.B., Windsor,E.A., Sumaroka,A., Cheung,A.Y., Steinberg,J.D., Roman,A.J., Stone,E.M., Sheffield,V.C., and Jacobson,S.G. (2006). Retinal disease expression in Bardet-Biedl syndrome-1 (BBS1) is a spectrum from maculopathy to retina-wide degeneration. Invest Ophthalmol. Vis. Sci. *47*, 5004-5010.

5. Badano,J.L., Mitsuma,N., Beales,P.L., and Katsanis,N. (2006). The ciliopathies: an emerging class of human genetic disorders. Annu. Rev. Genomics Hum. Genet. *7*, 125-148.

6. Bainbridge,J.W. (2009). Prospects for gene therapy of inherited retinal disease. Eye (Lond) *23*, 1898-1903.

7. Bainbridge,J.W., Smith,A.J., Barker,S.S., Robbie,S., Henderson,R., Balaggan,K., Viswanathan,A., Holder,G.E., Stockman,A., Tyler,N., Petersen-Jones,S., Bhattacharya,S.S., Thrasher,A.J., Fitzke,F.W., Carter,B.J., Rubin,G.S., Moore,A.T., and Ali,R.R. (2008). Effect of gene therapy on visual function in Leber's congenital amaurosis. N. Engl. J. Med. *358*, 2231-2239.

8. Beales,P.L., Badano,J.L., Ross,A.J., Ansley,S.J., Hoskins,B.E., Kirsten,B., Mein,C.A., Froguel,P., Scambler,P.J., Lewis,R.A., Lupski,J.R., and Katsanis,N. (2003). Genetic interaction of BBS1 mutations with alleles at other BBS loci can result in non-Mendelian Bardet-Biedl syndrome. Am. J. Hum. Genet. *72*, 1187-1199.

9. Beales,P.L., Elcioglu,N., Woolf,A.S., Parker,D., and Flinter,F.A. (1999). New criteria for improved diagnosis of Bardet-Biedl syndrome: results of a population survey. J. Med. Genet. *36*, 437-446.

10. Blacque,O.E. and Leroux,M.R. (2006). Bardet-Biedl syndrome: an emerging pathomechanism of intracellular transport. Cell Mol. Life Sci. *63*, 2145-2161.

11. Brenner,S. and Malech,H.L. (2003). Current developments in the design of onco-retrovirus and lentivirus vector systems for hematopoietic cell gene therapy. Biochim. Biophys. Acta *1640*, 1-24.

12. Church,D.M., Stotler,C.J., Rutter,J.L., Murrell,J.R., Trofatter,J.A., and Buckler,A.J. (1994). Isolation of genes from complex sources of mammalian genomic DNA using exon amplification. Nat. Genet. *6*, 98-105.

13. Cideciyan,A.V., Aleman,T.S., Boye,S.L., Schwartz,S.B., Kaushal,S., Roman,A.J., Pang,J.J., Sumaroka,A., Windsor,E.A., Wilson,J.M., Flotte,T.R., Fishman,G.A., Heon,E., Stone,E.M., Byrne,B.J., Jacobson,S.G., and Hauswirth,W.W. (2008). Human gene therapy for RPE65 isomerase deficiency activates the retinoid cycle of vision but with slow rod kinetics. Proc. Natl. Acad. Sci. U. S. A *105*, 15112-15117.

14. Cooper,T.A., Wan,L., and Dreyfuss,G. (2009). RNA and disease. Cell *136*, 777-793.

15. Fan,Y., Esmail,M.A., Ansley,S.J., Blacque,O.E., Boroevich,K., Ross,A.J., Moore,S.J., Badano,J.L., May-Simera,H., Compton,D.S., Green,J.S., Lewis,R.A., van Haelst,M.M., Parfrey,P.S., Baillie,D.L., Beales,P.L., Katsanis,N., Davidson,W.S., and Leroux,M.R. (2004). Mutations in a member of the Ras superfamily of small GTP-binding proteins causes Bardet-Biedl syndrome. Nat. Genet. *36*, 989-993.

16. Fauser,S., Munz,M., and Besch,D. (2003). Further support for digenic inheritance in Bardet-Biedl syndrome. J. Med. Genet. *40*, e104.

17. Faustino,N.A. and Cooper,T.A. (2003). Pre-mRNA splicing and human disease. Genes Dev. *17*, 419-437.

18. Gerth,C., Zawadzki,R.J., Werner,J.S., and Heon,E. (2008). Retinal morphology in patients with BBS1 and BBS10 related Bardet-Biedl Syndrome evaluated by Fourier-domain optical coherence tomography. Vision Res. *48*, 392-399.

19. Gudbjartsson,D.F., Jonasson,K., Frigge,M.L., and Kong,A. (2000). Allegro, a new computer program for multipoint linkage analysis. Nat. Genet. *25*, 12-13.

20. Hichri,H., Stoetzel,C., Laurier,V., Caron,S., Sigaudy,S., Sarda,P., Hamel,C., Martin-Coignard,D., Gilles,M., Leheup,B., Holder,M., Kaplan,J., Bitoun,P., Lacombe,D., Verloes,A., Bonneau,D., Perrin-Schmitt,F., Brandt,C., Besancon,A.F., Mandel,J.L., Cossee,M., and Dollfus,H. (2005). Testing for triallelism: analysis of six BBS genes in a Bardet-Biedl syndrome family cohort. Eur. J. Hum. Genet. *13*, 607-616.

21. Jin,H., White,S.R., Shida,T., Schulz,S., Aguiar,M., Gygi,S.P., Bazan,J.F., and Nachury,M.V. (2010). The conserved Bardet-Biedl syndrome proteins assemble a coat that traffics membrane proteins to cilia. Cell *141*, 1208-1219.

22. Katsanis,N. (2004). The oligogenic properties of Bardet-Biedl syndrome. Hum. Mol. Genet. *13 Spec No 1*, R65-R71.

23. Katsanis,N., Ansley,S.J., Badano,J.L., Eichers,E.R., Lewis,R.A., Hoskins,B.E., Scambler,P.J., Davidson,W.S., Beales,P.L., and Lupski,J.R. (2001). Triallelic inheritance in Bardet-Biedl syndrome, a Mendelian recessive disorder. Science *293*, 2256-2259.

24. Kim,S.K., Shindo,A., Park,T.J., Oh,E.C., Ghosh,S., Gray,R.S., Lewis,R.A., Johnson,C.A., Attie-Bittach,T., Katsanis,N., and Wallingford,J.B. (2010). Planar cell polarity acts through septins to control collective cell movement and ciliogenesis. Science *329*, 1337-1340.

25. Leroux,M.R. (2007). Taking vesicular transport to the cilium. Cell *129*, 1041-1043.

26. Lund,E. and Dahlberg,J.E. (1984). True genes for human U1 small nuclear RNA. Copy number, polymorphism, and methylation. J. Biol. Chem. *259*, 2013-2021.

27. Maguire,A.M., Simonelli,F., Pierce,E.A., Pugh,E.N., Jr., Mingozzi,F., Bennicelli,J., Banfi,S., Marshall,K.A., Testa,F., Surace,E.M., Rossi,S., Lyubarsky,A., Arruda,V.R., Konkle,B., Stone,E., Sun,J., Jacobs,J., Dell'Osso,L., Hertle,R., Ma,J.X., Redmond,T.M., Zhu,X., Hauck,B., Zelenaia,O., Shindler,K.S., Maguire,M.G., Wright,J.F., Volpe,N.J., McDonnell,J.W., Auricchio,A., High,K.A., and Bennett,J. (2008). Safety and efficacy of gene transfer for Leber's congenital amaurosis. N. Engl. J. Med. *358*, 2240-2248.

28. Mykytyn,K., Nishimura,D.Y., Searby,C.C., Beck,G., Bugge,K., Haines,H.L., Cornier,A.S., Cox,G.F., Fulton,A.B., Carmi,R., Iannaccone,A., Jacobson,S.G., Weleber,R.G., Wright,A.F., Riise,R., Hennekam,R.C., Luleci,G., Berker-Karauzum,S., Biesecker,L.G., Stone,E.M., and Sheffield,V.C. (2003). Evaluation of complex inheritance involving the most common Bardet-Biedl syndrome locus (BBS1). Am. J. Hum. Genet. *72*, 429-437.

29. Mykytyn,K., Nishimura,D.Y., Searby,C.C., Shastri,M., Yen,H.J., Beck,J.S., Braun,T., Streb,L.M., Cornier,A.S., Cox,G.F., Fulton,A.B., Carmi,R., Luleci,G., Chandrasekharappa,S.C., Collins,F.S., Jacobson,S.G., Heckenlively,J.R., Weleber,R.G., Stone,E.M., and Sheffield,V.C. (2002). Identification of the gene (BBS1) most commonly involved in Bardet-Biedl syndrome, a complex human obesity syndrome. Nat. Genet. *31*, 435-438.

30. Nachury,M.V., Loktev,A.V., Zhang,Q., Westlake,C.J., Peranen,J., Merdes,A., Slusarski,D.C., Scheller,R.H., Bazan,J.F., Sheffield,V.C., and Jackson,P.K. (2007). A core complex of BBS proteins cooperates with the GTPase Rab8 to promote ciliary membrane biogenesis. Cell *129*, 1201-1213.

31. Neidhardt,J., Glaus,E., Barthelmes,D., Zeitz,C., Fleischhauer,J., and Berger,W. (2007). Identification and characterization of a novel RPGR isoform in human retina. Hum. Mutat. *28*, 797-807.

32. Nishimura,D.Y., Fath,M., Mullins,R.F., Searby,C., Andrews,M., Davis,R., Andorf,J.L., Mykytyn,K., Swiderski,R.E., Yang,B., Carmi,R., Stone,E.M., and Sheffield,V.C. (2004). Bbs2-null mice have neurosensory deficits, a defect in social dominance, and retinopathy associated with mislocalization of rhodopsin. Proc. Natl. Acad. Sci. U. S. A *101*, 16588-16593.

33. O'Connell,J.R. and Weeks,D.E. (1998). PedCheck: a program for identification of genotype incompatibilities in linkage analysis. Am. J. Hum. Genet. *63*, 259-266.

34. Pagani,F., Buratti,E., Stuani,C., Bendix,R., Dork,T., and Baralle,F.E. (2002). A new type of mutation causes a splicing defect in ATM. Nat. Genet. *30*, 426-429.

35. Pawlik,B., Mir,A., Iqbal,H., Li,Y., Nurnberg,G., Becker,C., Qamar,R., Nurnberg,P., and Wollnik,B. (2010). A Novel Familial BBS12 Mutation Associated with a Mild Phenotype: Implications for Clinical and Molecular Diagnostic Strategies. Mol. Syndromol. *1*, 27-34.

36. Riazuddin,S.A., Iqbal,M., Wang,Y., Masuda,T., Chen,Y., Bowne,S., Sullivan,L.S., Waseem,N.H., Bhattacharya,S., Daiger,S.P., Zhang,K., Khan,S.N., Riazuddin,S., Hejtmancik,J.F., Sieving,P.A., Zack,D.J., and Katsanis,N. (2010). A splice-site mutation in a retina-specific exon of BBS8 causes nonsyndromic retinitis pigmentosa. Am. J. Hum. Genet. *86*, 805-812.

37. Ruschendorf,F. and Nurnberg,P. (2005). ALOHOMORA: a tool for linkage analysis using 10K SNP array data. Bioinformatics. *21*, 2123-2125.

38. Stoetzel,C., Laurier,V., Davis,E.E., Muller,J., Rix,S., Badano,J.L., Leitch,C.C., Salem,N., Chouery,E., Corbani,S., Jalk,N., Vicaire,S., Sarda,P., Hamel,C., Lacombe,D., Holder,M., Odent,S., Holder,S., Brooks,A.S., Elcioglu,N.H., Silva,E.D., Rossillion,B., Sigaudy,S., de Ravel,T.J., Lewis,R.A., Leheup,B., Verloes,A., Amati-Bonneau,P., Megarbane,A., Poch,O., Bonneau,D., Beales,P.L., Mandel,J.L., Katsanis,N., and Dollfus,H. (2006). BBS10 encodes a vertebrate-specific chaperonin-like protein and is a major BBS locus. Nat. Genet. *38*, 521-524.

39. Stone,E.M. (2009). Progress toward effective treatments for human photoreceptor degenerations. Curr. Opin. Genet. Dev. *19*, 283-289.

40. Tanner,G., Glaus,E., Barthelmes,D., Ader,M., Fleischhauer,J., Pagani,F., Berger,W., and Neidhardt,J. (2009). Therapeutic strategy to rescue mutation-induced exon skipping in rhodopsin by adaptation of U1 snRNA. Hum. Mutat. *30*, 255-263.

41. Thiele,H. and Nurnberg,P. (2005). HaploPainter: a tool for drawing pedigrees with complex haplotypes. Bioinformatics. *21*, 1730-1732.

42. Villegas,J. and McPhaul,M. (2005). Establishment and culture of human skin fibroblasts. Curr. Protoc. Mol. Biol. *Chapter 28*, Unit.

43. Wahl,M.C., Will,C.L., and Luhrmann,R. (2009). The spliceosome: design principles of a dynamic RNP machine. Cell *136*, 701-718.

44. Wang,G.S. and Cooper,T.A. (2007). Splicing in disease: disruption of the splicing code and the decoding machinery. Nat. Rev. Genet. *8*, 749-761.

45. Werner,M., Kraunus,J., Baum,C., and Brocker,T. (2004). B-cell-specific transgene expression using a self-inactivating retroviral vector with human

CD19 promoter and viral post-transcriptional regulatory element. Gene Ther. *11*, 992-1000.

46. Zaghloul,N.A. and Katsanis,N. (2009). Mechanistic insights into Bardet-Biedl syndrome, a model ciliopathy. J. Clin. Invest *119*, 428-437.

47. Zhuang,Y. and Weiner,A.M. (1986). A compensatory base change in U1 snRNA suppresses a 5' splice site mutation. Cell *46*, 827-835.

3.2.8. Figures and Tables

Table 1 Clinical examinations of family members IV:9, IV:10, and IV:11

		Patient		
		IV:9	IV:10	IV:11
Demographic	Year of birth	1981	1974	1964
	gender	female	female	male
	height in cm	168	167	172
	BMI in kg/m^2	28.7	28.6	27.0
Diabetes mellitus		none	gestational diabetes in the second pregnancy	none
Limbs		No polydactyly, no other anomalies	No polydactyly, no other anomalies	No polydactyly, no other anomalies
Eye	night blindness	present since childhood	present since childhood	none
	VA (OD - OS)	20/800 - 20/400	20/400 - 20/200	20/20 - 20/20
	IOP (OD - OS)	12 - 12	12 - 14	14 - 14
	anterior segment	normal morphology	normal morphology	normal morphology
	fundus	bone spicules, attenuated vessels, epiretinal gliosis, atrophic retina, pale discs	bone spicules, narrowed vessels, atrophic retina, pale discs	normal
	ERG	extinguished	extinguished	normal rod- and cone-driven signals
	Visual field	severely concentrically constricted	severely constricted with only a small central island left	normal
Kidney	lab tests	within normal ranges	within normal ranges	within normal ranges
Liver	lab tests	within normal ranges	within normal ranges	within normal ranges
Hematologic system	lab tests	within normal ranges	within normal ranges	within normal ranges
Reproductive system	Ultrasound, hormonal status	irregular menstrual cycle, otherwise normal	normal, 2 healthy children with IV:11	normal, 2 healthy children with IV:10

BMI: Body Mass Index (weight in kg / (height in m)^2); VA: Visual acuity; IOP: Intraocular pressure in mmHg; ERG: Ganzfeld Electroretinography

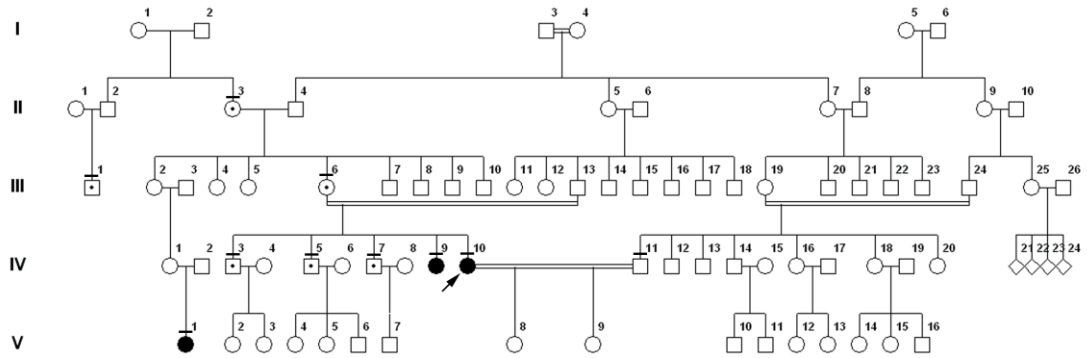

Figure 1 Pedigree of the consanguineous family 26223 segregating RP. Filled symbols represent affected family members whereas symbols with dots represent unaffected mutation carriers. Double lines indicate consanguinity. Analyzed patients are marked by horizontal bars

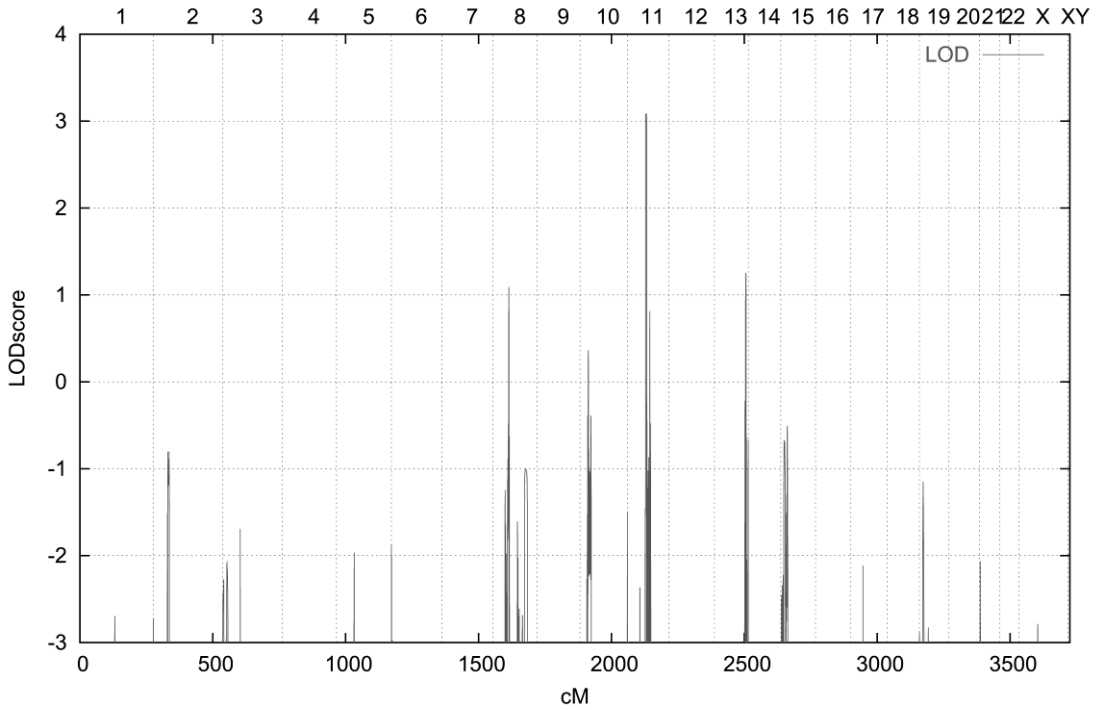

Figure 2 LOD scores across the genome for the RP phenotype in family 26223. Genetic map position (cM) and chromosome numbers are displayed horizontally. LOD scores are indicated on the vertical axis.

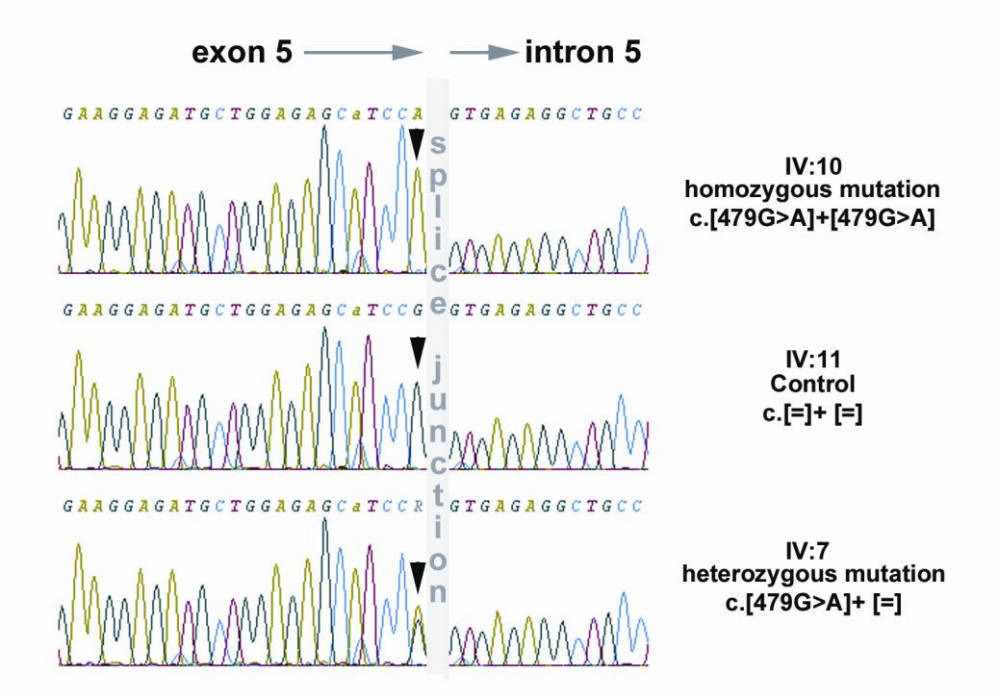

Figure 3 Electropherograms of parts of the exon/intron boundary containing the mutation c.479G>A found in *BBS1* exon 5 of affected family members. Three different electropherograms are shown representing homozygous (IV:10) and heterozygous (IV:7) mutations carriers as well as an unaffected family member (IV:11). The position of the mutation is marked by an arrow head. The exon/intron boundary at the *BBS1* exon 5 splice donor site is depicted as splice junction.

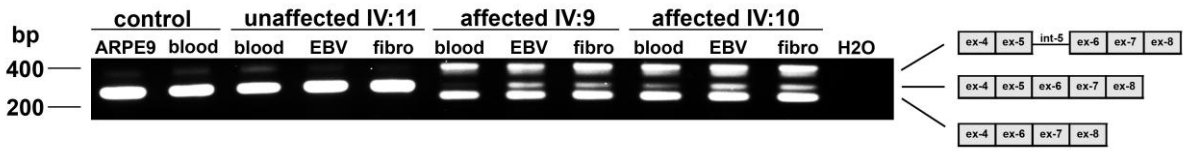

Figure 4 Amplification of *BBS1* transcripts in affected family members. RNA from blood, ARPE9, EBV-transformed lymphoblast (EBV) or fibroblast (fibro) cells from different family members was analyzed by RT-PCR using primers in exon 4 and exon 8. RT-PCR reaction lacking a template is indicated by H_2O. DNA marker sizes are given in base pairs (bp). Detected splice isoforms are illustrated by schematic drawings.

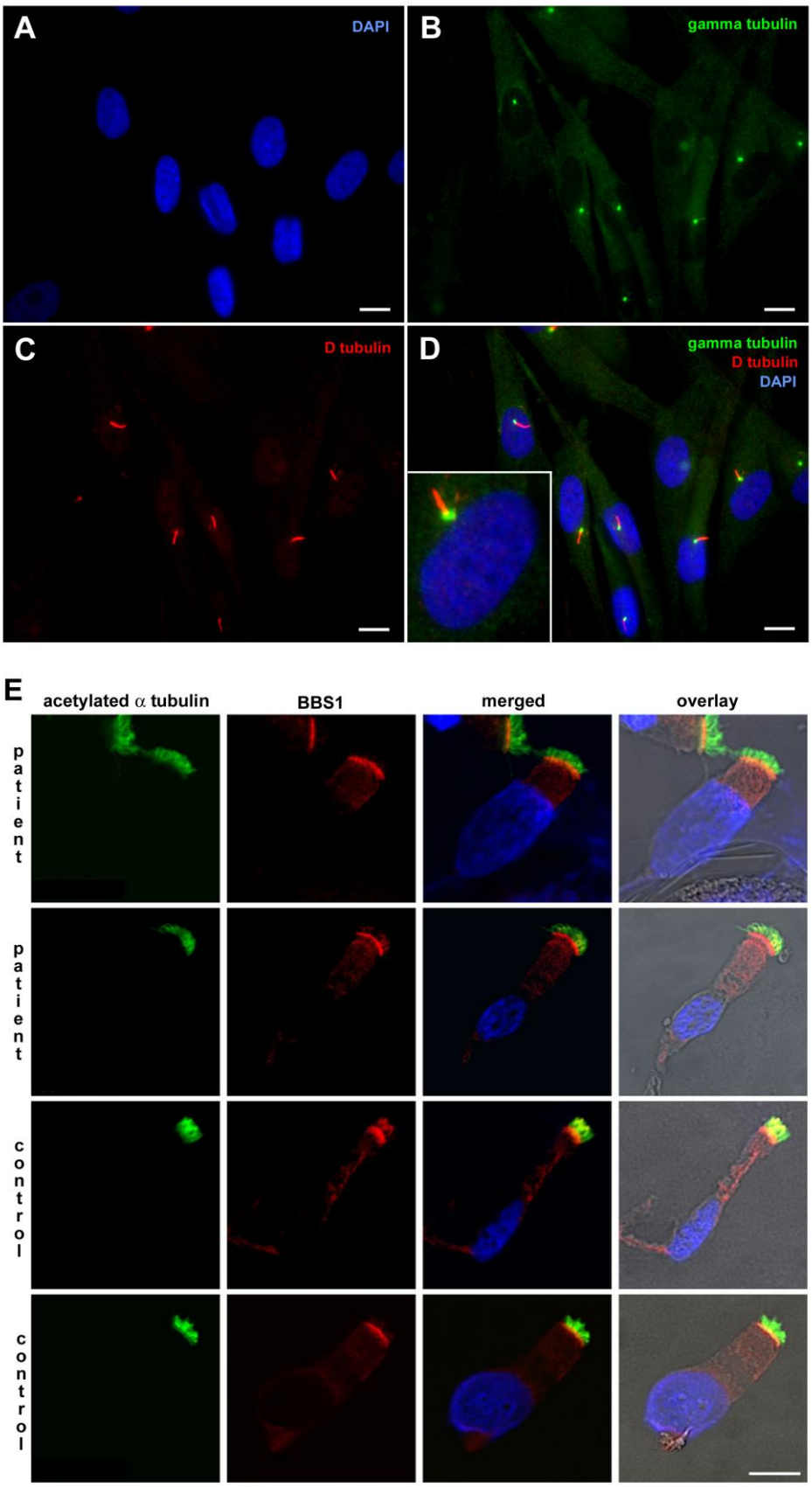

Figure 5 Immunostaining of patient-derived fibroblasts to detect cilia. Fluorescence images of serum-starved cells stained with **A** DAPI, **B** anti gamma tubulin, **C** anti D-tubulin are merged in **D**. **E** Patient-derived epithelial cells extracted from nose by brushing were stained with antibodies against acetylated α-tubulin or BBS1. Scale bars represent sizes of 10 μm.

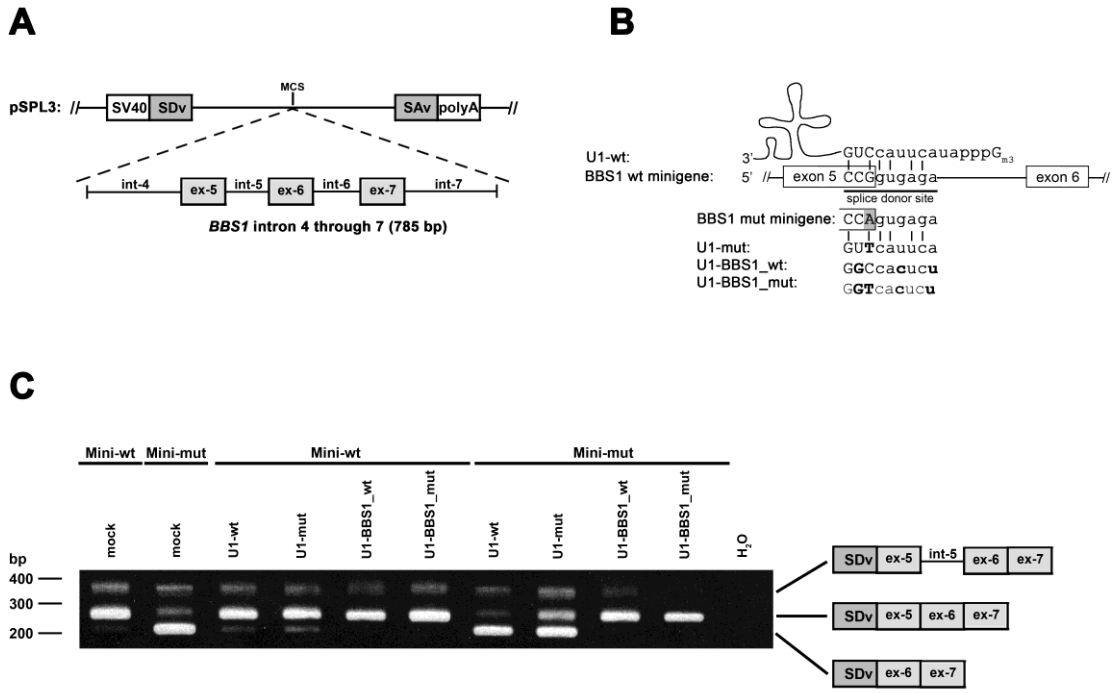

Figure 6 Amplification of minigene-derived *BBS1* transcripts by RT-PCR. **A** Graphical illustration of the minigene construct in pSPL3 containing the human genomic sequence of *BBS1* spanning intron 4 to 7. SDv: vector-derived splice donor; SAv: vector-derived splice acceptor. **B** Molecular interaction of wild-type U1 (U1-wt) with the splice donor site (SD) of *BBS1* exon 5. Watson and Crick base pairing is indicated by vertical lines. The position of the mutation c.479G>A in the mutated minigene (Mini-mut) is highlighted in gray. In addition to the construct expressing the U1-wt, we generated different modifications of U1 effecting its SD binding sequence: U1-mut (U1 adapted to the mutation c.479G>A only), U1-BBS1_wt (U1 adapted to the reference SD of *BBS1* exon 5) and U1-BBS1_mut (U1 fully adapted to the mutated SD). Adaptations of the SD are illustrated in bold letters. **C** Rescue of minigene-derived *BBS1* missplicing by co-transfection of wild type (Mini-wt) or mutated minigenes (Mini-mut) with adapted U1 isoforms or empty vector (mock) in COS-7 cells. RT-PCR reaction lacking a template is indicated by H_2O. DNA marker sizes are given in base pairs (bp). Detected splice isoforms are illustrated by schematic drawings.

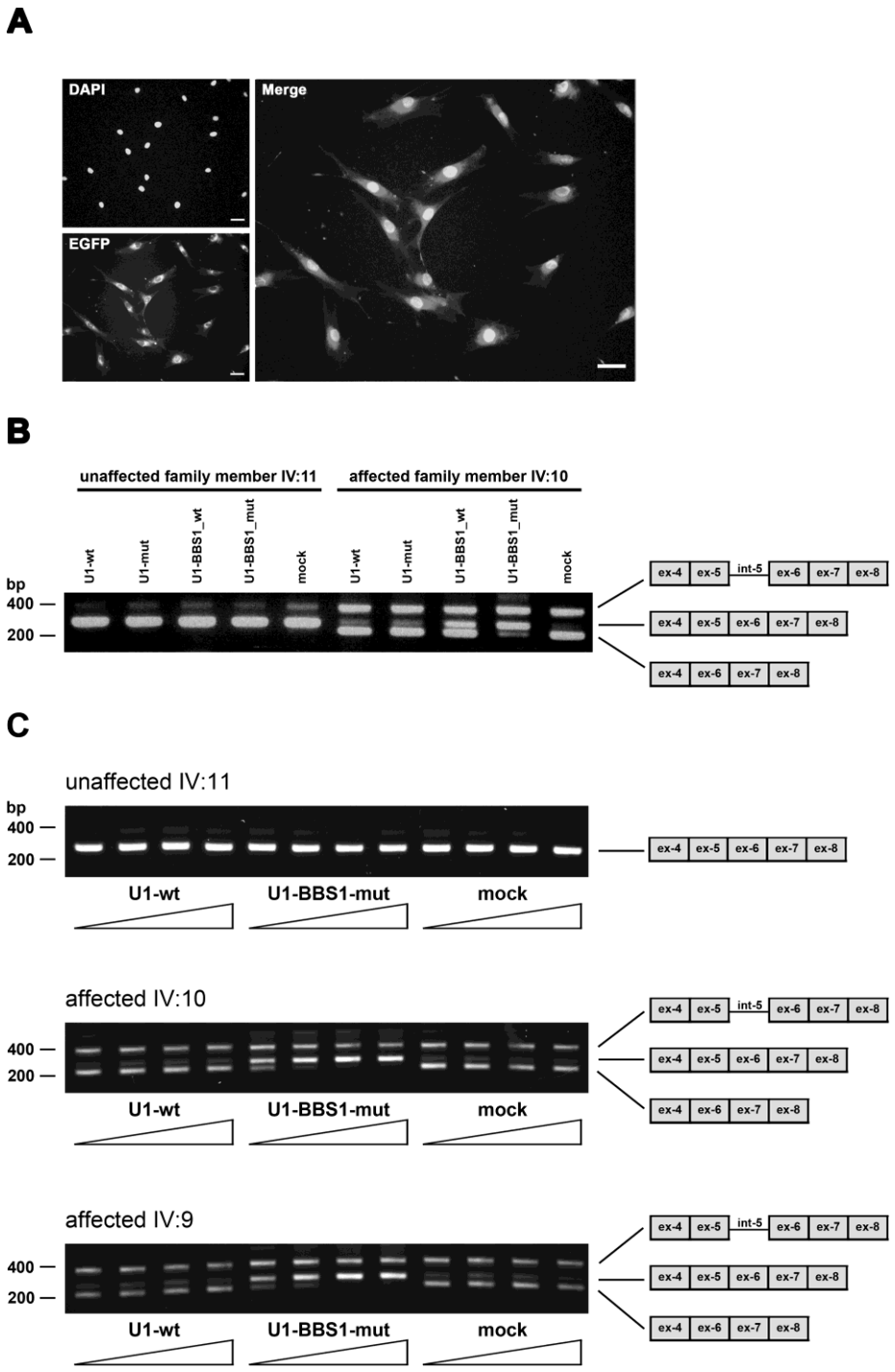

Figure 7 Correction of endogenously expressed *BBS1* transcripts in patient-derived fibroblasts. Cells were transduced with lentiviral vectors expressing adapted U1. **A** Fluorescence microscopy image of fibroblast cells transduced with lentiviral vectors expressing modified U1 and EGFP. Scale bars represents sizes of 100 μm. **B** RT-PCR amplification of exons 4 to 8 of endogenous *BBS1* transcripts in transduced fibroblasts from patient IV:10. Fibroblasts transduced with lentiviral particles containing no U1 are designated as mock. DNA marker sizes are given in base pairs (bp). **C** Stepwise increase of the amount of lentiviral shuttles containing fully adapted U1 to achieve higher correction efficiencies. Fibroblasts from patients IV:9 and IV:10 and the unaffected control IV:11 were transfected with either 1 ml, 3 ml, 6 ml or 9 ml culture medium containing lentiviral shuttles. Either wild-type U1 (U1-wt), fully adapted U1 (U1-BBS1_mut) or no U1 (mock) was encoded by the lentivirus. DNA marker sizes are given in bp. Detected splice isoforms are illustrated by schematic drawings.

3.2.9. Own contribution to the manuscript “U1 snRNA-mediated gene therapeutic correction of splice defects caused by an exceptionally mild BBS mutation”

Cell culture, adapting U1 snRNA, lentivirus production, transfection and transduction, evaluation of transduction efficiency, RT-PCR analysis of minigene-derived and endogenous *BBS1* splicing, contributions to data interpretation and manuscript writing

3.3. Search for downstream target genes of BBS1

Fabian Schmid [1], Ute Boettinger [1], Wolfgang Berger [1], John Neidhardt [1*]

[1] University of Zurich, Institute of Medical Molecular Genetics, Schorenstrasse 16, 8603 Schwerzenbach, Switzerland.

*Corresponding author

Manuscript in preparation

3.3.1. Abstract

We have identified a splice donor site mutation in the Bardet-Biedl-Syndrome 1 gene (*BBS1*) and characterized its effect on splicing of *BBS1*. The mutation was homozygous in three members of a consanguineous family affected by retinitis pigmentosa. By overexpression of a modified isoform of the U1 snRNA (U1), which features full complementary to the mutated splice donor site, we could significantly increase the amount of normal *BBS1* transcripts in patient derived fibroblasts. The correction of the splice defect might also result in altered expression of downstream targets or BBS1 interaction partners. In addition, the expression of the modified U1 might not only restore correct *BBS1* splicing, but may also interfere with normal splicing of other genes. Thus, we aimed to understand possible consequences of the treatment and focused on effects at the transcript level. To assess pre-mRNA splicing in treated fibroblasts from the patient, we used the Human Exon 1.0 ST array chip comparing the fully adapted U1 with the wild-type U1 treatment. The outcome of the study revealed only mild effects on splicing of non-target mRNAs upon treatment with fully adapted U1, especially for retinopathy-associated genes. Nevertheless, possible consequences of this therapeutic approach need to be further investigated with particular focus on retinal cells. Furthermore, we identified *CKAP5* as a potential downstream target gene the expression of which might be controlled by the function of BBS1.

3.3.2. Introduction

Bardet-Biedl syndrome (BBS) is a pleiotropic disorder affecting functions of cilia in different tissues. So far, all mutations found in *BBS1* cause BBS (Zaghloul and Katsanis, 2009). BBS1 has been found in a complex together with six other BBS proteins, called the BBSome (Nachury et al., 2007). One of its assumed cellular functions is the transport of membrane proteins to cilia (Jin et al., 2010). Cilia are present on many human cell types where they accomplish different functions. Mutation-induced dysfunctions of the cilium may cause the different disease symptoms associated with BBS.

We have previously identified a splice defect in patients with RP having a homozygous splice donor site (SD) mutation in *BBS1* (c.479G>A, p.Arg160Gln). The mutation leads to reduced levels of correctly spliced transcripts and skipping of exon 5. Moreover, we have developed a gene therapeutic approach using an adapted form of the U1 snRNA (U1) to correct the splice defect (see Results 3.2.4., page 77).

U1 interacts with splice donor sites in a pre-mRNA transcript through RNA base pairing and recruits other component of the spliceosome to initiate splicing (Wahl et al., 2009). In addition, it has been found that binding of U1 to the splice donor can be impaired by mutations (Zhuang and Weiner, 1986). In order to increase binding affinity and subsequent recognition of the exon, we modified U1 to have perfect complementarity to the mutated SD of *BBS1* exon 5 in the patients. Treatment with this fully adapted U1 (U1-BBS1_mut) significantly increased the amount of correctly spliced transcripts and abolished exon 5 skipping (see Results 3.2.4., page 80). Because the expression of an adapted form of U1 might affect splicing of other genes, we performed global analysis of splicing in patient derived fibroblast treated with either wild-type U1 (U1-wt) or U1-BBS1_mut using the Human Exon 1.0 ST array chip (Affymetrix). This gene expression array contains 1.4 million probe sets that cover exonic as well as intronic pre-mRNA sequences enable the detection of splice defects in almost all human gene transcripts. First results derived from this analysis revealed effects on splicing of only a few genes after a treatment with U1-BBS1_mut compared with U1-wt (Boettinger, 2009, Master Thesis).

Many studies reported that the primary cilium can influence the activity of serveral signaling pathways (Singla and Reiter, 2006; Lancaster and Gleeson, 2009; Goetz and Anderson, 2010). Based on these findings, we assumed that reduced levels of *BBS1* as found in the patients, might also affect transcription of target genes regulated by these

pathways in our patients. The exon array data served as the primary source to search for genes the expression of which might be regulated through the ciliary function of *BBS1*. Since increased levels of normal *BBS1* transcripts were obtain by the U1-BBS1_mut treatment, but not with U1-wt, a comparison of these two treatments could identify potential candidates regulated by the amount of BBS1 protein. The analysis of the expression of selected candidate genes using RT-PCR detected genes that have the potential to genetically and functionally interact with BBS1.

3.3.3. Methods and Results

Selection of potential candidate genes

In samples analyzed by the Human Exon 1.0 ST array, the correction efficiency of the splice defect mediated by U1 was confirmed by RT-PCR analysis. We detected higher frequencies of exon 5 inclusion after the U1-BBS1_mut treatment compared to U1-wt within a range between fold changes of - 0.9 and + 0.9 (Figure 1A). This result suggested a high reliability for the array data on exon level within this range.

In contrast, to find differences on the level of gene expression, the data from the Human Exon 1.0 ST array was processed at the Functional Genomics Center Zurich (FGCZ) by averaging all corresponding exonic probe sets of a gene. Thereby, a list of all genes showing their differences in expression between U1-wt (calibrator sample) and U1-BBS1_mut in patient IV:9 with corresponding p-values calculated from 3 replicates was created. We restricted our analysis to entries showing either fold changes lower than - 0.9 or higher than + 0.9 (Supplementary Table 1). Among that list, many genes were not consistently annotated comparing ENSEMBL and Entrez Gene (NCBI) databases. Therefore, we primarily selected genes that were validated as protein coding and correctly annotated in both databases. These selection criteria reduced the amount of candidates to 11 genes (Table 1, upper part).

Because fold changes on the level of gene expression might not be representative due to a loss of data during processing, we additionally sorted the raw list for p-values smaller than 0.05 and excluded genes with fold changes lower than 0.5. This created another list containing 286 genes (Supplementary Table 2) from which 10 potential candidates were selected (Table 1, middle part).

Since it is known that the primary cilium can influence activity of several signaling pathways, we extended our data analysis to select for genes clustered in the same signaling cascade. In order to find these, we used the GeneGo MetaCore (http://www.genego.com; open access through FGCZ) software focusing on pathways controlling cytoskeletal remodeling and cell cycle progression. We were also interested in genes of the canonical Wnt pathway, because it has been reported that the amount of functional BBS1 protein can influence Wnt signaling activity (Gerdes et al., 2007). Altogether, another 7 potential candidate genes have been selected (Table 1, lower part) which extended our list up to 28 potential candidate genes which we further analyzed by RT-PCR (Table 1).

Expression analysis of selected genes upon different U1 treatments

To verify changes in expression levels of candidate genes selected from the exon array data, we have established several RT-PCR assays. RT-PCR conditions and primer sequences are given in Supplementary Table 3. Reactions were performed on RNA from fibroblasts of patient IV:9 and IV:10 affected by the splice donor site mutation (c.479G>A) in *BBS1* and a unaffected control (IV:11) from the same family. The control was used to eliminate genes showing unspecific effects not due to increased *BBS1* transcript levels. Fibroblast cell lines were transduced with increasing amounts (1 ml, 3 ml, 6 ml, 9 ml) of lentiviral shuttles expressing either no U1 (mock), U1-wt or U1-BBS1_mut (see Results 3.2.4., page 80). The high increase of normal *BBS1* transcript levels found in both patient cell lines upon the U1-BBS1_mut treatment (Figure 1B) provides the basis to look for genetic interaction partners.

Expression analysis of selected candidate genes in transduced fibroblasts from patient IV:9 and a control detected several effects on transcript expression. We found that many genes showed differences in expression levels between control and patient. Furthermore, we could also identify adverse effects in patient and control, which were not specific to the U1-BBS1_mut treatment and caused a decrease of transcript levels in most of the cases (Table 2; Supplementary Figures 1-6). Interstingly, for two genes, *CCDC162* (coiled-coil domain containing 162 pseudogene) and *GRAP* (GBR2-related adaptor protein), we found higher expression levels (Supplementary Figure 1) which were specific for the U1-BBS1_mut treatment.

In contrast to the effects described above, *AP1S2* (adaptor-related protein complex 1, sigma subunit 2), *CKAP5* (cytoskeleton associated protein 5), *TCF4* (transcription factor 4) and *IDE* (insulin degrading enzyme) appeared to be reduced only in the patient upon the treatment with U1-BBS1_mut. In addition, expression levels of these genes were different between patient and control, thus making them good candidates to be regulated by BBS1 (Table 2; Supplementary Figures 2-4).

Confirmation of results in different fibroblast cell lines

To verify the significance of our findings we treated fibroblasts from the other patient (IV:10) and another control (Control II) accordingly. For *AP1S2*, *TCF4* and *IDE* we now detected changes in the expression level upon treatment with U1-BBS1_mut and/or mock in both cell lines indicating possible adverse effects (Figure 2). Interestingly, we again found changes in *CKAP5* expression upon treatment with U1-

BBS1_mut but only minor effects using mock in the patient. In contrast, the control showed no obvious effect among all treatments (Figure 2). In summary, these results still suggest that *CKAP5* expression might be specifically regulated through the amount of BBS1.

Quantification of lentiviral copy numbers in treated fibroblasts

The results from the expression analysis also indicated that lentiviral shuttles themself could affect the expression of certain genes. In order to compare treatments with similar lentivirus copy numbers, we quantified the amount of integrated proviral DNA into the host genome in transduced fibroblasts. To do so, we used a quantitative real-time PCR method which has been previously described (Lizee et al., 2003). For every cell line, we were able to find conditions with copy numbers of integrated proviral DNA at comparable levels among the different treatments (Figure 3). Under these conditions, we identified slight differences in *AP1S2* and *TCF4* transcript expression between U1-wt and U1-BBS1_mut treatments (asterisks in Figure 2 and Supplementary Figures 2 and 3), whereas for *IDE* we observed again a decrease upon treatment with U1-BBS1_mut in both cell lines (asterisks in Figure 2 and Supplementary Figure 4). Interestingly, expression levels of *CKAP5* transcripts were significantly reduced in both patients upon treatment with U1-BBS1_mut, but not or only slightly in the two controls (asterisks in Figure 2 and Supplementary Figure 4), still making *CKAP5* a good candidate gene to be regulated by BBS1.

3.3.4. Discussion

Most of the data from the exon array was in accordance with our results gained by the RT-PCR assays. However, for a few cases we were not able to confirm the data. Although olfactory receptor genes revealed high differences between expression levels among U1-wt and U1-BBS1_mut in the exon array, we could not detect any amplification product by RT-PCR. This result is not very surprising, because these receptors are specifically expressed in olfactory receptor neurons of the dorsal nasal cavity in human (Su et al., 2009) and thus, not found in fibroblasts of the skin. It still remains an open question why these genes seemed to be expressed according to the exon array data.

Many of the tested genes revealed only slight alterations in transcript expression due to U1-BBS1_mut and/or mock treatment. However, the impact of these adverse effects especially on the viability of retinal cells has to be further evaluated. For genes which reacted upon both U1-BBS1_mut and mock treatment, we conclude that integration of lentiviral shuttles alone must have a significant effect on their expression level. In particular, we assume that high amounts of integrated proviral DNA might influence cell cycle progression and thus also the expression of genes involved in this process.

Expression level changes detected only upon U1-BBS1_mut treatment in controls and patient-derived fibroblasts indicate that the fully adapted U1 snRNA might interfere with correct pre-mRNA splicing of non-target genes. These adverse effects showed either an increase or decrease in mRNA expression. We speculate that alterations in splicing induced by the U1-BBS1_mut treatment might lead to premature termination codon (PTC) containing gene transcripts which are subject to degradation by nonsense-mediated mRNA decay (NMD). The involvement of NMD in this process might be a reasonable explanation for the observed reduction of whole transcript levels upon U1-BBS1_mut treatment. In contrast, we have found an increase of transcript levels for *GRAP* and *CCDC162*. This finding can be explained through NMD too. In this case, U1-BBS1_mut might interfere with pre-mRNA splicing of genes that represent negative transcriptional regulators of *CCDC162* and *GRAP* leading finally to their degradation by NMD. For the latter, it is reasonable to suppose that the gene targeted by the fully adapted U1 snRNA is somehow involved in TGF-β signaling, because it is mentioned that this pathway regulates expression of *GRAP*

in cultured renal tubule cells (Cummins et al., 2010). However our exon array analysis did not identify a U1-BBS1_mut mediated reduction in the expression of genes involved in TGF-β signaling which would further support this idea. The identification of genes controlling expression of *GRAP* or *CCDC162* will help to further elucidate their cellular functions. We can not exclude that other NMD-independent mechanisms also cause the observed side effects.

The only gene that seemed to be significantly downregulated by higher amounts of *BBS1* was *CKAP5*. Since it has been demonstrated in different vertebrate cell types that BBS1 is important for correct functioning of the primary cilium (Kulaga et al., 2004; Gerdes et al., 2007; Shah et al., 2008; Tayeh et al., 2008), it is possible that *CKAP5* might be regulated by the activity of this organelle, rather than by the function of BBS1 itself. This might also hold true for other genes which could be regulated by BBS1. CKAP5 was primarily identified as overexpressed in human hepatomas and colonic tumors (Charrasse et al., 1995) and appeared to be a crucial player in spindle pole assembly and centrosome integrity (Gergely et al., 2003; Cassimeris and Morabito, 2004). Furthermore, the protein is annotated in the ciliary proteome database (http://www.ciliaproteome.org; Gherman et al., 2006) suggesting a functional link between CKAP5 and the cilium. Nevertheless, to verify the significance of these findings expression levels of *CKAP5* upon treatment of U1-wt, U1-BBS1_mut and mock have to be evaluated by quantitative real-time RT-PCR. Moreover, we have also detected slight effects on *CKAP5* expression, which were exclusively due to the lentiviral vector. To further clarify the correlation between BBS1 and CKAP5, it will be crucial to check whether *CKAP5* becomes upregulated upon RNAi-mediated *BBS1* knockdown in fibroblasts of healthy, unaffected individuals. The outcome of that experiment will finally help to clarify whether *CKAP5* is really regulated through the activity of BBS1 and will gain more insight into the function of CKAP5 and its connection with the primary cilium.

A comparison of data gained by a whole expression analysis in *BBS1* depleted cells with the data from the exon array will simplify our search for other candidate genes. The identification of these genes might extend our knowledge about the functions of the primary cilium and BBS1, and could also increase the number of genes associated with ciliopathies.

3.3.5. Acknowledgements

We are grateful to thank Esther Glaus for cloning lentiviral U1 snRNA constructs. Additional thanks goes to Catharine Aquino and Michal Okoniewski, two members of the Functional Genomics Center Zurich (FGCZ), who assisted us using the Human Exon 1.0 ST array chip. The study was funded by the Velux Foundation, the Forschungskredit of the University of Zurich, Schweizerische Fonds zur Verhütung und Bekämpfung der Blindheit, and the Hartmann Müller Foundation (to J.N.).

3.3.6. References

1. Boettinger, U. (2009). Nebenwirkungen eines therapeutischen Ansatzes zur Behandlung von pathogenem Exonverlust mittels U1snRNA Adaption. Diplomarbeit der Fakultät für Biologie der Eberhard Karls Universität Tübingen. Ausgeführt an der Universität Zürich.

2. Cassimeris,L. and Morabito,J. (2004). TOGp, the human homolog of XMAP215/Dis1, is required for centrosome integrity, spindle pole organization, and bipolar spindle assembly. Mol. Biol. Cell *15*, 1580-1590.

3. Charrasse,S., Mazel,M., Taviaux,S., Berta,P., Chow,T., and Larroque,C. (1995). Characterization of the cDNA and pattern of expression of a new gene over-expressed in human hepatomas and colonic tumors. Eur. J. Biochem. *234*, 406-413.

4. Cummins,T.D., Barati,M.T., Coventry,S.C., Salyer,S.A., Klein,J.B., and Powell,D.W. (2010). Quantitative mass spectrometry of diabetic kidney tubules identifies GRAP as a novel regulator of TGF-beta signaling. Biochim. Biophys. Acta *1804*, 653-661.

5. Gerdes,J.M., Liu,Y., Zaghloul,N.A., Leitch,C.C., Lawson,S.S., Kato,M., Beachy,P.A., Beales,P.L., DeMartino,G.N., Fisher,S., Badano,J.L., and Katsanis,N. (2007). Disruption of the basal body compromises proteasomal function and perturbs intracellular Wnt response. Nat. Genet. *39*, 1350-1360.

6. Gergely,F., Draviam,V.M., and Raff,J.W. (2003). The ch-TOG/XMAP215 protein is essential for spindle pole organization in human somatic cells. Genes Dev. *17*, 336-341.

7. Gherman,A., Davis,E.E., and Katsanis,N. (2006). The ciliary proteome database: an integrated community resource for the genetic and functional dissection of cilia. Nat. Genet. *38*, 961-962.

8. Goetz,S.C. and Anderson,K.V. (2010). The primary cilium: a signalling centre during vertebrate development. Nat. Rev. Genet. *11*, 331-344.

9. Jin,H., White,S.R., Shida,T., Schulz,S., Aguiar,M., Gygi,S.P., Bazan,J.F., and Nachury,M.V. (2010). The conserved Bardet-Biedl syndrome proteins assemble a coat that traffics membrane proteins to cilia. Cell *141*, 1208-1219.

10. Kulaga,H.M., Leitch,C.C., Eichers,E.R., Badano,J.L., Lesemann,A., Hoskins,B.E., Lupski,J.R., Beales,P.L., Reed,R.R., and Katsanis,N. (2004). Loss of BBS proteins causes anosmia in humans and defects in olfactory cilia structure and function in the mouse. Nat. Genet. *36*, 994-998.

11. Lancaster,M.A. and Gleeson,J.G. (2009). The primary cilium as a cellular signaling center: lessons from disease. Curr. Opin. Genet. Dev. *19*, 220-229.

12. Lizee,G., Aerts,J.L., Gonzales,M.I., Chinnasamy,N., Morgan,R.A., and Topalian,S.L. (2003). Real-time quantitative reverse transcriptase-polymerase chain reaction as a method for determining lentiviral vector titers and measuring transgene expression. Hum. Gene Ther. *14*, 497-507.

13. Nachury,M.V., Loktev,A.V., Zhang,Q., Westlake,C.J., Peranen,J., Merdes,A., Slusarski,D.C., Scheller,R.H., Bazan,J.F., Sheffield,V.C., and Jackson,P.K. (2007). A core complex of BBS proteins cooperates with the GTPase Rab8 to promote ciliary membrane biogenesis. Cell *129*, 1201-1213.

14. Shah,A.S., Farmen,S.L., Moninger,T.O., Businga,T.R., Andrews,M.P., Bugge,K., Searby,C.C., Nishimura,D., Brogden,K.A., Kline,J.N., Sheffield,V.C., and Welsh,M.J. (2008). Loss of Bardet-Biedl syndrome proteins alters the morphology and function of motile cilia in airway epithelia. Proc. Natl. Acad. Sci. U. S. A *105*, 3380-3385.

15. Singla,V. and Reiter,J.F. (2006). The primary cilium as the cell's antenna: signaling at a sensory organelle. Science *313*, 629-633.

16. Su,C.Y., Menuz,K., and Carlson,J.R. (2009). Olfactory perception: receptors, cells, and circuits. Cell *139*, 45-59.

17. Tayeh,M.K., Yen,H.J., Beck,J.S., Searby,C.C., Westfall,T.A., Griesbach,H., Sheffield,V.C., and Slusarski,D.C. (2008). Genetic interaction between Bardet-Biedl syndrome genes and implications for limb patterning. Hum. Mol. Genet. *17*, 1956-1967.

18. Wahl,M.C., Will,C.L., and Luhrmann,R. (2009). The spliceosome: design principles of a dynamic RNP machine. Cell *136*, 701-718.

19. Zaghloul,N.A. and Katsanis,N. (2009). Mechanistic insights into Bardet-Biedl syndrome, a model ciliopathy. J. Clin. Invest *119*, 428-437.

20. Zhuang,Y. and Weiner,A.M. (1986). A compensatory base change in U1 snRNA suppresses a 5' splice site mutation. Cell *46*, 827-835.

3.3.7. Figures and Tables

Table 1 Selection of genes from exon array data to further evaluate their expression upon treatment with either U1-BBS1_mut or U1 wt.

Gene Symbol	Fold change	P-value	Probe Sets	Selection
OR8G1*	1.000929433	0.160168194	1	fold change: <-0.9 or > 0.9
SERHL *	0.996271677	0.1033489	1	fold change: <-0.9 or > 0.9
OR10G2 *	0.967081652	0.141329187	1	fold change: <-0.9 or > 0.9
PLGLA1	-0.901545367	0.130864559	1	fold change: <-0.9 or > 0.9
CCDC144B	-0.920253259	0.097830558	1	fold change: <-0.9 or > 0.9
PCOLCE2	-1.036802132	0.000207559	1	fold change: <-0.9 or > 0.9
C2orf27A	-1.2537138	0.115494124	1	fold change: <-0.9 or > 0.9
CCDC162	0.910767977	0.015352589	5	fold change: <-0.9 or > 0.9; probe set: >1
SEC24A	-0.939305783	0.033251092	20	fold change: <-0.9 or > 0.9; probe set: >1
ORC6L	-1.008795795	0.010408435	6	fold change: <-0.9 or > 0.9; probe set: >1
ANAPC5	-1.012129768	0.000879074	11	fold change: <-0.9 or > 0.9; probe set: >1
GRAP	0.767820089	0.037558602	?	p-value <0.05; FC +/- 0.5
OR6B3 *	0.647933659	0.026703847	?	p-value <0.05; FC +/- 0.5
OR10H4 *	0.501354595	0.016606359	?	p-value <0.05; FC +/- 0.5
AP1S2	-0.556877562	0.007877637	?	p-value <0.05; FC +/- 0.5
PRDX3	-0.705029442	0.003791025	?	p-value <0.05; FC +/- 0.5
KIF20B	-0.712239297	0.036897943	?	p-value <0.05; FC +/- 0.5
CKAP5	-0.722091211	0.019759787	?	p-value <0.05; FC +/- 0.5
FAM111B	-0.747902385	0.032349634	?	p-value <0.05; FC +/- 0.5
IDE	-0.826560618	0.016511654	?	p-value <0.05; FC +/- 0.5
NDC80/KNTC2	-0.812153617	0.037874319	?	p-value <0.05; FC +/- 0.5 (also found in GeneGo)
EFNB3	0.296063081	0.047072584	?	GeneGo: Ephrin signaling in cytoskeletal remodeling
EPHB2	0.125229211	0.035425694	?	GeneGo: Ephrin signaling in cytoskeletal remodeling
TUBB4	0.177578585	0.033655026	?	GeneGo: Nek pathway in regulation of cell cycle
IRS1	0.150166445	0.00594226	?	GeneGo: Nek pathway in regulation of cell cycle
TUBA1A	-0.161051111	0.028263008	?	GeneGo: Nek pathway in regulation of cell cycle
H3F3B	-0.427254946	0.041089699	?	GeneGo: Nek pathway in regulation of cell cycle
TCF4	-0.161174107	0.222067531	?	GeneGo: Wnt signaling

Gene Symbol: gene symbol annotated by the Gene Chip® Human Exon 1.0 ST Array (Affimetrix)
Fold Change: difference between U1-BBS1_mut vs. U1-wt treatment of means derived from exonic probe sets of the gene and displayed on logarithmic scale
P-Value: p-value of the t-test on the means of exonic probe sets of the gene between U1-BBS1_mut vs. U1-wt treatment
Probe sets: number of exonic probe sets found for that gene which are higher or lower than a fold change of 0.9 or -0.9, respectively
Selection: desicion critera for RT-PCR analysis
* no amplification product

Table 2 Summary of results from RT-PCR expression analysis of selected candidate genes acquired by 3 independent transductions.

Gene Symbol	Difference	Rescue	Side effect
CCDC162 [2]	+	-	++
GRAP	+	-	++
EFNB3	+	-	(+/v)
TUBB4	?	?	?
IRS1	+	-	?
EPHB2	+	-	+/v
TUBA1A [2]	-	-	-
TCF4	+	+	(+/v)
H3F3B	-	-	-
AP1S2	++	+	(+/v)
PRDX3 [1]	-	-	+
KIF20B	+	-	+/v
CKAP5	+	+	-
FAM111B	++	-	+/v
NDC80/KNTC2	+	-	+/v
IDE	+	+	-
PLGLA1	-	-	-
CCDC144B	-	-	-
SEC24A [2]	-	-	+
ORC6L [2]	-	-	+
ANAPC5 [2]	-	-	+
PCOLCE2	?	?	?
C2orf27A	-	-	-

++: high +: low ?: inconsistent -: no effect +/v: additional virus effect

[1] replicated only one time

[2] weak rescue; different virus production

Gene Symbol: gene symbol annotated by the Gene Chip® Human Exon 1.0 ST Array (Affimetrix)
Difference: difference in expression levels between control and patient fibroblast
Rescue: expression level of the patient becomes similar to the control by the U1-BBS1_mut treatment
Side effect: side effect because of U1-BBS1_mut treatment

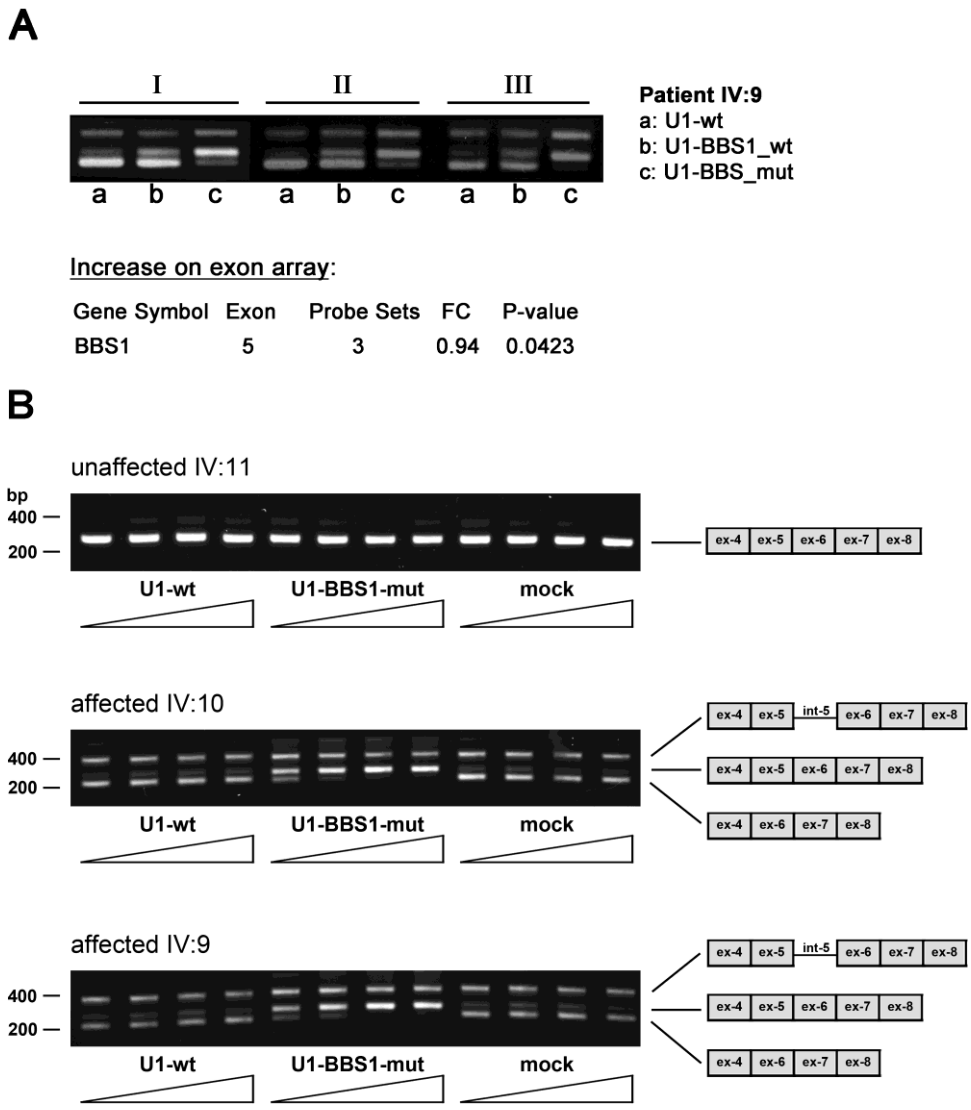

Figure 1 RT-PCR analysis of patient and control fibroblasts. **A** Efficiency of splice defect correction in fibroblasts from patient IV:9 used in exon array analysis. Cells were treated with either wild type U1 (U1-wt), U1 adapted to the splice donor site (U1-BBS1_wt) or fully adapted U1 (U1-BBS1_mut). Replicates of three independent transductions (I-III) have been analyzed. The increased amount of exon 5 inclusion into the *BBS1* transcript, detected by the exon array upon the U1-BBS1_mut treatment, is given in fold changes (FC) below. **B** Patient-derived fibroblasts IV:9 and IV:10 treated with increasing amounts (1 ml, 3 ml, 6 ml and 9 ml) of either U1-wt, U1-BBS1_mut or no (mock) U1 containing virus. A similar treatment in fibroblasts from the unaffected family member IV:11 was used as a control. The composition of the different BBS1 spliced products is illustrated graphically at most right. Product sizes are given in base pairs. This figure has been previously shown (see Results 3.2.4., page 75).

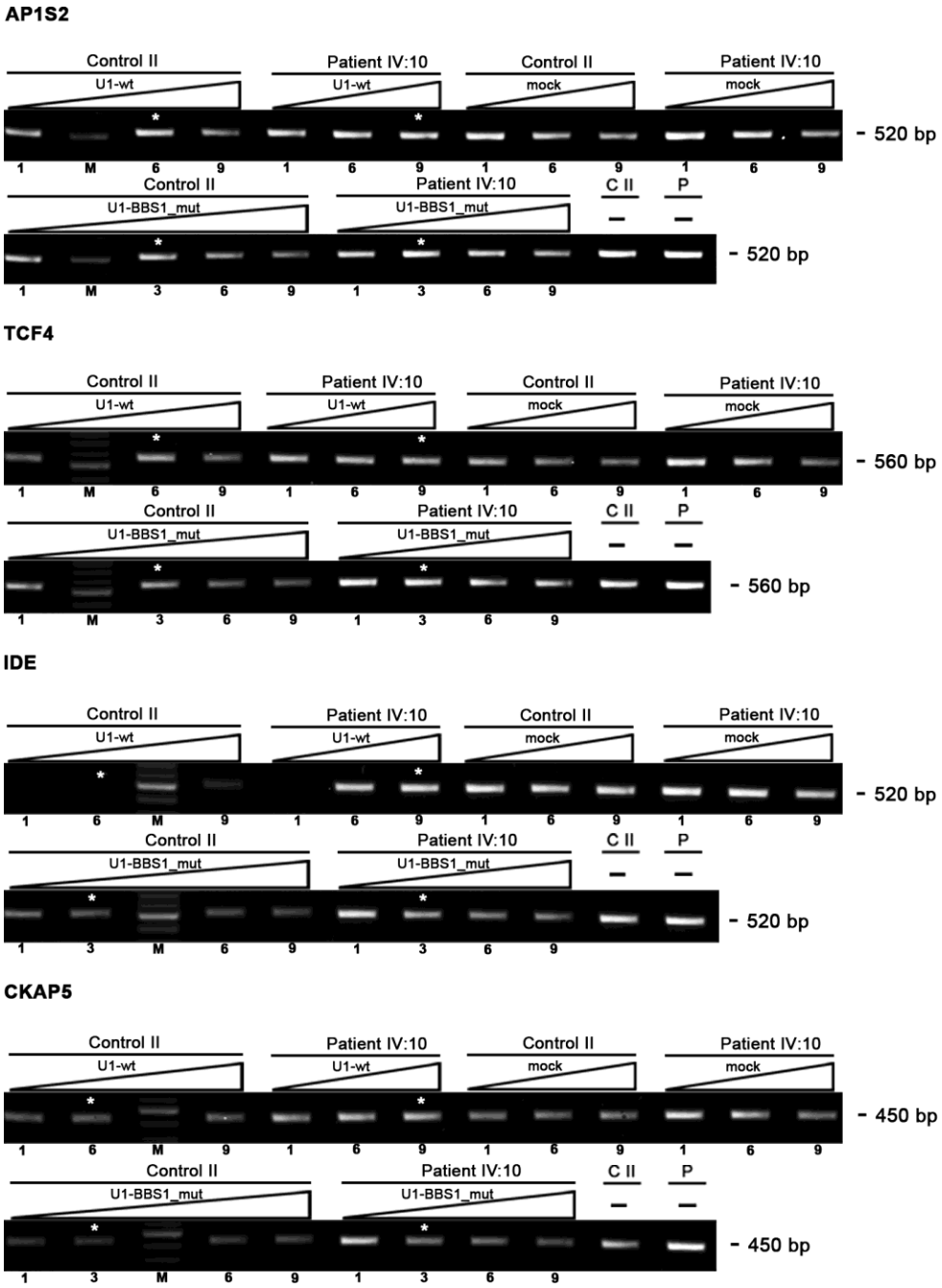

Figure 2 RT-PCR expression analysis of *AP1S2*, *TCF4*, *IDE* and *CKAP5* in U1-treated fibroblasts. Representative gel images from 3 replicates are shown. Fibroblasts from patient (IV:10) or the second control (Control II) were treated with increasing amounts of lentiviral shuttles expressing either wild type (U1-wt), fully adapted (U1-BBS1_mut) or no (mock) U1. Numbers below each lane define the amount (ml) of virus used in this sample. M labels the DNA ladder. Sizes of RT-PCR amplification products are given in base pairs (bp). Conditions with similar amounts of proviral DNA are labeled by asterisks and are only comparable within the same cell line.

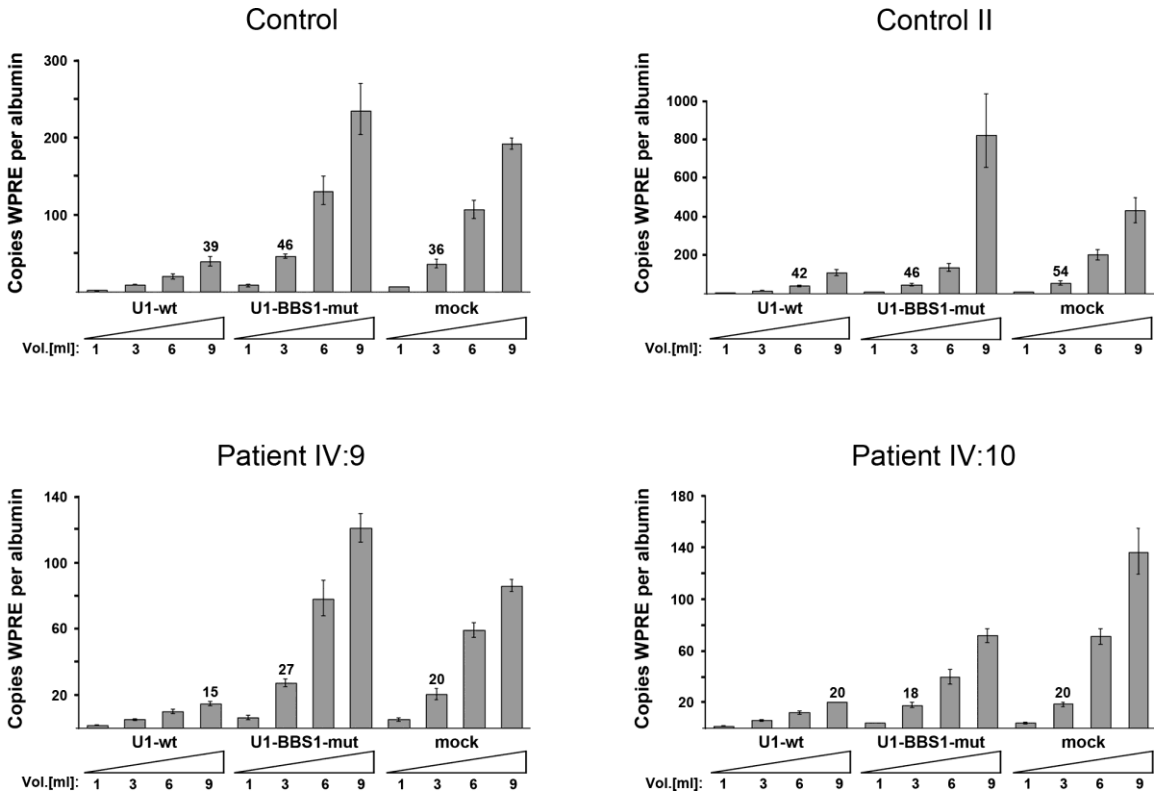

Figure 3 Relative amount of integrated proviral DNA into the host genome of transduced fibroblasts. Amounts of virus used for transduction is given in ml. The relative amount was determined by quantitative real-time PCR using the woodchuck hepatitis virus posttranscriptional regulatory element (WPRE) as target sequence and normalized to the expression level of human albumin. Numbers on the top of each data bar indicate comparable amounts of integrated provirus for each cell line.

3.3.8. Supplementary Material

Supplementary Figure 1

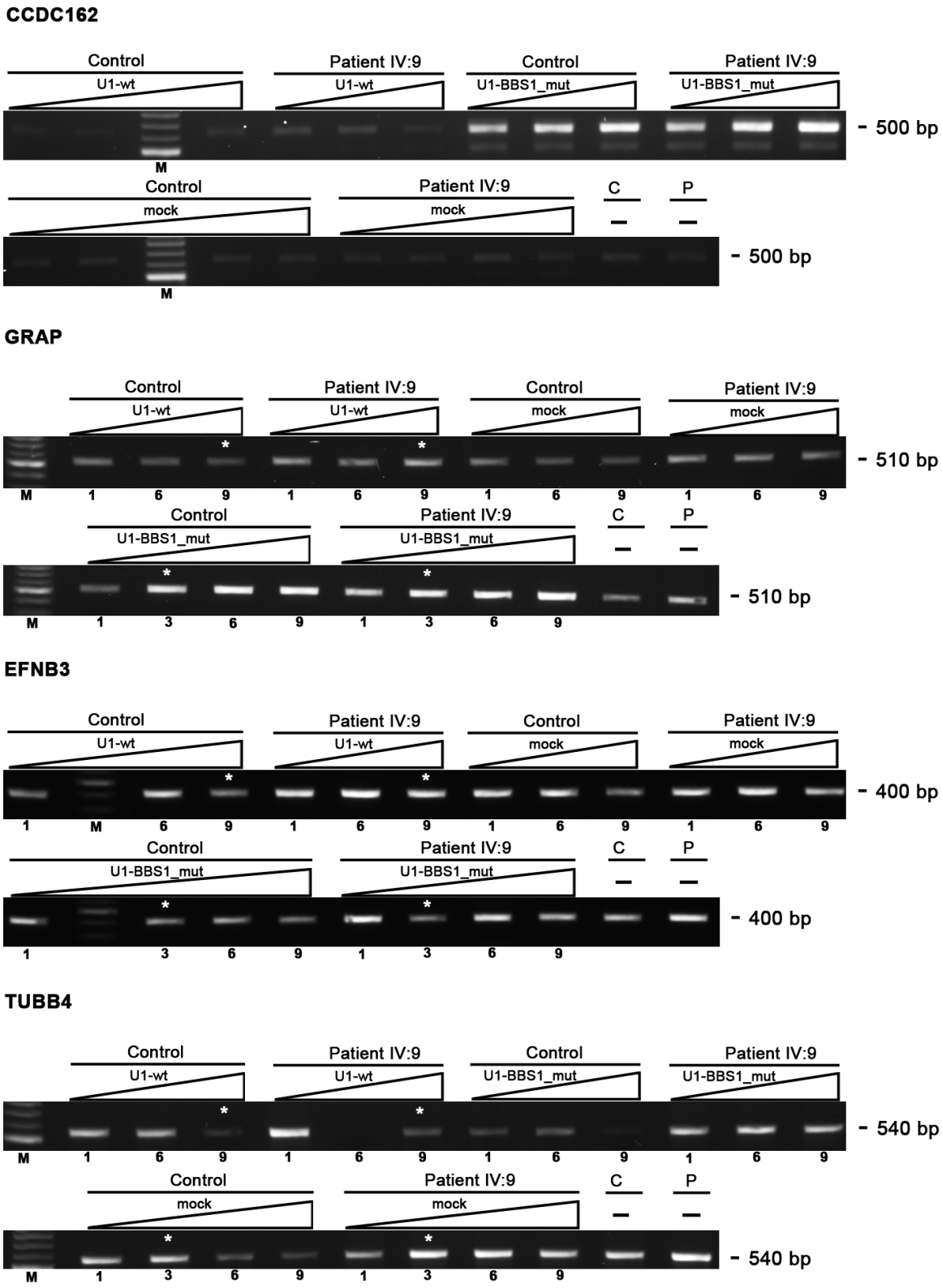

Supplementary Figure 2

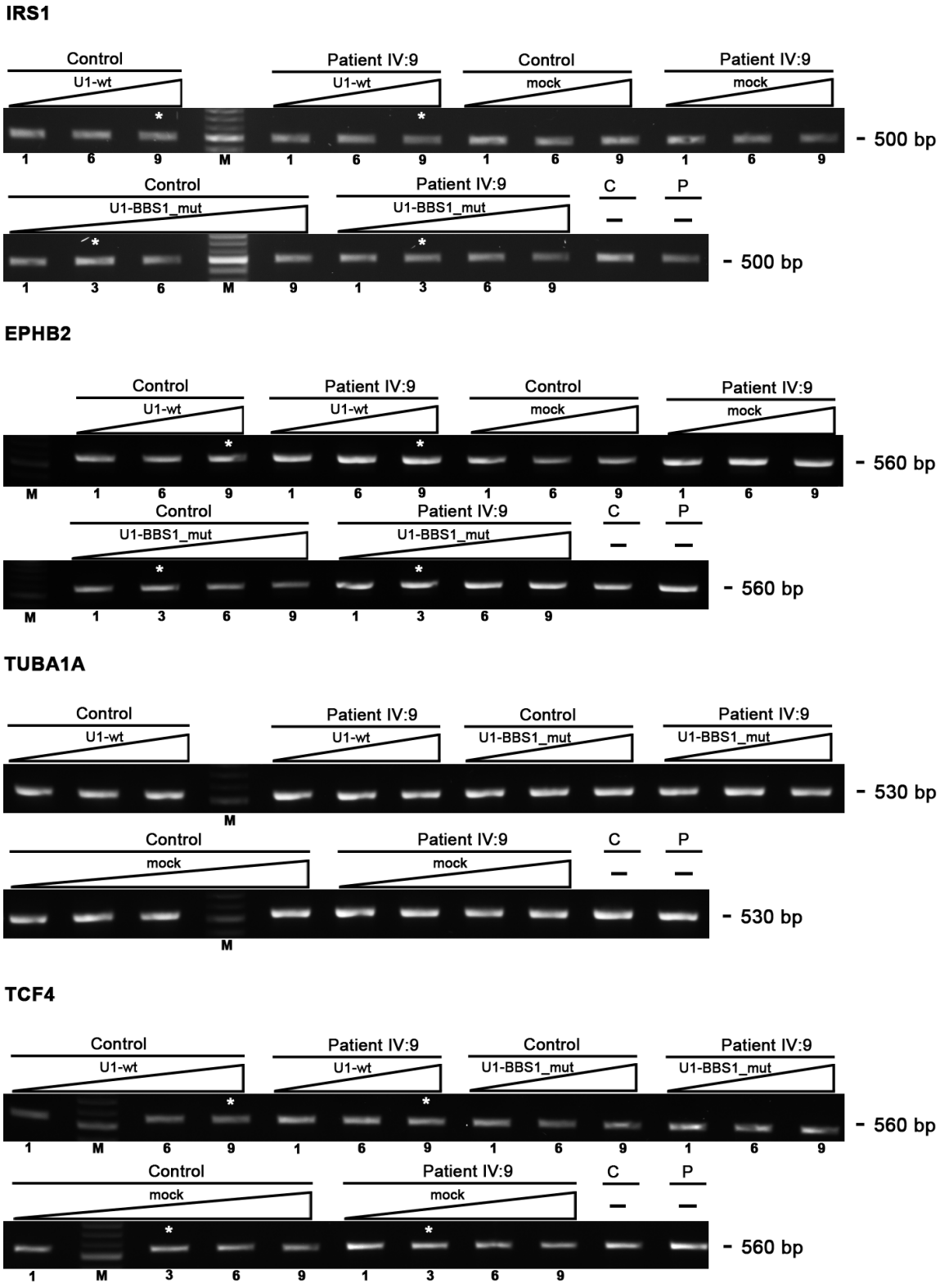

Supplementary Figure 3

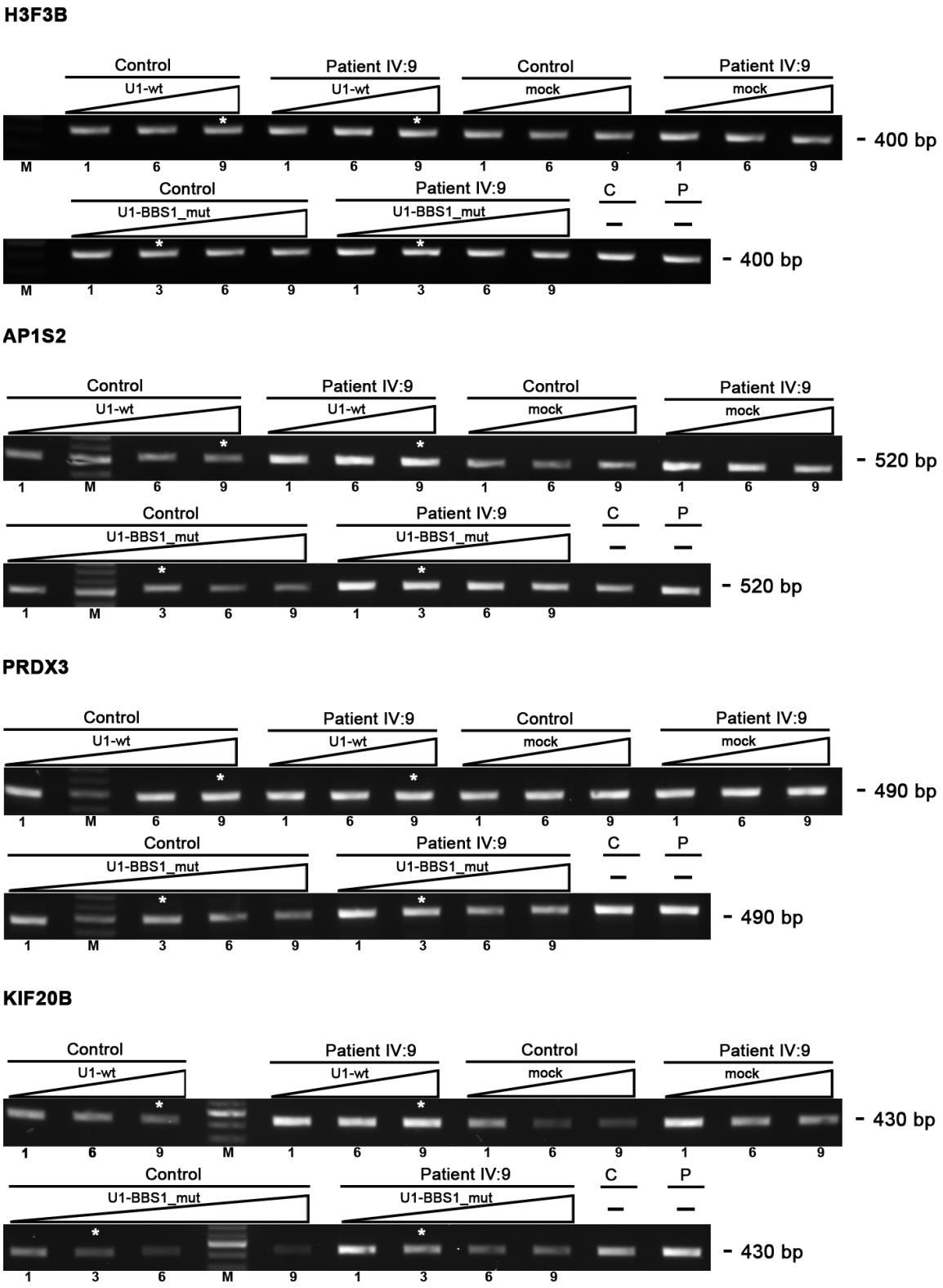

Supplementary Figure 4

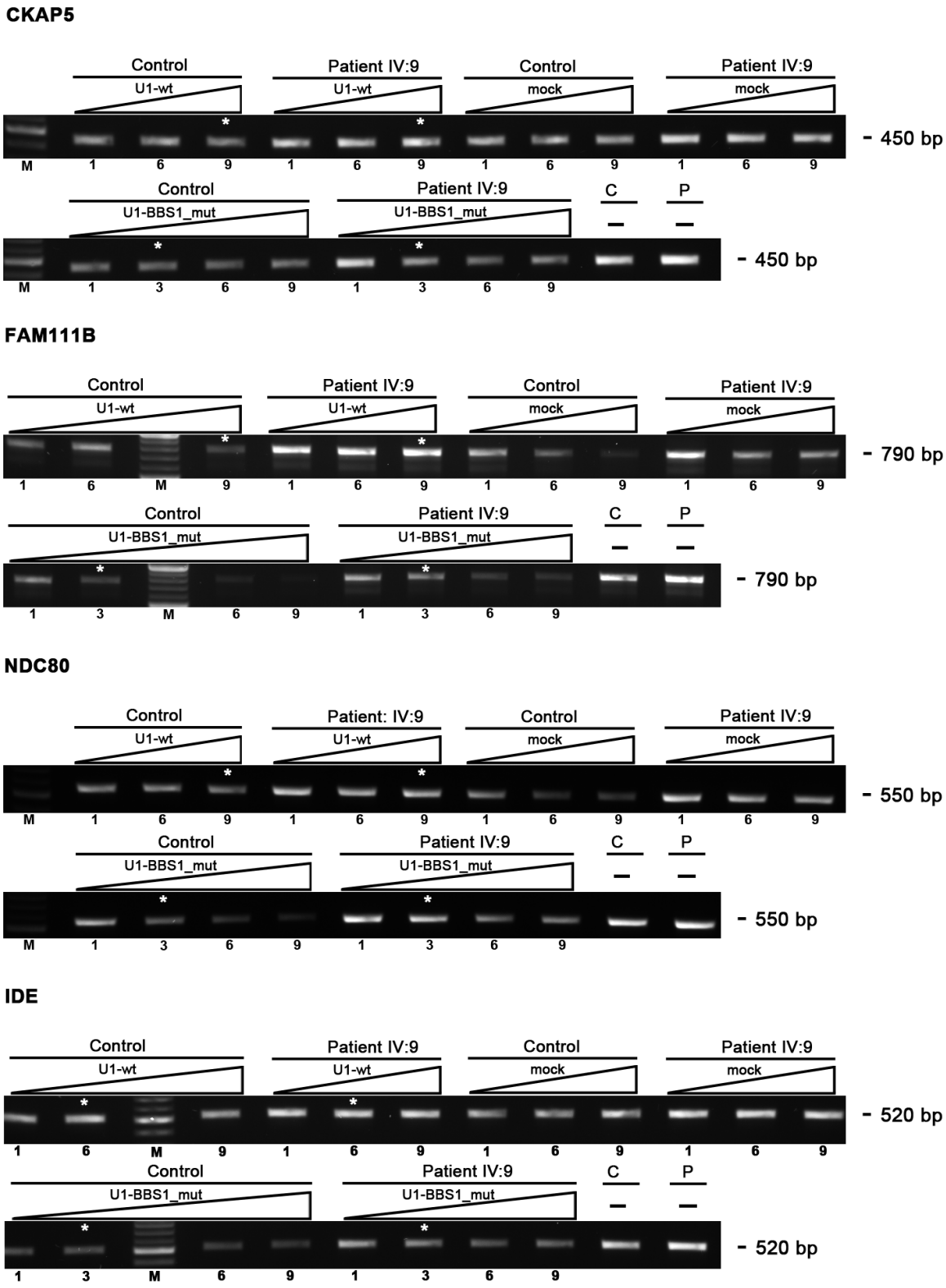

Supplementary Figure 5

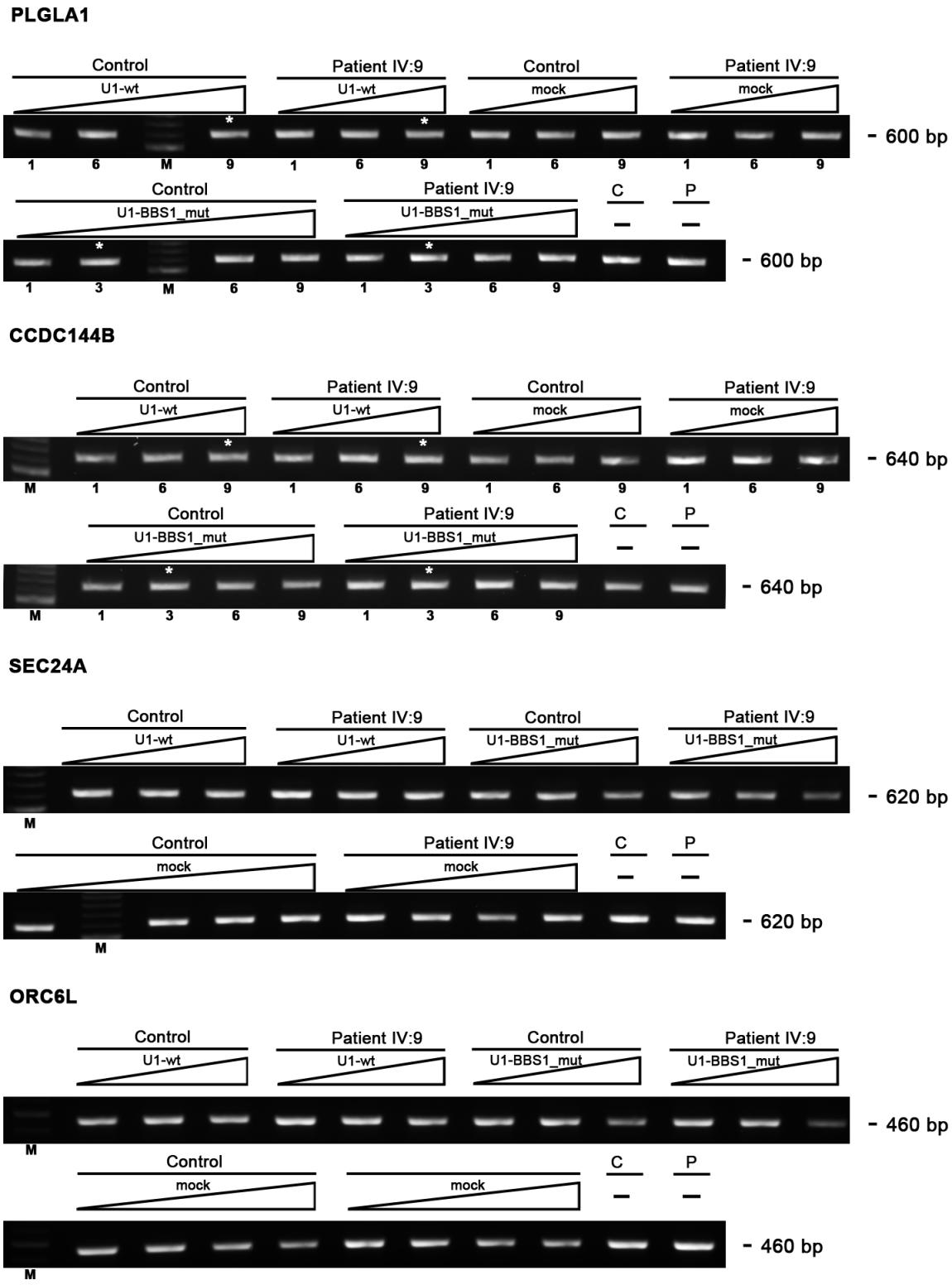

Supplementary Figure 6

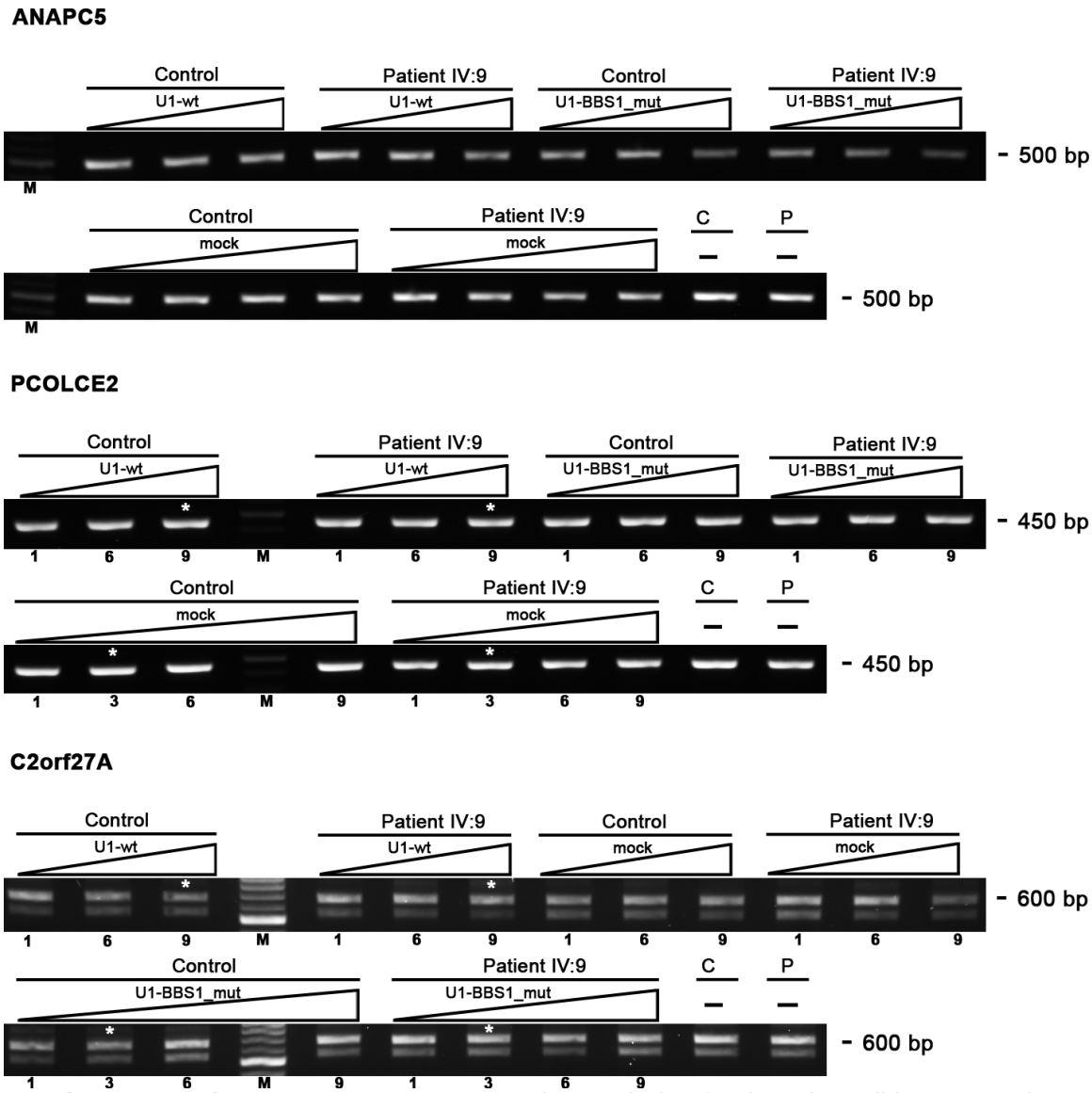

Supplementary Figures 1-6 RT-PCR expression analysis of selected candidate genes in transduced fibroblasts. Representative gel images from 3 replicates are shown. Fibroblasts from patient (IV:9) or the unaffected control (Control) were treated with increasing amounts of lentiviral shuttles expressing either wild type (U1-wt), fully adapted (U1-BBS1_mut) or no (mock) U1. Numbers below each lane define the volume (ml) of virus used in this sample. M labels the DNA ladder. Sizes of RT-PCR amplification products are given in base pairs (bp). Conditions with similar amounts of proviral DNA are labeled by asterisks and only comparable within the same cell line. *CCDC162*, *TUBA1A*, *SEC24A*, *ORC6L* and *ANAPC5* lack asterisks because the amount of proviral DNA was not determined.

Supplementary Table 1 List of genes differentially expressed between U1-BBS1_wt and U1-wt treatment with fold changes in the range of < -0.9 and > 0.9.

Gene Symbol	Fold Change	P-Value	ENSEMBL ID	Probe Sets	ENSEMBL Gene	Annotations from Entrez Gene (NCBI)
AL359711.18	3.889451976	0.001966179	ENSG00000208901	1	not found	CD164, CCDC162, RPL7P28, PPIL6, C6orf184
AC026740.6	1.88736613	0.0118438	ENSG00000215247	2	AC026740.1	TPPP, CEP72, LOC100132605, ZDHHC11
AL450023.21	1.678130162	9.81E-05	ENSG00000211022	1	not found	SSX2, SSX2B, SSXP5 etc.
AC011744.8	1.458691732	0.169987172	ENSG00000198787	1	AC011744.1	ZBTB49, OTOP1, OR4D12P, OR7E103P, OR7E99P, LYAR, TMEM128, UNC93B4
AL162376.15	1.382811293	0.029820921	ENSG00000206697	1	Y_RNA	not found
AC012435.13	1.354108139	0.061764049	ENSG00000212279	1	SNORD77	UBL7,LOC440288,SEMA7A
AC006357.5	1.171581475	0.008226601	ENSG00000213992	1	AC006357.1	LOC645249, MNX1, NOM1
IGLV11-55	1.160350228	0.15058778	ENSG00000211641	1	IGLV11-55	IGLV11-55
AL358780.22	1.159951483	0.015221737	ENSG00000207347	1	U6	MLLT10,C10orf114,C10orf140,MIR1915
AC108867.3	1.155289102	0.15691948	ENSG00000207188	1	U6	LOC100418792
AC015804.14	1.113945054	0.009179416	ENSG00000207107	1	not found	TNRC6B, FLJ45079
AC015980.4	1.105844832	0.076878667	ENSG00000201671	1	5S_rRNA	CAPN14,GALNT14
AL136163.15	1.086419311	0.025313397	ENSG00000208711	1	Not found	NCOA7
AL161450.14	1.075780518	0.06648095	ENSG00000210198	1	not found	INSL6, TRNAQ9, LOC100129107, JAK2, IGHEP2
hsa-mir-184	1.063481098	0.133515286	ENSG00000207695	1	hsa-mir-184	not found
AL450023.21	1.059426936	0.009858163	ENSG00000157965	1	SSX8	SSX2, SSX8, SSX7, SSXP5, SSXP4, SSXP1, LOC100420089, LOC791099, LOC791098, LOC791098, LOC791097, SSX2B, LOC100128981, LOC100288328, LOC100128321
AC097526.3	1.059301147	0.022776002	ENSG00000208748	1	not found	TRNAQ54P, TRNAI31
AC006120.1	1.051445058	0.172146009	ENSG00000211172	1	not found	CCDC46, PSMD7L, APOH
AC131055.10	1.040945532	0.065449957	ENSG00000209968	1	not found	TRNAS30P,LOC100289154,LOC100289127, LOC100289062,LOC100289032,LOC100288998
TMEM78	1.031015536	0.067085917	ENSG00000177800	1	TMEM78	TMEM78
AL158196.24	1.021895292	0.076878465	ENSG00000214488	1	not found	MED4, NUDT15, RP11-90M2.3
TRAV8-4	1.010188708	0.158268776	ENSG00000211790	1	AE000659.13	TRAV8-4
OR8G1	1.000929433	0.160168194	ENSG00000197849	1	OR8G1	OR8G1
AP003732.4	1.000295616	0.1136081	ENSG00000212416	1	5S_rRNA	CPT1A,MTL5

Gene Symbol	Fold Change	P-Value	ENSEMBL ID	Probe Sets	ENSEMBL Gene	Annotations from Entrez Gene (NCBI)
SERHL	0.996271677	0.1033489	ENSG00000172250	1	SERHL	SERHL
RP11-290P14.2	0.993920466	0.045809483	ENSG00000216496	1	not found	not found
AC140847.4	0.985484801	0.101164685	ENSG00000209785	1	not found	LOC260338, LOC100132086, LOC100131369
AL392105.13	0.974395802	0.117260695	ENSG00000208590	1	not found	GPR107, LOC100129785
AL159153.17	0.973986984	0.150115456	ENSG00000210514	1	not found	COL4A2, LOC100129836
AL391122.9	0.972967497	0.073749459	ENSG00000210366	1	not found	RPS6P23, RP11-122A8.1, LOC100129122, DOCK9
OR10G2	0.967081652	0.141329187	ENSG00000169202	1	OR10G2	OR10G2
TRGV1	0.965330375	0.109133179	ENSG00000211701	1	AC007245.3	TRGV1
RP5-931E15.4	0.96496641	0.058415107	ENSG00000213737	2	not found	not found
AL513168.4	0.961471015	0.166051694	ENSG00000202495	1	Y_RNA	not found
AL359712.12	0.956321451	0.002394581	ENSG00000177460	6	RP11-352J4.1	C6orf183, FJ37396
RP11-425D10.1	0.954266748	0.388475589	ENSG00000220527	1	not found	not found
AC096543.2	0.939412646	0.008419546	ENSG00000210790	1	not found	LOC199899
AL357150.7	0.93712017	0.014062357	ENSG00000211383	1	not found	PTBP2, RPL7P9, RPL7 3 75
AC004147.2	0.936932797	0.184062355	ENSG00000210348	1	not found	LOC100131744, ACCN1
AC117476.6	0.93453064	0.194568967	ENSG00000208537	1	not found	RNY5P3
GS1-466O4.5	0.929458224	0.123089442	ENSG00000217931	1	not found	not found
AC007283.3	0.925416138	0.039889153	ENSG00000208149	1	not found	LOC100130026,LOC729172,CASP10, CASP8,CFLAR,RNU7-45P
hsa-mir-181c	0.924109812	0.165612578	ENSG00000207613	1	hsa-mir-181c	not found
AC110777.3	0.923321908	0.080416816	ENSG00000209239	1	not found	NDST4
AC136896.6	0.922636885	0.048259244	ENSG00000200326	1	5S_rRNA	GABRG3, LOC653227
AC126389.7	0.919932324	0.04392405	ENSG00000201586	1	U6	PIK3C2A, RPL34P24
AP001924.5	0.918822853	0.016597138	ENSG00000211358	1	not found	LOC399959, MIR125B, BLID
AC094106.3	0.91102318	0.013371912	ENSG00000176183	1	AC233964.1	LOC402221, LOC100289160, LOC100289133, MRPS35P2
C6orf184	0.910767977	0.015352589	ENSG00000203799	5	C6orf184	CCDC162 or C6orf184
AC090465.15	0.903787009	0.213540653	ENSG00000207154	1	U1	not found
CYP2G1P	0.902874989	0.036528192	ENSG00000198461	1	AC008962.1	CYP2G1P
RP5-967N21.7	0.902112443	0.24580477	ENSG00000219953	1	not found	not found
AL591398.2	0.9020043	0.302762005	ENSG00000208538	1	not found	LOC100289259
PLGLA1	-0.901545367	0.130864559	ENSG00000169659	1	PLGLA	PLGLA1
AC004381.1	-0.906452457	0.167388486	ENSG00000209026	1	not found	THUMPD1, LOC730079, ACSM3, ERI2, LOC81691, LOC646810

Gene Symbol	Fold Change	P-Value	ENSEMBL ID	Probe Sets	ENSEMBL Gene	Annotations from Entrez Gene (NCBI)
AP001318.6	-0.906632149	0.246165888	ENSG00000209258	1	not found	TIRAP,FLJ39051,FOXRED1,LOC100289010, FAM118B,SRPR,DCPS,RPL35AP26,ST3GAL4
AC121344.5	-0.909095002	0.106485185	ENSG00000210617	1	not found	IL1RAPL1
AL390237.9	-0.915922975	0.019134966	ENSG00000214561	1	RP11-278J20.1	LOC727842, LOC100288628
AL731569.18	-0.917592779	0.070325642	ENSG00000212332	1	U6	LOC100289138, WAPAL
AC119041.6	-0.919963473	0.101323129	ENSG00000210218	1	not found	LOC100287892
AL109806.22	-0.920194795	0.321197247	ENSG00000210826	1	not found	C20orf107,LOC100130156, C20orf106,C20orf43, GCNT7
CCDC144B	-0.920253259	0.097830558	ENSG00000154874	1	CCDC144B	CCDC144B
AC124312.5	-0.925279867	0.122998901	ENSG00000206621	1	SNORD116	SNORDs and others
AP001273.4	-0.926384308	0.098565662	ENSG00000210825	1	SNORA40	SNORDs and others
AC068896.9	-0.929776527	0.06346643	ENSG00000207494	1	Y_RNA	LOC100287472, FAM53B, FAM175B
AP000240.1	-0.930857464	0.046255892	ENSG00000209835	1	not found	C21orf41, BACH1
AP000361.2	-0.932918193	0.08368405	ENSG00000220686	1	not found	not found
RP11-503K16.2	-0.933322582	0.081943938	ENSG00000217817	1	not found	not found
SEC24A	-0.939305783	0.033251092	ENSG00000113615	20	SEC24A	SEC24A
AL442663.3	-0.951746978	0.055331601	ENSG00000209100	1	not found	LOC100287446, TRNAC24, RBM25, RPS12P1, DCAF4, ZFYVE1
AF129075.3	-0.952042091	0.071420604	ENSG00000201984	1	Y_RNA	CCT8, USP16,RPL12P9,RWDD2B,C21orf7, RPL23P2,RNF160
AC108477.5	-0.952326163	0.157711254	ENSG00000201433	1	U6	C4orf41, RWDD4A
AP001160.4	-0.952689543	0.357605781	ENSG00000206653	1	SNORD29	SNORDs and others
AC068056.7	-0.955983274	0.302330713	ENSG00000208171	1	not found	MYO1B
AL391728.19	-0.961892033	0.030061379	ENSG00000210993	1	not found	LRC7, PIN1L
AC008635.6	-0.96311748	0.048732443	ENSG00000210192	1	not found	STRN4, PRKD2
AC011747.5	-0.965584758	0.232356308	ENSG00000182367	1	not found	not found
RP11-11N7.2	-0.979310805	0.163617309	ENSG00000188206	1	C1orf199	NCRNA00201
AC099337.2	-0.980956923	0.001558388	ENSG00000201493	1	U1	RRP15
AC009884.8	-0.982763079	0.090000943	ENSG00000201157	1	SNORA62	PSD3
RP4-566D2.1	-0.98800418	0.168112795	ENSG00000205179	1	not found	not found
AL132989.5	-1.00034451	0.040970153	ENSG00000209824	1	not found	HMGB1L14,ACTR10,TRNAK13,FLJ31306, ARID4A,PSMA3
AL136305.14	-1.006727472	0.114783319	ENSG00000209103	1	not found	RBM24

Gene Symbol	Fold Change	P-Value	ENSEMBL ID	Probe Sets	ENSEMBL Gene	Annotations from Entrez Gene (NCBI)
AL451165.19	-1.007873917	0.091409653	ENSG00000210647	1	not found	C6orf106, LOC100131607
ORC6L	-1.008795795	0.010408435	ENSG00000091651	6	ORC6L	ORC6L
ANAPC5	-1.012129768	0.000879074	ENSG00000089053	11	ANAPC5	ANAPC5
AL049542.10	-1.016193066	0.010906895	ENSG00000201034	1	Y_RNA	RAB11FIP3
AC023389.13	-1.022713709	0.107565341	ENSG00000200961	1	not found	SSH2
AC104653.5	-1.027414746	0.029883558	ENSG00000208621	1	not found	not found
RP11-697G4.3	-1.02744096	0.148381901	ENSG00000217466	1	not found	not found
AL359540.19	-1.029461862	0.216752337	ENSG00000210479	1	not found	MUTYH,TESK2,TOE,LOC100288481,HPDL, hCG 1820661
AC122179.6	-1.033203074	0.055741884	ENSG00000209444	1	not found	WEE1
PCOLCE2	-1.036802132	0.000207559	ENSG00000163710	1	PCOLCE2	PCOLCE2
hsa-mir-32	-1.038626557	0.1007958	ENSG00000207698	1	hsa-mir-32	MIR32
AL161450.14	-1.041676617	0.049580201	ENSG00000210157	1	not found	INSL6, TRNAQ9, LOC100129107, JAK2, IGHEP2
AC064799.6	-1.042178938	0.004699737	ENSG00000175333	1	not found	THSD4, RPL17P39
AL355608.11	-1.048207268	0.04766562	ENSG00000207268	1	SNORA70	SNORA70C, ASTN2, RPL10P3
AL451005.9	-1.088393151	0.240406689	ENSG00000208765	1	not found	CUL4B
AC073575.30	-1.095881176	0.042243036	ENSG00000200688	1	Y_RNA	ERP29,TRAFD1,C12orf30, C12orf51, LOC728543, LOC100287839,TMEM116
AC090510.4	-1.098824275	0.228918193	ENSG00000210523	1	not found	LOC100289126, STARD9,CDAN1,TTBK2
AC021654.25	-1.11504749	0.175734028	ENSG00000208651	1	not found	SCHIP1
AL121809.6	-1.13078268	0.027531616	ENSG00000214919	1	AL121809.3	FKBP3,SNORD127,C14orf106,PRPF39,FANCM, FAM179B
AC092868.2	-1.132295402	0.040175367	ENSG00000199512	1	U6	MYO1E,LOC100132644
AL049712.12	-1.142341904	0.015872884	ENSG00000207262	1	SNORD57	SNORD56,57,88,110 etc
AL445648.18	-1.143706916	0.216724119	ENSG00000212350	1	not found	SRRM1,CLIC4
AP001160.4	-1.151870699	0.079744505	ENSG00000207437	1	SNORD28	SNORD22 +25-31, and others
AL449963.2	-1.153615665	0.142490702	ENSG00000210401	1	not found	ADAMTSL1
AL591807.1	-1.185913859	0.022237101	ENSG00000201376	1	SNORA70	TMX1
AC124312.5	-1.186376975	0.04912134	ENSG00000209418	1	SNORD64	div SNORDs and others
AC087650.12	-1.187113008	0.100497145	ENSG00000210609	1	not found	LOC100130581,RNU2-4P,DHX8,RPL29P31,MIR2117, ARL4D
AC093602.5	-1.204175229	0.151055081	ENSG00000208967	1	not found	ELF2,CCRN4L

Gene Symbol	Fold Change	P-Value	ENSEMBL ID	Probe Sets	ENSEMBL Gene	Annotations from Entrez Gene (NCBI)
AC003043.1	-1.205655359	0.015727766	ENSG00000210683	1	not found	not found
C2orf27	-1.2537138	0.115494124	ENSG00000197927	1	C2orf27A	C2orf27A
AC007016.5	-1.264953481	0.077124883	ENSG00000214165	1		CC2D2A,LOC100288116,C1QTNF7
EIF1AX	-1.265205141	0.085168458	ENSG00000173674	1	EIF1AX	EIF1AX, IPO13, EIF5, EIF2S1, EIF5B, EIF3C
AL732366.7	-1.265205141	0.085168458	ENSG00000201882	1	snoU2-30	MAP7D2,EIF1AX,SCARNA9L,LOC729609,RPS6KA3
AL109897.30	-1.266087527	0.107674918	ENSG00000211267	1	not found	MYO6,SENP6
AC069483.6	-1.333991077	0.122955078	ENSG00000206676	1	Y_RNA	MEIS2
AL360091.28	-1.336648887	0.007571362	ENSG00000201544	1	SNORA16	PPP2R5A,TMEM206,SNORA16B,RPL23AP18
AC019209.3	-1.337538973	0.05639091	ENSG00000205706	1	not found	LOC645233
AL136170.14	-1.366582839	0.128413781	ENSG00000208317	1	SNORD78	div. SNORDs and others
AC005104.1	-1.389958657	0.072518332	ENSG00000208039	1	not found	SEPT2,FARP2
AL139021.6	-1.403286842	0.064646933	ENSG00000209829	1	not found	TOMM20L,HSBP1P1,TIMM9,KIAA0586,ARID4A
RP11-444I9.2	-1.408900617	0.006261549	ENSG00000219530	1	not found	not found
AL136162.18	-1.417658561	0.137158587	ENSG00000201367	1	U6	JARID2
RPL39P	-1.420316171	0.123536336	ENSG00000216467	1	not found	RPL39P
AL592166.16	-1.433050238	0.143336603	ENSG00000207421	1	SNORD38	div. SNORDs, KIF2C,RPS8,TCTEX1D4,PLK3, BTBD19,RPS15AP11,BEST4,PTCH2
RP11-220I1.4	-1.441177157	0.050584163	ENSG00000217860	1	not found	not found
AC073195.5	-1.452884236	0.136903814	ENSG00000207086	1	Y_RNA	LOC100127913,YWHAQ,ADAM17
AL513497.21	-1.481301716	0.123623914	ENSG00000201808	1	SNORA73	SNORDs and others
AL589675.5	-1.54464195	0.014316349	ENSG00000187770	1	not found	KIAA0020,CARM1L, LOC138234,LOC392281
AP001065.1	-1.568805669	0.047596025	ENSG00000210065	1	not found	TRPM2,PIRC105,C21orf30,LBRC3
AL732366.7	-1.71746527	0.019786683	ENSG00000206663	1	Y_RNA	MAP7D2,EIF1AX,SCARNA9L,LOC729609,RPS6KA3
AC087292.14	-2.14096641	0.013508814	ENSG00000207390	1	Y_RNA	CYB5D2,ANKFY1,ZZEF1

Gene Symbol: gene symbol or GeneBank accession number annotated by the Gene Chip® Human Exon 1.0 ST Array (Affimetrix)
Fold Change: difference between U1-BBS1_mut vs. U1-wt treatment of means derived from exonic probe sets of the gene and dsiplayed on logarithmic scale
P-Value: p-value of the t-test on the means of exonic probe sets of the gene between U1-BBS1_mut vs. U1-wt treatment
Probe sets: number of exonic probe sets found for that gene which are higher or lower than a fold change of 0.9 or -0.9, respectively
ENSEMBL Gene: gene symbol annotated by ENSEMBL

Supplementary Table 2 List of genes differently expressed between U1-BBS1_mut and U1-wt treatment showing p-values lower than 0.05 and fold changes larger than 0.5.

Gene Symbol	ENSEMBL ID	Fold Change	P-value
AL450023.21	ENSG00000211022	1.678130162	9.81E-05
PCOLCE2	ENSG00000163710	-1.036802132	0.000208
AL445663.10	ENSG00000184353	-0.562778942	0.000531
ANAPC5	ENSG00000089053	-1.012129768	0.000879
AL365260.11	ENSG00000208881	-0.66237004	0.000962
AL391382.10	ENSG00000206787	0.641892817	0.00111
AC015550.19	ENSG00000198751	-0.681534812	0.001233
AC048348.25	ENSG00000209178	-0.803167174	0.00124
AL133387.8	ENSG00000210922	-0.696550324	0.001256
AL137226.3	ENSG00000188831	0.77435412	0.001498
GINS1	ENSG00000101003	-0.544718551	0.001527
AC099337.2	ENSG00000201493	-0.980956923	0.001558
AL359711.18	ENSG00000208901	3.889451976	0.001966
PYY3	ENSG00000204474	0.833171179	0.002123
RP11-318G11.2	ENSG00000219290	-0.513575233	0.002371
AL359712.12	ENSG00000177460	0.956321451	0.002395
AL359878.13	ENSG00000205740	0.692406079	0.003583
PRDX3	ENSG00000165672	-0.705029442	0.003791
AC032011.15	ENSG00000182015	0.771048419	0.003792
AC064799.6	ENSG00000175333	-1.042178938	0.0047
RP11-176F3.9	ENSG00000219724	-0.580993978	0.004784
AL357374.11	ENSG00000210251	0.804439742	0.00494
AC098817.3	ENSG00000208842	-0.557425933	0.00499
AL008721.1	ENSG00000206062	0.69842191	0.005322
AC105050.2	ENSG00000208615	0.656636603	0.005393
AC010761.10	ENSG00000206735	-0.637481934	0.005447
AP001273.4	ENSG00000207145	-0.773167975	0.005808
RP11-444I9.2	ENSG00000219530	-1.408900617	0.006262
RP11-481A12.2	ENSG00000220508	0.566748961	0.006693
RP3-391O22.3	ENSG00000196114	0.510048292	0.006891
AC018720.5	ENSG00000170092	-0.868953104	0.007173
AC012183.9	ENSG00000210394	0.596764102	0.007413
AL160270.19	ENSG00000210712	0.579439039	0.007552
AL360091.28	ENSG00000201544	-1.336648887	0.007571
AL135998.6	ENSG00000199716	0.633140154	0.007757
AC016876.10	ENSG00000207152	-0.628983588	0.007849
AP1S2	ENSG00000182287	-0.556877562	0.007878
AC006357.5	ENSG00000213992	1.171581475	0.008227
AC117395.5	ENSG00000208760	0.863103858	0.008313
AC096543.2	ENSG00000210790	0.939412646	0.00842
AC092964.8	ENSG00000208521	-0.651084024	0.008795
AL358790.22	ENSG00000203886	0.660903474	0.009132
AC015804.14	ENSG00000207107	1.113945054	0.009179
AF347015.1	ENSG00000211459	-0.555399384	0.009488
TRAJ15	ENSG00000211874	0.593821413	0.009519
AC093106.3	ENSG00000172400	0.641682857	0.009617
AC012314.8	ENSG00000210694	-0.53850507	0.00971

Gene Symbol	ENSEMBL ID	Fold Change	P-value
AL132989.5	ENSG00000180189	-0.702257354	0.009799
AL450023.21	ENSG00000157965	1.059426936	0.009858
AC025731.12	ENSG00000210355	0.543061714	0.009936
AL391557.11	ENSG00000209185	0.726136225	0.010164
AL158155.24	ENSG00000206784	-0.780370413	0.010186
AL357037.13	ENSG00000213525	0.544175528	0.010306
AC008942.6	ENSG00000201223	-0.724953713	0.010405
ORC6L	ENSG00000091651	-1.008795795	0.010408
AC078953.20	ENSG00000208522	0.791273058	0.010701
AL355305.9	ENSG00000203800	0.798289373	0.010737
AL590708.18	ENSG00000208605	0.820515191	0.010749
AL049542.10	ENSG00000201034	-1.016193066	0.010907
AC093844.3	ENSG00000219943	0.628270489	0.011576
RP11-468L18.1	ENSG00000217870	0.57144147	0.011642
AC026740.6	ENSG00000215247	1.88736613	0.011844
AC068228.8	ENSG00000208604	-0.898204404	0.01239
AF111169.2	ENSG00000213379	-0.664054691	0.012894
AP001629.1	ENSG00000196847	0.608994411	0.012995
DEFB112	ENSG00000180872	-0.607080633	0.013242
AC094106.3	ENSG00000176183	0.91102318	0.013372
AC087292.14	ENSG00000207390	-2.14096641	0.013509
AC006271.2	ENSG00000188314	0.582617153	0.013713
hsa-mir-296	ENSG00000207950	0.576270751	0.013778
AC107071.3	ENSG00000206601	-0.638567124	0.01379
CDKN3	ENSG00000100526	-0.627590769	0.013883
AL357150.7	ENSG00000137970	0.93712017	0.014062
AL357150.7	ENSG00000211383	0.93712017	0.014062
C11orf81	ENSG00000205872	0.607386877	0.014165
AL589675.5	ENSG00000187770	-1.54464195	0.014316
AC009309.4	ENSG00000200241	0.513730703	0.014403
RP11-70K10.2	ENSG00000217321	0.514017316	0.015076
AL358780.22	ENSG00000207347	1.159951483	0.015222
RP1-20I3.3	ENSG00000220016	-0.575022174	0.015228
C6orf184	ENSG00000203799	0.910767977	0.015353
AP000080.1	ENSG00000206871	0.69331703	0.015449
hsa-mir-133a-2	ENSG00000207764	0.715562551	0.015647
AC003043.1	ENSG00000221496	-1.205655359	0.015728
AC003043.1	ENSG00000210683	-1.205655359	0.015728
RP11-294H11.4	ENSG00000216977	-0.848758322	0.015792
AL137849.13	ENSG00000211334	0.549692959	0.015843
AL049712.12	ENSG00000207262	-1.142341904	0.015873
RP11-570F6.1	ENSG00000217615	-0.522390396	0.016065
AC020629.6	ENSG00000209911	-0.719217838	0.016295
IDE	ENSG00000119912	-0.826560618	0.016512
AL590396.13	ENSG00000208077	-0.870167661	0.016512
AC004932.4	ENSG00000208274	-0.517530547	0.016596
AP001924.5	ENSG00000211358	0.918822853	0.016597
OR10H4	ENSG00000176231	0.501354595	0.016606
AL731546.4	ENSG00000209535	0.723895785	0.016683
AL671966.1	ENSG00000208802	-0.588029241	0.016685
AC025429.6	ENSG00000210449	0.644506349	0.016747
AL139404.9	ENSG00000206605	-0.706499137	0.01676
AC139070.3	ENSG00000199728	0.604178586	0.01691

Gene Symbol	ENSEMBL ID	Fold Change	P-value
PSIP1	ENSG00000164985	-0.52573609	0.017164
AC004522.3	ENSG00000199711	0.742106734	0.018269
AC006070.12	ENSG00000218712	-0.645853416	0.018321
AC005067.2	ENSG00000201643	0.850567538	0.01891
OR2C1	ENSG00000168158	-0.535261844	0.019002
AC114810.4	ENSG00000210538	-0.557849619	0.019063
AL390237.9	ENSG00000214561	-0.915922975	0.019135
AL390196.17	ENSG00000209037	-0.623829132	0.01941
RP11-235D19.2	ENSG00000218727	-0.717320745	0.019557
CKAP5	ENSG00000175216	-0.722091211	0.01976
AL732366.7	ENSG00000206663	-1.71746527	0.019787
AL122013.5	ENSG00000213482	-0.610721759	0.019983
USP3	ENSG00000140455	-0.500231685	0.020154
USP3	ENSG00000140455	-0.500231685	0.020154
AL137009.8	ENSG00000208773	0.660116538	0.020369
AC020907.6	ENSG00000203404	0.562557535	0.020398
AL513526.19	ENSG00000175658	0.595253082	0.020562
AC139143.1	ENSG00000216482	0.506718601	0.020856
AL355336.15	ENSG00000201483	0.84416656	0.021313
IGLC4	ENSG00000214522	0.72359719	0.02135
ZBTB40	ENSG00000184677	0.629924418	0.021682
RP11-271B5.1	ENSG00000218366	-0.705410647	0.021918
AC007535.3	ENSG00000200475	0.664932866	0.021919
PPY2	ENSG00000126657	0.719038248	0.022179
AL591807.1	ENSG00000201376	-1.185913859	0.022237
AC079789.7	ENSG00000213370	-0.525792681	0.022368
RP11-244N20.7	ENSG00000218423	-0.658708986	0.022724
AC097526.3	ENSG00000208748	1.059301147	0.022776
ARHGAP11B	ENSG00000187951	-0.591719589	0.022837
AC119618.4	ENSG00000200852	0.895077394	0.023044
AL049780.4	ENSG00000206924	-0.649837988	0.023143
MBOAT4	ENSG00000177669	0.5566696	0.023303
TRAV12-3	ENSG00000211794	0.532708016	0.023346
AC007880.2	ENSG00000199964	0.626889944	0.023725
RP13-465B17.2	ENSG00000216546	0.636483476	0.023735
RP11-185C18.4	ENSG00000218696	-0.814500004	0.02396
OR52E1P	ENSG00000216987	0.510529099	0.024179
AC010287.9	ENSG00000206952	-0.715363419	0.024816
AC080112.15	ENSG00000131747	-0.582868832	0.024869
C6orf185	ENSG00000203798	0.816996034	0.025028
RP11-134A8.1	ENSG00000218425	0.531449412	0.025148
AC098477.2	ENSG00000201962	0.59350445	0.025305
AL136163.15	ENSG00000208711	1.086419311	0.025313
HS6ST1	ENSG00000136720	0.607115489	0.025317
AC016585.8	ENSG00000210667	0.526603272	0.025406
AC018892.8	ENSG00000144188	0.512404393	0.025412
GLYATL2	ENSG00000156689	-0.766470533	0.025596
RP4-666O22.1	ENSG00000218392	-0.562425659	0.025648
AC006132.1	ENSG00000210152	0.685018715	0.026064
AL139240.9	ENSG00000210069	0.678835257	0.026603
OR6B3	ENSG00000178586	0.647933659	0.026704
RP1-106C24.1	ENSG00000220366	-0.553247092	0.02702
AL121809.6	ENSG00000214919	-1.13078268	0.027532

Gene Symbol	ENSEMBL ID	Fold Change	P-value
AC010260.7	ENSG00000211056	-0.68201634	0.028056
AL662914.8	ENSG00000201447	0.725860813	0.028107
ACSL4	ENSG00000068366	-0.531582519	0.028164
DGKI	ENSG00000157680	0.69509023	0.028517
AC003013.1	ENSG00000179418	0.678775283	0.028616
AC112166.3	ENSG00000209898	0.797852137	0.028642
BX322799.22	ENSG00000214358	0.51357186	0.028872
RP11-50K12.1	ENSG00000218777	0.518995935	0.028922
AC103590.2	ENSG00000208180	-0.762446382	0.029212
AC018628.13	ENSG00000200842	-0.880541997	0.029288
RP1-321E8.2	ENSG00000217987	-0.524266513	0.029638
AC079148.9	ENSG00000207170	-0.793755846	0.029666
C14orf70	ENSG00000196273	0.613187073	0.029707
AL662871.9	ENSG00000212240	-0.624359738	0.029722
AL449214.6	ENSG00000212344	-0.573099445	0.029814
AL162376.15	ENSG00000206697	1.382811293	0.029821
AC104653.5	ENSG00000208621	-1.027414746	0.029884
AP001324.4	ENSG00000171579	-0.547989621	0.029979
CCNE2	ENSG00000175305	-0.676237668	0.030033
AL391728.19	ENSG00000210993	-0.961892033	0.030061
RP11-569O4.4	ENSG00000220289	0.549215327	0.030861
AC002457.2	ENSG00000209318	0.772732659	0.031023
AF070718.1	ENSG00000199354	0.869899651	0.031272
RP11-156G14.6	ENSG00000218082	-0.691765171	0.031478
NUSAP1	ENSG00000137804	-0.647275496	0.031583
RPL18A	ENSG00000105640	0.781637385	0.031595
AC005796.1	ENSG00000207166	0.781637385	0.031595
AC104170.2	ENSG00000210578	-0.601163181	0.031613
RGS4	ENSG00000117152	-0.659466495	0.032323
FAM111B	ENSG00000189057	-0.747902385	0.03235
CCL19	ENSG00000172724	0.533551978	0.032609
AC002064.1	ENSG00000207488	-0.51600327	0.032612
RP11-254N18.1	ENSG00000217496	-0.673034548	0.032649
AC104967.4	ENSG00000214954	0.516604997	0.032941
APPL2	ENSG00000136044	-0.55233265	0.033038
SEC24A	ENSG00000113615	-0.939305783	0.033251
AC079804.5	ENSG00000155070	0.655559992	0.033827
AL353660.11	ENSG00000206617	-0.768418022	0.033883
RPL12P3	ENSG00000217037	-0.57533243	0.034021
hsa-mir-24-2	ENSG00000209707	0.50158958	0.034043
OR52L2P	ENSG00000180923	0.545012613	0.034076
AC017100.4	ENSG00000209937	-0.660208879	0.034339
C13orf3	ENSG00000165480	-0.697289229	0.034347
ANKRD26	ENSG00000107890	-0.53547385	0.034434
AC131009.7	ENSG00000200516	0.526493424	0.034454
SHCBP1	ENSG00000171241	-0.519861728	0.034482
AC023933.9	ENSG00000208905	-0.610114264	0.034503
RP1-144F13.4	ENSG00000212671	-0.628703982	0.034566
RP13-60P5.2	ENSG00000218677	0.579239949	0.034725
AC087632.10	ENSG00000219244	-0.50664587	0.035079
Z82185.1	ENSG00000183822	0.841979254	0.035489
STAG3L4	ENSG00000106610	0.576280835	0.03577
DIAPH1	ENSG00000131504	-0.621646194	0.035886

Gene Symbol	ENSEMBL ID	Fold Change	P-value
CASC5	ENSG00000137812	-0.517446529	0.035907
AC093900.3	ENSG00000206820	-0.794995568	0.036451
CYP2G1P	ENSG00000198461	0.902874989	0.036528
EFTUD2	ENSG00000108883	-0.513148337	0.036563
MPHOSPH1	ENSG00000138182	-0.712239297	0.036898
RP11-543N17.2	ENSG00000220795	0.615545977	0.036931
AC004668.1	ENSG00000214221	0.507182849	0.036936
AL356115.9	ENSG00000178429	-0.558325527	0.036989
AL445431.16	ENSG00000201364	0.76624801	0.037019
GRAP	ENSG00000154016	0.767820089	0.037559
AL392104.19	ENSG00000199535	-0.729597136	0.037726
KNTC2	ENSG00000080986	-0.812153617	0.037874
AC021451.8	ENSG00000210898	-0.878090609	0.0379
AC022394.7	ENSG00000200789	0.620641884	0.038088
AC009464.8	ENSG00000209242	-0.623060248	0.038241
AL135842.15	ENSG00000183586	-0.723940545	0.0383
AC134509.2	ENSG00000199465	0.669112324	0.038377
AL109823.23	ENSG00000199507	-0.752874669	0.038581
AL137792.11	ENSG00000214812	-0.8914577	0.039057
U52112.2	ENSG00000211524	0.894856789	0.039263
C9orf71	ENSG00000181778	0.54510016	0.039313
WDR76	ENSG00000092470	-0.587284949	0.03981
AC007283.3	ENSG00000208149	0.925416138	0.039889
AL358117.11	ENSG00000210379	0.796879735	0.039957
RP11-117O7.2	ENSG00000218149	0.827586838	0.040015
AC092868.2	ENSG00000199512	-1.132295402	0.040175
AC121344.5	ENSG00000201356	0.783519987	0.040211
AC008732.9	ENSG00000212382	0.520177677	0.040422
AC011447.7	ENSG00000187928	0.569879528	0.040505
OR6S1	ENSG00000181803	0.671792533	0.040594
AL022149.2	ENSG00000202410	0.513279222	0.04069
RP11-38M15.4	ENSG00000219849	0.666442396	0.040843
AL132989.5	ENSG00000209824	-1.00034451	0.04097
AL353092.6	ENSG00000212571	0.566366109	0.041154
AL645940.4	ENSG00000202441	-0.760766885	0.041202
TRIM55	ENSG00000147573	-0.565026446	0.041389
GTF2E2	ENSG00000197265	-0.550804181	0.041619
CENPI	ENSG00000102384	-0.673194359	0.041815
hsa-mir-223	ENSG00000207939	0.84585314	0.041924
AC073575.30	ENSG00000200688	-1.095881176	0.042243
AL158205.12	ENSG00000204446	0.557184014	0.04232
AC006023.2	ENSG00000199273	0.509275132	0.042584
AC105224.8	ENSG00000210248	-0.805199976	0.043051
AC091057.6	ENSG00000210161	-0.888035143	0.043542
IGHV3-35	ENSG00000211957	0.680687694	0.043631
AC126389.7	ENSG00000201586	0.919932324	0.043924
RP11-35N6.4	ENSG00000220198	0.871230507	0.044102
GAS2L3	ENSG00000139354	-0.532301905	0.044834
AL589947.3	ENSG00000209206	0.89014805	0.044851
AL589947.3	ENSG00000221455	0.89014805	0.044851
AC096587.1	ENSG00000202216	0.741869484	0.044987
AL137247.14	ENSG00000212293	-0.588736741	0.045137
HELLS	ENSG00000119969	-0.72964393	0.045574

Gene Symbol	ENSEMBL ID	Fold Change	P-value
AC073995.6	ENSG00000135976	-0.655681679	0.04567
RP11-290P14.2	ENSG00000216496	0.993920466	0.045809
AP000240.1	ENSG00000209835	-0.930857464	0.046256
RP11-163N15.1	ENSG00000217002	0.787588111	0.046369
AC098591.4	ENSG00000200455	-0.691386241	0.046623
AL049576.19	ENSG00000209629	0.609039096	0.046776
hsa-mir-21	ENSG00000199004	-0.532589084	0.046945
AC004073.1	ENSG00000211376	-0.722250067	0.047389
AC100852.2	ENSG00000210020	-0.877957658	0.047575
AP001065.1	ENSG00000210065	-1.568805669	0.047596
AL355608.11	ENSG00000207268	-1.048207268	0.047666
AC091167.19	ENSG00000208939	0.544409037	0.047788
AC087672.7	ENSG00000212348	0.51209892	0.047882
AC136896.6	ENSG00000200326	0.922636885	0.048259
OR51B4	ENSG00000183251	0.571861332	0.04837
AL358253.16	ENSG00000209591	-0.849563993	0.048416
AL138919.12	ENSG00000211435	-0.584688743	0.048468
AC008635.6	ENSG00000210192	-0.96311748	0.048732
RPS6KA3	ENSG00000177189	-0.540531222	0.048802
PARP14	ENSG00000173193	-0.537432059	0.048992
AC124312.5	ENSG00000209418	-1.186376975	0.049121
AL161450.14	ENSG00000210157	-1.041676617	0.04958
RP1-313I6.8	ENSG00000217751	0.767445006	0.04988
ARHGDIB	ENSG00000111348	-0.676303212	0.049943
AL121890.34	ENSG00000212536	0.540164615	0.049974

Gene Symbol: gene symbol or GeneBank accession number annotated by the Gene Chip® Human Exon 1.0 ST Array (Affimetrix)
Fold Change: difference between U1-BBS1_mut vs. U1-wt treatment of means derived from exonic probe sets of the gene and displayed on logarithmic scale
P-Value: p-value of the t-test on the means of exonic probe sets of the gene between U1-BBS1_mut vs. U1-wt treatment

Supplementary Table 3 List of primers used for RT-PCR analysis of candidate genes.

Gene	Primer Name	Sequence	Tm [°C]	Product size [bp]
OR8G1	OR8G1_E1F	5' ctctcagaacagccagagctccag	60.8	690
	OR8G1_E1R	5' caacatgtgggagctacaagtgctg	60.2	
SERHL	SERHL_E1F	5' ggcctggaactgcaggatacactc	59.6	550
	SERHL_E7R	5' tgctctatggctctccgcttgtag	59.9	
OR10G2	OR10G2_E1F	5' ctggatgccgtggtgacagatttc	60.1	550
	ORG10G2_E1R	5' ctcaatactgcgcggatgtcacag	59.9	
CCDC162	CCDC162_E1F	5' cgatgtttgctgtcagcggatgg	60.7	500
	CCDC162_E4R	5' ggtatctgggctgttactcataactggg	60.1	
GRAP	GRAP_E4F	5' agctggtcgacttctaccgcac	60.6	510
	GRAP_E5R	5' acagctggcagccaatggaaag	60.5	
OR6B3	OR6B3_E1F	5' gtacctgctcttcctcctcttcctg	60.1	520
	OR6B3_E1R	5' accagctctgcagtggagaagtc	60.5	
OR10H4	OR10H4_E1F	5' caaccttctcatcatggccacaatctg	59.9	520
	OR10H4_E1R	5' gaataaacagcctatcagggctgtgac	59.3	
EFNB3	EFNB3_E1F	5' cctggagcctgtctactggaactc	60.4	400
	EFNB3_E4R	5' ccttcatgcctctggttaggcac	59.9	
TUBB4	TUBB4_E2F	5' aggttatcagtgacgaacatggcatcg	60.3	540
	TUBB4_E4R	5' gatgcagtaggtctcatccgtattctcc	59.7	
IRS1	IRS1_E1F	5' cctatgccagcatcagtttccagaag	59.6	500
	IRS1_E2R	5' atactctctccacccaacgtgaacag	59.7	
EPHB2	EPHB2_E5F	5' cctcgtctacaacatcatctgcaagagc	60.7	560
	EPHB2_E8R	5' gtggcaacttctcctggatgcttg	60.4	
TUBA1A	TUBA1A_E1F	5' cttacatcgaccgcctaagagtcgc	60.7	530
	TUBA1A_E4R	5' agaaccagttcccccaccaaag	59.3	
TCF4	TCF4_E2F	5' gccttagggacggacaaagagc	59.9	560
	TCF4_E9R	5' agtcggcagtgcttgctgatg	60	
H3F3B	H3F3B_E1F	5' ggagaagtggcctaaaacttcggc	60.2	400
	H3F3B_E3R	5' catgatggtgactctcttagcgtggatg	60.4	
AP1S2	AP1S2_E2F	5' agtcgtcagggaaagcttcgactgc	60.4	520
	AP1S2_E5R	5' catggacatgaagggagtgaccatc	59.3	
PRDX3	PRDX3_E4F	5' ttgcttttagtgacaaagctaacg	60	490
	PRDX3_E7R	5' tttcaactgtggttcttctctcag	60	
KIF20B	KIF20B_E23F	5' aacagtatgagagagcatgcaaag	60	430
	KIF20B_E26R	5' tccatttcattctgttgcttaaaa	60	
CKAP5	CKAP5_E6F	5' tgctcctagacctactcgatttct	59.9	450
	CKAP5_E10R	5' ctctttgaatttctccaagatggt	60	
FAM111B	FAM111B_E1F	5' ataaaagagcagtctttccagcac	60.3	790
	FAM11B_E4R	5' tagcaacaacatgaaaaagaatgc	60.5	
NDC80	NDC80_E5F	5' tgtgcccctcatacgaacttcctg	60.5	550
	NDC80_E10R	5' gagactccaaattgctcatgtatgcctg	59.6	

Gene	Primer Name	Sequence	Tm [°C]	Product size [bp]
IDE	IDE_E2F	5’ gacaagcgagaatatcgagggctagag	59.9	520
	IDE_E5R	5’ ccttcttggtttggtctagtctccagag	59.9	
PLGLA1	PLGLA_E1F	5’ gcaggaagcagagaagaatgtgcag	60.2	600
	PLGLA_E3R	5’ gggttccacatccacaaattcaaccaac	60.7	
CCDC144B	CCDC144B_E5F	5’ gcaaggaacccagaagtggttacg	60.1	640
	CCDC144B_E9R	5’ gtgtcttggattcttggtaggctagcag	60.5	
SEC24A	Sec24A_E3F	5’ ctcacgcccctgacatcatcatatagag	59.8	620
	Sec24A_E8R	5’ caattgtactggaggtaaccacaggc	59.1	
ORC6L	ORC6L_E2F	5’ agtgcagtcatgtgcctggaccttg	60.7	460
	ORC6L_E6R	5’ ccgtggtggagtagctacatctcc	60.3	
ANAPC5	ANAPC5_E3F	5’ ctggaactgaaccagaggttcacaaaac	59.8	500
	ANAPC5_E7R	5’ cggctccggtaagaatcagacgatc	60.7	
PCOLCE2	PCOLCE2_E3F	5’ catagacctcgagagtgacaacctgtg	60	450
	PCOLCE2_E5R	5’ ttctagcatcgttgacttccccgc	60.7	
C2orf27A	C2orf27A_E1F	5’ aatgtacagactagcacagaagctggac	59.7	550
	C2orf27A_E4R	5’ ggctctacaggaggtgccatgaag	59.4	

3.3.9. Own contributions to the manuscript “Search for downstream target genes of BBS1”

Cell culture, lentivirus production, candidate gene selection, RT-PCR analysis, qPCR analysis of integrated proviral DNA, contributions to data interpretation and manuscript writing

4. General Discussion

4.1. Ciliopathies

We have identified and characterized splice defects in two ciliary genes, designated *BBS1* and *RPGR*, which cause RP. We speculate that photoreceptor degeneration is caused by mislocalization of RHO or other proteins transported through the CC. Ectopic localization of RHO has been associated with *RPGR* mutations in both RP mouse models (Hong et al., 2000; Brunner et al., 2010) and human patients (Adamian et al., 2006). It was also found in different BBS mouse models (Nishimura et al., 2004; Mykytyn et al., 2004; Fath et al., 2005). The mislocalization of RHO is generally assumed to occur because of impaired transport along the connecting cilium.

The connecting cilium is a specialized structure which derives from a primary cilium (see General Introduction 1.1.4., page 11). Almost all human cell types carry this single, non-motile cilium which can act as a sensor for e.g. odor or mechanical stimuli. A complete list of tissues with a primary cilium can be found at http://www.bowserlab.org/primarycilia/cilia3.htm. Cilia are evolutionary conserved microtubule-based cell organelles which represent protrusions of the plasma membrane on the surface of the cell. These organelles are involved in many processes in the human body including for instance movement of extracellular fluid in epithelial cells, establishment of the left-right asymmetry and processing of external signals (Fliegauf et al., 2007). The ciliary membrane contains different receptors or ion channels that bind proteins like growth factors or sonic hedgehog and link the presence of these ligands to intracellular transduction cascades (Satir and Christensen, 2007). Consequently, mutations in genes disrupting the morphology or functions of cilia can result in a broad range of human disorders which are summarized by the term ciliopathies (Badano et al., 2006a). Dysfunctions in cilia can lead to defects in kidney, retina, developing limbs, pancreas, liver, spleen, bone, and several parts of the central nervous system. Interestingly, in all cilia-associated disorders, only a fraction of ciliated tissues are affected. These findings point towards the fact that mutated genes accomplish distinct ciliary tasks in different tissues. The mutations identified in *BBS1* and *RPGR* may only disrupt their properties necessary for correct functioning of photoreceptors which is for instance the proper localization of RHO to OS. This may

finally lead to the tissue-specific, ocular phenotype. A further explanation for the variable disease symptoms in ciliopathies could be that ciliary proteins may have other functions which are not limited to the cilium and only important in certain tissues. This might be in part due to variable protein redundancies and/or buffering capacities of individual tissues and cell types (Badano et al., 2006a). Although many studies have elucidated the pathogenic mechanisms in ciliopathies, the question how defects in this almost ubiquitous cell organelle can lead to variable and diverse phenotypes is not fully understood.

4.1.1. Ciliary genes *BBS1* and *RPGR*

Most mutations in *BBS1* lead to different symptoms associated with BBS. In contrast, *RPGR* mutations generally cause a non-pleiotropic disorder showing only retinal degeneration. Consequently, it is assumed that BBS1 has a more general ciliary function, whereas the function of RPGR is restricted to the retina.

BBS1 interacts in a complex with other BBS proteins, called the BBSome (Nachury et al., 2007). This complex is involved in active transport of membrane protein-containing vesicles to the cilium (Jin et al., 2010). Thus mutations in *BBS1* may impair transport of proteins to cilia. Several lines of evidence demonstrated that the BBSome accomplishes transport of important signaling receptors into the ciliary membrane. Mislocalization of somatostatin receptor type 3 (Sstr3) was found in neurons of mice lacking BBS genes (Berbari et al., 2008). Since aberrant levels of somatostatin are linked to cognitive impairment in humans, this aberrant localization of the receptor might explain the learning disabilities usually observed in BBS patients. Furthermore, the obesity phenotype in BBS could be due to impaired signaling by the leptin receptor (LepR) or the melanin-concentrating hormone receptor 1 (Mchr1). These receptors are both involved in the regulation of food intake in the CNS and do not localize to cilia in BBS knock out mice (Berbari et al., 2008; Seo et al., 2009). Likewise, another ciliary disease, termed polycystic kidney disease (PKD), might also occur because of defective trafficking of signaling pathway proteins to cilia. Cyst formation in the kidney is presumed to result from defects in the planar cell polarity pathway (PCP) (Fischer et al., 2006). PCP regulates mitotic spindle orientation to promote oriented cell division which is necessary for correct development of the kidney morphology (Fischer and Pontoglio, 2009). Because disruption of some BBS proteins leads to defects in planar cell polarity in mice (Ross

et al., 2005) there might be a link between PCP signaling, the cilium and PKD in BBS patients. Together, these findings may explain why mutations in *BBS1* can lead to a pleiotropic disorder.

In contrast to *BBS1* mutations, sequence alterations in *RPGR* mainly affect retinal function. RPGR proteins localize to the basal body and photoreceptor connecting cilium (Shu et al., 2005; Khanna et al., 2005) and directly interact with the RPGR interacting protein 1 (RPGRIP1) at centrioles and basal bodies (Roepman et al., 2000; Shu et al., 2005). RPGRIP1 was found to be mutated in LCA patients suggesting that both proteins play an important role in the retina (Dryja et al., 2001). Many other interaction partners of RPGR have been identified. All these findings support a model in which RPGR is in a complex with many other ciliary proteins at the basal body of the photoreceptor connecting cilium. There, RPGR might have different functions necessary for survival of photoreceptors. To date, these functions remain very speculative. Of note, mislocalization of RHO was found in *RPGR* mutant mice (Hong et al., 2000; Brunner et al., 2010). These findings together with its interaction with microtubule-associated proteins, IFT motors, RAB8A and its localization to the connecting cilium (Khanna et al., 2005; Murga-Zamalloa et al., 2010), suggest a role for RPGR in IFT transport. It seems that RPGR may act as a scaffold protein which clusters essential components of the IFT machinery at the connecting cilium. The clustering of these IFT components might be essential to accomplish the high intersegmental protein transport, needed in photoreceptors. Consequently, lower trafficking efficiencies induced by mutations in *RPGR* might lead to RP. Other disease phenotypes occasionally observed in patients with *RPGR* mutations could also be explained by this model. Although RPGR is expressed in many cell types, it might not be essential for correct functioning of cilia in other tissues than retina. This may be due to protein redundancies or lower rates of ciliary protein transport in these cell types. Nevertheless, it cannot be excluded that *RPGR* mutations could have a dominant negative effect by retaining essential ciliary components at the basal body. As a consequence, these components cannot perform their specific functions which may also result in defects of motile cilia, which are the flagella of sperms or multi-cilia on lung epithelial cells. This could explain infertility and lung infections present in PCD patients with *RPGR* mutations (Moore et al., 2006). Supportively, male infertility was also found in RPGR overexpressing mice (Brunner et al., 2008).

4.1.2. Genotype-phenotype correlations in *BBS1*- and *RPGR*-associated ciliopathies

Our studies in patients affected by mutations in ciliary genes *BBS1* and *RPGR*, revealed variations in disease expression which are usually not associated with mutations in either of these two genes. To give an example, the two patients with the splice site mutation in *BBS1* showed only RP, although *BBS1* mutations are usually associated with multiple phenotypes (Mykytyn et al., 2002). The observed phenotypic differences in expressivity of the disease suggest the presence of disease modifying factors.

The position of the mutation and its effect on protein function is one aspect which should be considered in order to make phenotype-genotype correlations. A major hot spot for *RPGR* mutations is in the alternative exon ORF15 whereas a minor fraction has been found in consitutive exons 1 to 14 and none in exons 16 to 19 (Vervoort et al., 2000; Vervoort and Wright, 2002; Pelletier et al., 2007; Neidhardt et al., 2008). Interestingly, mutations in exon ORF15 were reported to cause less severe forms of RP (Sharon et al., 2003). This might be reasonable because many of the mutations ranging from exons 1 to 14 lay in the conserved RCC1-like domain, through which important interactions with many other proteins may be performed. Supportively, a deletion spanning the entire RCC1-like domain was identified in patients with very severe RP symptoms (Jin et al., 2005).

In BBS, one of the most frequent mutation is p.M390R in *BBS1* (Mykytyn et al., 2002). It accounts for more than 70% of the total *BBS1* mutational load in Caucasian families and is considered to be a founder mutation (Mykytyn et al., 2003; Beales et al., 2003; Muller et al., 2010). Many other *BBS1* mutations have been identified to a minor fraction in the other exons, but none was initially found at extreme N and C termini. Recently, a mutation affecting the first nucleotide of the gene (c.1A>G, p.M1?) has been identified in a BBS patient showing more severe, abnormal morphologies of inner retinal layers compared to patients with mutations laying more distal at the N terminus (Gerth et al., 2008). Nevertheless, a clear phenotype-genotype correlation couldn't be established in this study.

The expression of the disease phenotype can also be modified by other genes. At least seven BBS proteins genes reside in the BBSome complex (Nachury et al., 2007). Mutations that disrupt BBSome assembly are very likely to cause BBS. Triallelic inheritance and the variable phenotypic expression in BBS might be thus explained by

the accumulation of defects in interactions of BBS proteins gained through additional mutations in other BBS loci. Likewise, mutations in other genes, not directly associated with BBS, might also disturb interactions at the BBSome. For instance, a heterozygous splice site mutation in the gene *CCDC28B* increases disease severity in BBS patients, whereas the homozygous mutations in *CCDC28B* alone did not cause BBS. CCDC28B interacts biochemically with all tested BBS proteins and localizes to the basal body (Badano et al., 2006b). In summary, these findings suggest that *CCDC28B* might be a modifier of the disease phenotype in patients with BBS.

Recently, several groups have reported the existence of modifier genes responsible for the additional ocular manifestation found in several ciliopathies. A common allele in *RPGRIP1L* has been associated with syndromic phenotypes that always include RP as a disease component (Khanna et al., 2009). More recently, it has been published that certain alleles in the genes *PDZD7* or *AHI1* can also contribute to the retinal phenotype in ciliary disorders (Ebermann et al., 2010; Louie et al., 2010). Together, these findings further indicate the high complexity of pathogenic mechanisms leading to the different forms of ciliopathies, which makes it very difficult to predict phenotypes from genotypes.

Genetic modifiers could also exist in RP patients described in our studies. In these cases, sequence alterations in modifier genes may have either a protective (for the patients with mutations in *BBS1*) or a deteriorating effect on the disease pathogenesis (for the patients with mutations in *RPGR*). It would be of further interest to screen our patients for sequence alterations in genetic modifiers as mentioned above which are associated with retinal degeneration. The outcome might probably help to explain the observed phenotypes in our patients.

4.1.3. Splicing as a modifier in *RPGR*- associated ciliopathies

The manifestation of the disease could also be modified by aberrant pre-mRNA splicing. Many reports have demonstrated that defects in splicing can modulate the severity of the disease (Nissim-Rafinia and Kerem, 2002; Garcia-Blanco et al., 2004; Nissim-Rafinia and Kerem, 2005). In two RP patients, we have found mutations in *RPGR* that changed the expression level of a specific, alternative transcript isoform. In addition, we observed variability in the expression of the disease (see Results Discussion 3.1.5, page 50). These findings suggest that misregulation of alternative *RPGR* splicing acts as a modifier. Mutation-induced differences in expression of

alternative *RPGR* isoforms may influence expression of the disease through different pathogenic mechanisms.

We have identified four novel *RPGR* transcript isoforms which were differently expressed among tissues examined (see Results 3.1.4., page 48). These results confirm previous findings demonstrating tissue-specific *RPGR* splicing (Kirschner et al., 1999; Vervoort et al., 2000; Neidhardt et al., 2007). From our expression analysis, we assume that *RPGR* transcript isoforms have specific functions, especially in tissues where expression levels are high. Of note, very high expression was detected for the isoform skipping exon 12 ($RPGR^{skipEx12}$) in lung and kidney, whereas simultaneous skipping of exons 14 and 15 ($RPGR^{skipEx14/15}$) was very frequently observed in brain. These findings suggest that $RPGR^{skipEx12}$ and $RPGR^{skipEx14/15}$ perform specific functions in lung and kidney or in brain, respectively. Distinct complexes of RPGR and tissue-specifc interactions partners might be essential for ciliary properties in these tissues. As a consequence, misregulation of alternative splicing may reduce the amount of protein isoforms needed to build up these RPGR complexes. Lack of these protein variants could thereby cause the additional phenotypic manifestations observed in a few patients. On one hand, downregulation of $RPGR^{skipEx12}$ could explain why patients sometimes exhibit additional defects in the respiratory system. On the other hand, we are not aware of cases showing dysfunctions of the kidney or the central nervous system. Therefore, the physiological function of these isoforms remains to be elucidated. Furthermore, it is unclear to what extend a reduction in their expression could contribute to the pathogenesis of the disease.

Mutation-induced overexpression of an alternative transcript isoform can also cause a disease phenotype. This idea is supported by the finding that overexpression of a cone-specific RPGR isoform causes retinal degeneration (Neidhardt et al., 2007). Given that RPGR protein isoforms bind tissue-specific interaction partners, the increased presence of a protein variant in a tissue, where it is normally expressed at lower levels, might induce the disease through a dominant negative effect. Thereby, it might prevent precise assembly of the tissue-specific RPGR complex and will subsequently lead to dysfunctions of the cilium. Interestingly, we found affected female carriers in the family of the patient who showed increased levels of exon 11a containing *RPGR* transcripts ($RPGR^{+Ex11a}$). The elevated level is most probably due to a sequence alteration in the alternative exon creating a novel ESE binding site. The *RPGR* exon 11a contains a stop codon and is assumed to generate a truncated protein

when introduced into the transcript. Competing with constitutive and alternative ORF15 protein isoforms for interaction partners, a higher amount of *RPGR*$^{+Ex11a}$ derived proteins may impair correct formation of the complex at the connecting cilium. This mechanism could explain the unusual dominant mode of inheritance in this XlRP family. To further confirm the hypothesis it would be crucial to find overexpression of *RPGR*$^{+Ex11a}$ also in affected female carriers. Unfortunately, material from other family members that would allow expression analysis of *RPGR*$^{+Ex11a}$ transcripts is not available.

It has not been proven so far whether the four alternative *RPGR* transcript isoforms identified, give rise to a functional protein as previously shown for the *RPGR*$^{+Ex9a}$ isoform (Neidhardt et al., 2007). *RPGR*$^{+Ex11a}$, *RPGR*^{skipEx12}, *RPGR*^{skipEx14} and *RPGR*^{skipEx15} all contain a PTC making them more susceptible for degradation mediated by NMD. Alternative splicing events that result in PTC containing transcripts and their subsequent degradation by NMD can also be used by the cell to regulate gene expression. The cellular mechanism which couples alternative splicing (AS) with NMD is referred to as AS-NMD and used for instance as an autoregulatory process to control the expression of certain splicing factors (McGlincy and Smith, 2008). We assume that AS-NMD could also participate in the maintenance of a certain level of functional RPGR proteins. Since overexpression of RPGR can cause ciliary defects (Brunner et al., 2008), a precise control of its expression might be crucial for correct functioning of cilia in several tissues. Consequently, an abnormal change in the amount of an AS-NMD-generated *RPGR* isoform used to control RPGR expression, might alter the level of functionally relevant RPGR leading to a pathogenic effects in different tissues. Interestingly, preliminary data indicate (data not shown) that at least *RPGR*$^{+Ex11a}$ might be partially degraded by NMD in human blood lymphoblasts. However, we did not find any indication that normal *RPGR* transcript levels were affected by increased levels of *RPGR*$^{+Ex11a}$ in the patient, which would point towards a pathogenic mechanism mediated by AS-NMD. To date, this mechanism has never been found to cause pathogenesis of the disease. It could be of interest to know whether AS-NMD is used to control the amount of RPGR proteins in certain tissues.

4.2. Therapy of splice defects by adaptation of the U1 snRNA

We have found that defects in mRNA splicing can cause a reduction of the transcript, the presence of aberrant splice products, or the ectopic expression of tissue-specific alternative isoforms, which could all be toxic for the cell. This further implicates that the restoration of normal splicing patterns may lead to a successful treatment of the splice defect. Thus, the therapeutic intervention must act on the level of pre-mRNA splicing. We have demonstrated that the expression of a modified form of the U1 snRNA significantly improved correct splicing of the mRNA in fibroblast from RP patients with a splice defects in *BBS1*. The U1 snRNA was fully adapted to the mutated splice donor site in exon 5 of *BBS1* with the aim to restore normal binding affinities of the U1snRNP to this site. The treatment abolished mutation-induced exon 5 skipping and increased the amount of normal *BBS1* transcripts (see Results 3.2.4., page 79 and 80).

4.2.1. Functional assays

A recent publication demonstrated that the U1 approach can increase the amount of functional protein in fibroblasts from Fanconi anemia patients (Hartmann et al., 2010). Likewise, we performed several functional assays to verify whether the correction of the splice defect in *BBS1* can restore the amount of functional BBS1 protein. Moreover, we presumed that an increase in BBS1 protein will subsequently improve functional properties of the primary cilium. Depletion of BBS1 has been shown to increase activity of the Wnt signaling pathway (Gerdes et al., 2007). Since the amount of normal *BBS1* transcripts is reduced in our patients and could be significantly restored by the U1-mediated approach, we expected increased BBS1 protein levels in fully adapted U1-treated fibroblasts, which should decrease Wnt activity. However, we did not detect conclusive differences in Wnt signaling comparing these fibroblasts with wild type U1 and untreated cells (data not shown). Technical difficulties complicated the conclusions from these experiments. Nevertheless, there are alternative pathways reflecting the performance of the primary cilium in fibroblasts. There is accumulating evidence that hedgehog-mediated signal transduction is highly dependent on correct functioning of the cilium. In addition, signaling accomplished by the platelet-derived growth factor receptor-α might be the

most promising pathway, because it depends on the primary cilium of fibroblasts (Goetz and Anderson, 2010).

Furthermore, we evaluated the expression of different genes which might be regulated through the cilium. We could identify *CKAP5* as a potential candidate gene whose expression might be regulated through the ciliary function of BBS1 (see Results 3.3.3., page 105). However, further experiments need to be done to confirm these findings. Finally, we counted the amount of primary cilia in patient and control fibroblasts treated with or without the adapted U1 snRNA, because the lack of BBS1 has already been linked to lower amounts of primary cilia in cultured cells (Nachury et al., 2007). Counting of cilia revealed no clear differences between treated and untreated control and patient fibroblasts.

Together, these results led to the assumption that the number of primary cilia as well as the ciliary function in fibroblasts is not dramatically affected by the lower amount of *BBS1* found in the patient. These findings might indicate that the reduced BBS1 level causes the disease through a photoreceptor-specific effect. We cannot exlude that we have overlooked mild alterations of the ciliary properties. The amino acid change in BBS1 (p.Arg160Gln) could also be relevant to modify the ciliary phenotype.

4.2.2. Side effects and improvements of the U1-based approach

The modification of the ubiquitously used U1 snRNA might bear the risk to interfere with splicing of other genes. The process of pre-mRNA splicing is highly dynamic. During splicing, many spliceosome components enter and exit the complex. Thus changes in binding properties of certain splicing factors could cause aberrant splicing. Alterations in binding affinities of the U1 snRNA might lead to a reduction or an increase in the usage of a classical splice site. Furthermore, it may also activate utilization of cryptic splice sites.

We tested for splice defects after the treatment with a modified U1 snRNA with particular interest on genes associated with retinal degenerations (Boettinger, 2009, Master Thesis). We identified 80 to 90% sequence complementarity of the fully adapted U1 snRNA to splice donor sites in genes *SEMA4A*, *PRPF31*, *PRPF8* and *RPGR* that primarily cause RP. To check whether these genes showed splice defects after the U1 treatment, we analyzed the expression of affected exons by RT-PCR using flanking primers. Our studies revealed normal splicing for all tested genes

(Boettinger, 2009, Master Thesis). In order to get a more general overview about possible adverse effects on splicing, we performed mRNA expression analyses in U1 treated fibroblasts with the Human Exon 1.0 ST array. Comparing fibroblasts treated either with wt or fully adapted U1 snRNA we found changes in splicing of 5 retinopathy-associated genes (Boettinger, 2009, Master Thesis). Nevertheless, a further analysis by RT-PCR is necessary to clarify whether these genes show aberrant splicing due to the U1 treatment. Expression analysis of other gene transcripts selected from the array demonstrated only mild effects upon treatment with fully adapted U1 (see Results 3.3.3., page 101). Finally, the study of animal models will be needed to evaluate the balance between benefits and side effects caused by the U1 treatment on the physiologic level.

The specificity of the U1 approach might be increased by nucleotide extensions at the 5' end of the U1 snRNA. A U1 snRNA extended by nucleotides (nt) complementary to the intronic sequence downstream of the splice donor site might have higher affinities to the target site and should reduce its interaction with non-target splice sites. We expanded the 5' splice site of the adapted U1 snRNA by 15 nts which were fully complementary to the intronic sequence following the splice donor site of exon 5 in *BBS1*. The efficiency of the extended U1 snRNA was then evaluated by co-transfection with minigenes comprising genomic sequence of *BBS1* spanning from intron 4 to intron 7, as previously described (see Results 3.2.4., page 79). For both, wt and mutant minigenes, co-expression of the extended U1 snRNA had no effect on the splice pattern suggesting that the generated U1 snRNP is not functional (data not shown). Probably, there might be a size limitation in the U1 snRNA which is crucial for correct maturation of the U1 snRNP. The threshold might be exceeded by the addition of 15 nts making the snRNP non-functional. However, successful treatment of a mouse model for Duchenne muscular dystrophy using 54 nts antisense oligonucleotides linked to the U1 snRNA has been reported (Denti et al., 2006). These findings show that the generated U1 snRNP is functional and contradicts our hypothesis. Probably, dimerization of sequences at the 5' end of the U1 snRNA might better explain why our extended U1 snRNA appeared to be not functional. Since this mechanism may block binding of U1 to its target sequence, 5' extensions shorter than 15 nucleotides could be more favorable. In order to achieve high specificity of the treatment and most efficient correction of the splice defect, the ideal extension length at 5' end of the U1 snRNA has to be determined in further experiments.

4.3. Concluding remarks

Taken together, we have detected splice defects in *RPGR* and *BBS1* in patients whose disease phenotypes were different from those which are normally associated with mutations in these genes. The findings indicated that defects in mRNA splicing might modify the phenotype and will further help to clarify disease pathogenesis in the patients.

To prevent deleterious effects of aberrant splicing, we have developed a therapeutic approach that significantly corrected splicing in patient-derived fibroblasts. Following successful treatment in animal models, these promising results might lead to the development of a gene therapy in patients with eye diseases caused by splice defects.

4.4. References General Discussion

1. Adamian,M., Pawlyk,B.S., Hong,D.H., and Berson,E.L. (2006). Rod and cone opsin mislocalization in an autopsy eye from a carrier of X-linked retinitis pigmentosa with a Gly436Asp mutation in the RPGR gene. Am. J. Ophthalmol. *142*, 515-518.

2. Badano,J.L., Leitch,C.C., Ansley,S.J., May-Simera,H., Lawson,S., Lewis,R.A., Beales,P.L., Dietz,H.C., Fisher,S., and Katsanis,N. (2006a). Dissection of epistasis in oligogenic Bardet-Biedl syndrome. Nature *439*, 326-330.

3. Badano,J.L., Mitsuma,N., Beales,P.L., and Katsanis,N. (2006b). The ciliopathies: an emerging class of human genetic disorders. Annu. Rev. Genomics Hum. Genet. *7*, 125-148.

4. Beales,P.L., Badano,J.L., Ross,A.J., Ansley,S.J., Hoskins,B.E., Kirsten,B., Mein,C.A., Froguel,P., Scambler,P.J., Lewis,R.A., Lupski,J.R., and Katsanis,N. (2003). Genetic interaction of BBS1 mutations with alleles at other BBS loci can result in non-Mendelian Bardet-Biedl syndrome. Am. J. Hum. Genet. *72*, 1187-1199.

5. Berbari,N.F., Lewis,J.S., Bishop,G.A., Askwith,C.C., and Mykytyn,K. (2008). Bardet-Biedl syndrome proteins are required for the localization of G protein-coupled receptors to primary cilia. Proc. Natl. Acad. Sci. U. S. A *105*, 4242-4246.

6. Boettinger, U. (2009). Nebenwirkungen eines therapeutischen Ansatzes zur Behandlung von pathogenem Exonverlust mittels U1snRNA Adaption. Diplomarbeit der Fakultät für Biologie der Eberhard Karls Universität Tübingen. Ausgeführt an der Universität Zürich.

7. Brunner,S., Colman,D., Travis,A.J., Luhmann,U.F., Shi,W., Feil,S., Imsand,C., Nelson,J., Grimm,C., Rulicke,T., Fundele,R., Neidhardt,J., and Berger,W. (2008). Overexpression of RPGR leads to male infertility in mice due to defects in flagellar assembly. Biol. Reprod. *79*, 608-617.

8. Brunner,S., Skosyrski,S., Kirschner-Schwabe,R., Knobeloch,K.P., Neidhardt,J., Feil,S., Glaus,E., Luhmann,U.F., Ruther,K., and Berger,W. (2010). Cone versus rod disease in a mutant Rpgr mouse caused by different genetic backgrounds. Invest Ophthalmol. Vis. Sci. *51*, 1106-1115.

9. Denti,M.A., Rosa,A., D'Antona,G., Sthandier,O., De Angelis,F.G., Nicoletti,C., Allocca,M., Pansarasa,O., Parente,V., Musaro,A., Auricchio,A., Bottinelli,R., and Bozzoni,I. (2006). Body-wide gene therapy of Duchenne muscular dystrophy in the mdx mouse model. Proc. Natl. Acad. Sci. U. S. A *103*, 3758-3763.

10. Dryja,T.P., Adams,S.M., Grimsby,J.L., McGee,T.L., Hong,D.H., Li,T., Andreasson,S., and Berson,E.L. (2001). Null RPGRIP1 alleles in patients with Leber congenital amaurosis. Am. J. Hum. Genet. *68*, 1295-1298.

11. Ebermann,I., Phillips,J.B., Liebau,M.C., Koenekoop,R.K., Schermer,B., Lopez,I., Schafer,E., Roux,A.F., Dafinger,C., Bernd,A., Zrenner,E., Claustres,M., Blanco,B., Nurnberg,G., Nurnberg,P., Ruland,R., Westerfield,M., Benzing,T., and Bolz,H.J. (2010). PDZD7 is a modifier of retinal disease and a contributor to digenic Usher syndrome. J. Clin. Invest *120*, 1812-1823.

12. Fath,M.A., Mullins,R.F., Searby,C., Nishimura,D.Y., Wei,J., Rahmouni,K., Davis,R.E., Tayeh,M.K., Andrews,M., Yang,B., Sigmund,C.D., Stone,E.M., and Sheffield,V.C. (2005). Mkks-null mice have a phenotype resembling Bardet-Biedl syndrome. Hum. Mol. Genet. *14*, 1109-1118.

13. Fischer,E., Legue,E., Doyen,A., Nato,F., Nicolas,J.F., Torres,V., Yaniv,M., and Pontoglio,M. (2006). Defective planar cell polarity in polycystic kidney disease. Nat. Genet. *38*, 21-23.

14. Fischer,E. and Pontoglio,M. (2009). Planar cell polarity and cilia. Semin. Cell Dev. Biol. *20*, 998-1005.

15. Fliegauf,M., Benzing,T., and Omran,H. (2007). When cilia go bad: cilia defects and ciliopathies. Nat. Rev. Mol. Cell Biol. *8*, 880-893.

16. Garcia-Blanco,M.A., Baraniak,A.P., and Lasda,E.L. (2004). Alternative splicing in disease and therapy. Nat. Biotechnol. *22*, 535-546.

17. Gerdes,J.M., Liu,Y., Zaghloul,N.A., Leitch,C.C., Lawson,S.S., Kato,M., Beachy,P.A., Beales,P.L., DeMartino,G.N., Fisher,S., Badano,J.L., and Katsanis,N. (2007). Disruption of the basal body compromises proteasomal function and perturbs intracellular Wnt response. Nat. Genet. *39*, 1350-1360.

18. Gerth,C., Zawadzki,R.J., Werner,J.S., and Heon,E. (2008). Retinal morphology in patients with BBS1 and BBS10 related Bardet-Biedl Syndrome evaluated by Fourier-domain optical coherence tomography. Vision Res. *48*, 392-399.

19. Goetz,S.C. and Anderson,K.V. (2010). The primary cilium: a signalling centre during vertebrate development. Nat. Rev. Genet. *11*, 331-344.

20. Hartmann,L., Neveling,K., Borkens,S., Schneider,H., Freund,M., Grassman,E., Theiss,S., Wawer,A., Burdach,S., Auerbach,A.D., Schindler,D., Hanenberg,H., and Schaal,H. (2010). Correct mRNA Processing at a Mutant TT Splice Donor in FANCC Ameliorates the Clinical Phenotype in Patients and Is Enhanced by Delivery of Suppressor U1 snRNAs. Am. J. Hum. Genet. *87*, 480-493.

21. Hong,D.H., Pawlyk,B.S., Shang,J., Sandberg,M.A., Berson,E.L., and Li,T. (2000). A retinitis pigmentosa GTPase regulator (RPGR)-deficient mouse model for X-linked retinitis pigmentosa (RP3). Proc. Natl. Acad. Sci. U. S. A *97*, 3649-3654.

22. Jin,H., White,S.R., Shida,T., Schulz,S., Aguiar,M., Gygi,S.P., Bazan,J.F., and Nachury,M.V. (2010). The conserved Bardet-Biedl syndrome proteins assemble a coat that traffics membrane proteins to cilia. Cell *141*, 1208-1219.

23. Jin,Z.B., Liu,X.Q., Uchida,A., Vervoort,R., Morishita,K., Hayakawa,M., Murakami,A., Matsumoto,N., Niikawa,N., and Nao-i N (2005). Novel deletion spanning RCC1-like domain of RPGR in Japanese X-linked retinitis pigmentosa family. Mol. Vis. *11*, 535-541.

24. Khanna,H., Davis,E.E., Murga-Zamalloa,C.A., Estrada-Cuzcano,A., Lopez,I., den Hollander,A.I., Zonneveld,M.N., Othman,M.I., Waseem,N., Chakarova,C.F., Maubaret,C., Diaz-Font,A., MacDonald,I., Muzny,D.M., Wheeler,D.A., Morgan,M., Lewis,L.R., Logan,C.V., Tan,P.L., Beer,M.A., Inglehearn,C.F., Lewis,R.A., Jacobson,S.G., Bergmann,C., Beales,P.L., Attie-Bitach,T., Johnson,C.A., Otto,E.A., Bhattacharya,S.S., Hildebrandt,F., Gibbs,R.A., Koenekoop,R.K., Swaroop,A., and Katsanis,N. (2009). A common allele in RPGRIP1L is a modifier of retinal degeneration in ciliopathies. Nat. Genet. *41*, 739-745.

25. Khanna,H., Hurd,T.W., Lillo,C., Shu,X., Parapuram,S.K., He,S., Akimoto,M., Wright,A.F., Margolis,B., Williams,D.S., and Swaroop,A. (2005). RPGR-ORF15, which is mutated in retinitis pigmentosa, associates with SMC1, SMC3, and microtubule transport proteins. J. Biol. Chem. *280*, 33580-33587.

26. Kirschner,R., Rosenberg,T., Schultz-Heienbrok,R., Lenzner,S., Feil,S., Roepman,R., Cremers,F.P., Ropers,H.H., and Berger,W. (1999). RPGR transcription studies in mouse and human tissues reveal a retina-specific isoform that is disrupted in a patient with X-linked retinitis pigmentosa. Hum. Mol. Genet. *8*, 1571-1578.

27. Louie,C.M., Caridi,G., Lopes,V.S., Brancati,F., Kispert,A., Lancaster,M.A., Schlossman,A.M., Otto,E.A., Leitges,M., Grone,H.J., Lopez,I., Gudiseva,H.V., O'Toole,J.F., Vallespin,E., Ayyagari,R., Ayuso,C., Cremers,F.P., den Hollander,A.I., Koenekoop,R.K., Dallapiccola,B., Ghiggeri,G.M., Hildebrandt,F., Valente,E.M., Williams,D.S., and Gleeson,J.G. (2010). AHI1 is required for photoreceptor outer segment development and is a modifier for retinal degeneration in nephronophthisis. Nat. Genet. *42*, 175-180.

28. McGlincy,N.J. and Smith,C.W. (2008). Alternative splicing resulting in nonsense-mediated mRNA decay: what is the meaning of nonsense? Trends Biochem. Sci. *33*, 385-393.

29. Moore,A., Escudier,E., Roger,G., Tamalet,A., Pelosse,B., Marlin,S., Clement,A., Geremek,M., Delaisi,B., Bridoux,A.M., Coste,A., Witt,M., Duriez,B., and Amselem,S. (2006). RPGR is mutated in patients with a complex X linked phenotype combining primary ciliary dyskinesia and retinitis pigmentosa. J. Med. Genet. *43*, 326-333.

30. Muller,J., Stoetzel,C., Vincent,M.C., Leitch,C.C., Laurier,V., Danse,J.M., Helle,S., Marion,V., Bennouna-Greene,V., Vicaire,S., Megarbane,A., Kaplan,J., Drouin-Garraud,V., Hamdani,M., Sigaudy,S., Francannet,C., Roume,J., Bitoun,P., Goldenberg,A., Philip,N., Odent,S., Green,J., Cossee,M., Davis,E.E., Katsanis,N., Bonneau,D., Verloes,A., Poch,O., Mandel,J.L., and Dollfus,H. (2010). Identification of 28 novel mutations in the Bardet-Biedl syndrome

genes: the burden of private mutations in an extensively heterogeneous disease. Hum. Genet. *127*, 583-593.

31. Murga-Zamalloa,C.A., Atkins,S.J., Peranen,J., Swaroop,A., and Khanna,H. (2010). Interaction of retinitis pigmentosa GTPase regulator (RPGR) with RAB8A GTPase: implications for cilia dysfunction and photoreceptor degeneration. Hum. Mol. Genet. *19*, 3591-3598.

32. Mykytyn,K., Mullins,R.F., Andrews,M., Chiang,A.P., Swiderski,R.E., Yang,B., Braun,T., Casavant,T., Stone,E.M., and Sheffield,V.C. (2004). Bardet-Biedl syndrome type 4 (BBS4)-null mice implicate Bbs4 in flagella formation but not global cilia assembly. Proc. Natl. Acad. Sci. U. S. A *101*, 8664-8669.

33. Mykytyn,K., Nishimura,D.Y., Searby,C.C., Beck,G., Bugge,K., Haines,H.L., Cornier,A.S., Cox,G.F., Fulton,A.B., Carmi,R., Iannaccone,A., Jacobson,S.G., Weleber,R.G., Wright,A.F., Riise,R., Hennekam,R.C., Luleci,G., Berker-Karauzum,S., Biesecker,L.G., Stone,E.M., and Sheffield,V.C. (2003). Evaluation of complex inheritance involving the most common Bardet-Biedl syndrome locus (BBS1). Am. J. Hum. Genet. *72*, 429-437.

34. Mykytyn,K., Nishimura,D.Y., Searby,C.C., Shastri,M., Yen,H.J., Beck,J.S., Braun,T., Streb,L.M., Cornier,A.S., Cox,G.F., Fulton,A.B., Carmi,R., Luleci,G., Chandrasekharappa,S.C., Collins,F.S., Jacobson,S.G., Heckenlively,J.R., Weleber,R.G., Stone,E.M., and Sheffield,V.C. (2002). Identification of the gene (BBS1) most commonly involved in Bardet-Biedl syndrome, a complex human obesity syndrome. Nat. Genet. *31*, 435-438.

35. Nachury,M.V., Loktev,A.V., Zhang,Q., Westlake,C.J., Peranen,J., Merdes,A., Slusarski,D.C., Scheller,R.H., Bazan,J.F., Sheffield,V.C., and Jackson,P.K. (2007). A core complex of BBS proteins cooperates with the GTPase Rab8 to promote ciliary membrane biogenesis. Cell *129*, 1201-1213.

36. Neidhardt,J., Glaus,E., Barthelmes,D., Zeitz,C., Fleischhauer,J., and Berger,W. (2007). Identification and characterization of a novel RPGR isoform in human retina. Hum. Mutat. *28*, 797-807.

37. Neidhardt,J., Glaus,E., Lorenz,B., Netzer,C., Li,Y., Schambeck,M., Wittmer,M., Feil,S., Kirschner-Schwabe,R., Rosenberg,T., Cremers,F.P., Bergen,A.A., Barthelmes,D., Baraki,H., Schmid,F., Tanner,G., Fleischhauer,J., Orth,U., Becker,C., Wegscheider,E., Nurnberg,G., Nurnberg,P., Bolz,H.J., Gal,A., and Berger,W. (2008). Identification of novel mutations in X-linked retinitis pigmentosa families and implications for diagnostic testing. Mol. Vis. *14*, 1081-1093.

38. Nishimura,D.Y., Fath,M., Mullins,R.F., Searby,C., Andrews,M., Davis,R., Andorf,J.L., Mykytyn,K., Swiderski,R.E., Yang,B., Carmi,R., Stone,E.M., and Sheffield,V.C. (2004). Bbs2-null mice have neurosensory deficits, a defect in social dominance, and retinopathy associated with mislocalization of rhodopsin. Proc. Natl. Acad. Sci. U. S. A *101*, 16588-16593.

39. Nissim-Rafinia,M. and Kerem,B. (2002). Splicing regulation as a potential genetic modifier. Trends in Genetics *18*, 123-127.

40. Nissim-Rafinia,M. and Kerem,B. (2005). The splicing machinery is a genetic modifier of disease severity. Trends Genet. *21*, 480-483.

41. Pelletier,V., Jambou,M., Delphin,N., Zinovieva,E., Stum,M., Gigarel,N., Dollfus,H., Hamel,C., Toutain,A., Dufier,J.L., Roche,O., Munnich,A., Bonnefont,J.P., Kaplan,J., and Rozet,J.M. (2007). Comprehensive survey of mutations in RP2 and RPGR in patients affected with distinct retinal dystrophies: genotype-phenotype correlations and impact on genetic counseling. Hum. Mutat. *28*, 81-91.

42. Roepman,R., Bernoud-Hubac,N., Schick,D.E., Maugeri,A., Berger,W., Ropers,H.H., Cremers,F.P., and Ferreira,P.A. (2000). The retinitis pigmentosa GTPase regulator (RPGR) interacts with novel transport-like proteins in the outer segments of rod photoreceptors. Hum. Mol. Genet. *9*, 2095-2105.

43. Ross,A.J., May-Simera,H., Eichers,E.R., Kai,M., Hill,J., Jagger,D.J., Leitch,C.C., Chapple,J.P., Munro,P.M., Fisher,S., Tan,P.L., Phillips,H.M., Leroux,M.R., Henderson,D.J., Murdoch,J.N., Copp,A.J., Eliot,M.M., Lupski,J.R., Kemp,D.T., Dollfus,H., Tada,M., Katsanis,N., Forge,A., and Beales,P.L. (2005). Disruption of Bardet-Biedl syndrome ciliary proteins perturbs planar cell polarity in vertebrates. Nat. Genet. *37*, 1135-1140.

44. Satir,P. and Christensen,S.T. (2007). Overview of structure and function of mammalian cilia. Annu. Rev. Physiol *69*, 377-400.

45. Seo,S., Guo,D.F., Bugge,K., Morgan,D.A., Rahmouni,K., and Sheffield,V.C. (2009). Requirement of Bardet-Biedl syndrome proteins for leptin receptor signaling. Hum. Mol. Genet. *18*, 1323-1331.

46. Sharon,D., Sandberg,M.A., Rabe,V.W., Stillberger,M., Dryja,T.P., and Berson,E.L. (2003). RP2 and RPGR mutations and clinical correlations in patients with X-linked retinitis pigmentosa. Am. J. Hum. Genet. *73*, 1131-1146.

47. Shu,X., Fry,A.M., Tulloch,B., Manson,F.D., Crabb,J.W., Khanna,H., Faragher,A.J., Lennon,A., He,S., Trojan,P., Giessl,A., Wolfrum,U., Vervoort,R., Swaroop,A., and Wright,A.F. (2005). RPGR ORF15 isoform co-localizes with RPGRIP1 at centrioles and basal bodies and interacts with nucleophosmin. Hum. Mol. Genet. *14*, 1183-1197.

48. Vervoort,R., Lennon,A., Bird,A.C., Tulloch,B., Axton,R., Miano,M.G., Meindl,A., Meitinger,T., Ciccodicola,A., and Wright,A.F. (2000). Mutational hot spot within a new RPGR exon in X-linked retinitis pigmentosa. Nat. Genet. *25*, 462-466.

49. Vervoort,R. and Wright,A.F. (2002). Mutations of RPGR in X-linked retinitis pigmentosa (RP3). Hum. Mutat. *19*, 486-500.

5. Acknowledgements

During the lifetime as a PhD student one experiences ups and downs. On the trail, I arrived at several crossroads having difficulties to find the right way which leads to the final destination. Input from many people was necessary to finally achieve the goal. Thus, I like to thank all the people that were somehow involved in the process to make this thesis possible.

First of all I like to thank my supervisor John Neidhardt for his constant support all the years I have spent here in Schwerzenbach and for his significant contributions to this thesis. He was always willing to come upstairs as soon as possible when I had questions (extraordinary fitness!). We had always fruitful discussions about our projects and about science in general. Furthermore, I liked the time we have spent together in New York visiting Jazz Clubs and eating large steaks.

I'm also grateful to Prof. Wolfgang Berger who gave me the opportunity to perform my PhD work in his lab. I always liked his insightful inputs on experiments, written papers and presentations.

I would also like to thank Esther Glaus for helpful discussions and technical support. I was glad to work together with Esther, who was always willing to listen to the problems I encountered (sometimes there was no chance for her to escape!).

Additional thank goes to Sandra Brunner, Silke Feil, Barbara Kloeckener-Gruissem, Gaby Tanner, Mariana Wittmer, Romain Da Costa, Martin Fritzsche, István Magyar, Lucas Mohn, Nikolaus Schäfer, Jurian Zürcher and all the other members of the Berger lab for their valuable input to ongoing projects and technical assistance.

Finally I like to thank my family, my friends and my girlfriend for all their support during this time.

6. Curriculum vitae

Name:	Fabian Schmid
Current address:	Lindenstrasse 15, 5430 Wettingen
Date of birth:	23.07.1980
Place of birth:	KS Baden (AG), Switzerland
Native Place:	Schübelbach (SZ)

Basic Education:

1987-1990	Primary School, Stetten AG
1991-1995	Bezirksschule, Mellingen AG
1996-2001	Kantonsschule: Neusprachlicher Typus (D), Wettingen AG

Academic Education:

2001-2003	Basic Studies in Biology at the University of Zurich.
2003-2004	Specialization in Molecular Biology (Main Subject) and Developmental Biology (Minor Subject).
2005-2006	Diploma thesis at the Institute of Molecular Biology in the Lab of Prof. Dr. Markus Noll at the University of Zurich. Title: "Analysis of the *poxn* function in the adult brain of *Drosophila melanogaster.*"
2006	Diploma in Molecular Biology at the University of Zurich.
2006 to date	PhD position at the Institute of Medical Molecular Genetics, University of Zurich, Switzerland.

Publications

Schmid F, Glaus E, Barthelmes D, Fliegauf M, Gaspar H, Nürnberg G, Nürnberg P, Omran H, Berger W, Neidhardt J. U1 snRNA-mediated gene therapeutic correction of splice defects caused by an exceptionally mild BBS mutation. *Hum Mutat*, 2011, submitted.

Glaus,E., **Schmid,F**., Da,C.R., Berger,W., and Neidhardt,J. (2011). Gene Therapeutic Approach Using Mutation-adapted U1 snRNA to Correct a RPGR Splice Defect in Patient-derived Cells. *Mol. Ther*. (Epub ahead of print)

Schmid F, Glaus E, Cremers FPM, Kloeckener-Gruissem B, Berger W, Neidhardt J (2010) Mutation- and tissue-specific alterations of *RPGR* transcripts. *Invest Ophthalmol Vis Sci* 51:1628-1635

Neidhardt J, Glaus E, Lorenz B, Netzer C, Li Y, Schambeck M, Wittmer M, Feil S, Kirschner-Schwabe R, Rosenberg T, Cremers FPM, Bergen AAB, Barthelmes D, Baraki H, **Schmid F**, Tanner G, Fleischhauer J, Orth U, Becker C, Wegscheider E, Nurnberg G, Nurnberg P, Bolz HJ, Gal A, Berger W (2008) Identification of novel mutations in X-linked retinitis pigmentosa families and implications for diagnostic testing. *Mol Vis* 14:1081-1093

Contributions to conferences and symposia:

Schmid F, Glaus E, Feil S, Roepman R, Cremers FPM, Berger W, Neidhardt J
Identification of novel *RPGR* splice variants and their relevance in X-linked retinitis pigmentosa. *Swiss Eye Research Meeting (SERM), Brunnen, 14th to 15th February 2008*, oral presentation.

Schmid F, Glaus E, Feil S, Roepman R, Cremers FPM, Berger W, Neidhardt J
Splicing of *RPGR* as a modifier of retinitis pigmentosa. *Pro Retina Deutschland Meeting, Potsdam (D), 28th to 29th March 2008*, poster presentation

Schmid F, Glaus E, Cremers FPM, Kloeckener-Gruissem B, Berger W, Neidhardt J
Mutation- and tissue-specific *RPGR* isoforms. *Swiss Eye Research Meeting (SERM), Biel, 27th to 28th January 2010*, oral presentation.

Schmid F, Glaus E, Cremers FPM, Kloeckener-Gruissem B, Berger W, Neidhardt J Alterations in *RPGR* splicing as a potential modifier of retinitis pigmentosa. *Association for Research in Vision and Ophthalmology (ARVO) Annual Meeting, Fort Lauderdale (FL, USA), 2nd to 6th May 2010*, poster presentation.